

The Ceramic Water Filter

Investigation Critical Parameters in the Production of Ceramic Water Filters

October 2011



Isabelle GENSBURGER

Acknowledgements

This study was executed by:



Engineers Without Borders Australia

99 Howard Street
North Melbourne
VIC Australia
www.ewb.org.au



Resource Development International Cambodia

Royal Brick Road, Preaek Thom Village, Kbal Kaoh Commune, Kean Svay District, Kandal Province
Cambodia
www.rdic.org



Delft University of Technology

Postbus 5
2600 AA Delft
The Netherlands
www.tudelft.nl



Practica Foundation

Oosteind 47
3356 AB Papendrecht
The Netherlands
www.practicafoundation.nl



Het Waterlaboratorium

J.W. Lucasweg 2
2031 BE Haarlem
The Netherlands
www.hetwaterlaboratorium.nl



Waterlaboratorium Noord

Rijksstraatweg 85
9756 AD Glimmen
The Netherlands
www.wln.nl



Aqua for All Foundation

Koningskade 40
2596 AA The Hague
The Netherlands
www.aquaforall.nl



Watercycle Research Institute

KWR Watercycle Research Institute

Groningerhaven 7, 3433 PE Nieuwegein
The Netherlands
www.kwrwater.nl

The author would like to give special thanks to:

- Dr. Bas Heijman for his regular technical support throughout the duration of the project;
- Ir. Guus Soppe for facilitating the Dutch Research Group meetings and helping with logistics and communications;
- Jan Nederstigt (from Practica), John Burnette, Som Vanna and Chan Saroeun (from RDIC) for their support in setting up the research production line;
- Dr. Ineke van der Veer and Dr. Jan Kroesbergen from Het Water Laboratory for their training in *E. coli* testing and help in resolving laboratory issues;
- Son Kosal for his dedicated assistance in the preparation and testing all the filter batches through the project period;
- Andrew Shantz from RDIC for his advice via meetings to discuss procedures, results and questions/issues;
- Chai Ratana from WaterSHED Cambodia for providing cultures of non-pathogenic *E. coli* B for this research;
- Ohm Mon from RDIC for his assistance in cutting discs from the pots for the strength test and solving technical problems related to machinery; and
- Kim Axworthy and Alexandra Ford from EWB Australia for supporting me throughout my placement in Cambodia.



Group photo (from left to right): Ir. Guus Soppe, Marc Hall, Andrew Shantz, Alex Ford, Isabelle Gensburger and Dr. Bas Heijman

Executive Summary

A ceramic pot filter is a point-of-use water treatment system produced in small factories in developing countries. The main treatment goal is disinfection of the water. In Hunter's 2009 meta-study, the ceramic pot filter appeared to be the most efficient household water treatment system out of four evaluated systems, especially on the long term. Worldwide, 22 factories produce ceramic filter pots. It is a relatively simple production process.

The porous pot is currently filtering water at a rate of 1-3 litres per hour. Although scrubbing has been shown to temporarily increase the flow rate, filters did not return to their original flow rate after scrubbing and flow rates continued to decrease to an extent which tends to be insufficient to meet drinking water needs. Accordingly, the objectives of this research were: (i) to better understand the production components and variables and move towards an international certification programme; and (ii) to investigate ways to increase the flow rate without compromising the water quality and strength of the filter.

In this research project, 15 batches of six pots were produced out of a mixture of clay, laterite and rice husk in a small pilot plant in Cambodia under controlled conditions, and tested for flow rate, log-reduction value of bacteria (*E. coli* being used as indicator) and strength of the pots. It appeared that the flow rate of the pot could be increased in two ways: 1) by increasing the porosity of the filter, by increasing the quantity of burn-out material (rice husk in this case) in the clay mix; and 2) by increasing the pore size. The pore size can be changed by either changing the particle size distribution of the burnout material or by changing the maximum firing temperature. The results are summarized as follows:

1. When the quantity of rice husk in the clay mix was increased from 9.7 kg to 14 kg per batch containing 30 kg of clay and 1 kg of laterite (i.e. from the rice husk to clay ratio 0.32:1 and 0.47:1), the average flow rate increases from 7.4 LPH to 22.8 LPH, the average LRV of *E. coli* stays approximately constant at 2.4, and the average MOR decreased from 2.4 MPa to 1.3 MPa.
2. When the maximum firing temperature was increased from 800 deg. C to 950 deg. C, the average flow rate increases from 3.8 LPH to 8.0 LPH, the average LRV of *E. coli* decreases slightly from 2.3 to 1.9, and the average MOR increases from 1.1 MPa to 2.9 MPa.
3. When the rice husk particle size increases from [0 – 1] mm to [0.5 – 1] mm, the average flow rate increases from 3.0 LPH to 6.7 LPH, the average LRV of *E. coli* decreases from 1.7 to 0.7, and the average MOR decreased from 2.4 MPa to 1.3 MPa.

The main conclusion is that a higher porosity does not appear to affect the removal of bacteria, but that a bigger pore size decreases the bacteria removal. More rice husks in the clay mixture gives a higher porosity in the pot; and porosity and flow rate are linearly related. The particle size distribution of the rice husk affects the pore size distribution in the clay wall. The maximum firing temperature is very important for sintering. During the sintering process which starts from about 850 deg. C, some small pores can merge to one bigger pore; and larger pores cause larger flow rates.

A two-month flow rate test was also done on pots with different porosities. This test emulated field conditions by feeding the pots with 20 L/day of locally available raw pond and well water of turbidity less than 30 NTU and scrubbing the pots when the flow rates became too low, i.e. lower than 1 LPH. Results indicate that pots of higher porosities did not need to be scrubbed as often as pots of lower porosities. Filters of lowest porosities (batch of rice husk to clay ratio 0.32:1) had to be scrubbed for the first time after 60 L of throughput, and there were six scrubbing events in the two-month test period. The filters of highest porosity (batch of rice husk to clay ratio 0.47:1) had to be scrubbed for the first time after 120 L of throughput, and there were only two scrubbing in the same testing period. Filters of higher porosities (i.e. rice husk to clay ratios of 0.40:1 to 0.47:1) managed to maintain flow rates above 2 LPH at all times whereas the lower porosity pots (i.e. rice husk to clay ratios of 0.32:1 to 0.37:1) either had flow rates lower than 2 LPH to start with or had to be scrubbed a few times to maintain that flow rate. Rapid clogging is not desirable because the user will have to scrub the filter to restore flow rates and is likely to contaminate or break the filter in this process. The less handling the better. The durability of pots with higher porosities needs to be investigated under field conditions.

Table of Contents

Acknowledgements	ii
Executive Summary	iv
Table of Contents	vi
List of Figures	x
List of Tables	xiv
1.0 Introduction	1
1.1 Background.....	1
1.2 Project Aims.....	2
1.3 Research Scope	3
1.3.1 Set up and test the research production line (Stage 1).....	3
1.3.2 Test reproducibility of RDI filters by mimicking RDI processes from mixing to firing and cooling (Stage 2).....	6
1.3.3 Make the first series of batches of filters (dry season) (Stage 3)	7
1.3.4 Make the second series of batches of filters (wet season) (Stage 4).....	7
1.3.5 Make a batch with rice husks of larger particle sizes (wet season) (Stage 5) ..	7
1.3.6 Strength tests and Quality control tests (stage 6)	8
2.0 Methodology	9
2.1 Sourcing of the Raw Materials	9
2.1.1 Rice husk.....	9
2.1.2 Clay and laterite.....	9
2.1.3 Water	11
2.2 Filter Making Procedure	11
2.2.2 Weighing raw materials	12

2.2.3	Mixing	13
2.2.4	Pressing.....	15
2.2.5	Surface Finishing	16
2.2.6	Labeling	16
2.2.7	Polishing.....	17
2.2.8	Drying	17
2.2.9	Firing and Cooling.....	18
2.2.10	Application of Silver Solution	22
2.3	Flow rate testing.....	23
2.4	E. coli testing with and without silver.....	24
2.5	Long-term Test.....	26
2.6	Strength test.....	28
3.0	Results	34
3.1	Rice husk quantity variations	34
3.1.1	Flow rates of the first and second batch series.....	34
3.1.2	LRV's of E. coli of the first and second batch series with and without silver ..	37
3.1.3	Strength test results for the second batch series with silver	42
3.2	Maximum firing temperature variations	44
3.2.1	Flow rates	44
3.2.2	LRVs of E. coli for filters fired at different maximum firing temperatures	45
3.2.3	Strength test results of the filters with silver	47
3.3	Rice husk particle size variations	49
3.3.1	Flow rates for filters with various rice husk particle sizes.....	49
3.3.2	LRV's of E. coli for filters with various rice husk particle sizes	50

3.3.3 Strength test results for filters with silver.....	52
3.4 Long-Term Flow Rate Testing.....	53
3.4.1 Highly turbid feed water	53
3.4.2 Less turbid feed water	54
4. Discussion	57
4.1 Raw Material Characteristics 4.1.1 Clay and Laterite (TCKI)	57
4.1.2 Rice husk.....	57
4.2 Rice Husk Quantity Variations	58
4.3 Maximum Firing Temperature Variations	59
4.4 Rice Husk Particle Size Variations.....	60
4.5 Reproducibility	61
4.6 Clogging test.....	62
4.7 Strength test.....	62
5.0 Conclusions.....	64
6.0 Recommendations for future research	65
References.....	66
Appendices.....	I
APPENDIX I: Analysis of the Raw Materials (by TCKI).....	II
APPENDIX II: Initial E. Coli Testing Procedure (First Batch Series)	V
APPENDIX III: Adapted E. Coli Testing Procedure (Second Batch Series)	IX
APPENDIX III: Raw and Calculated Data (First Batch Series).....	XII
APPENDIX V: Raw E. coli Data (First Batch Series)	XIV
APPENDIX VI: Raw and Calculated Data (Second Batch Series)	XIX
APPENDIX VII. Sensitivity Analysis (First Batch Series)	XXI

APPENDIX VIII: Raw and Calculated Data (Maximum Firing Temperature Variations)	XXIII
APPENDIX IX: Mercury Intrusion Porosimetry Results from the Technical University of Delft in the Netherlands	I
APPENDIX X: Detailed Results of the Strength Tests by GERES	I
APPENDIX XI: Raw Data (Rice Husk Size Variations)	I
APPENDIX XII: Rice husk particle size distribution analysis of the rice husk samples used in the dry and wet seasons	III
APPENDIX XIII: Long-term Flow Rate Raw Data (Pond Water – part 1)	VII
APPENDIX XIV: Long-term Flow Rate Raw Data (Well Water – part 2)	VIII
APPENDIX XV: DIA of SEM photomicrographs from Cultrone et al. (2003)	IX

List of Figures

Figure 1. Location of RDI where the research project was based	3
Figure 2. Planning of the layout of the research unit and facilities in early August 2010.	4
Figure 3. Roof of the shed in the process of being built in late August 2010.....	4
Figure 4. Water and power connection completed and all necessary equipment purchased in November 2010	5
Figure 5. Necessary research equipment (including buckets, tarpaulin and so on) was purchased in November 2010	5
Figure 6. Upgraded kiln ready for firing	6
Figure 7. Temperature regulation system for the gas-operated research kiln	6
Figure 8. Rice husk sample from RDIC	9
Figure 9. Clay bricks used at RDIC	10
Figure 10. Laterite sample from RDIC.....	10
Figure 11. Freshly constructed rainwater harvesting concrete tanks	11
Figure 12. hammer mill used for grinding the clay and laterite	12
Figure 13. Sieving of the raw materials	12
Figure 14. Weighing of the raw materials.....	12
Figure 15. Mixing of the clay mixture after water is added	13
Figure 16. Extraction of the wet mixture on the tarpaulin	14
Figure 17. Formation of cubes for pressing.....	14
Figure 18. Cubic block ready for pressing	15
Figure 19. Cubic block turned into a pot shape	15
Figure 20. Surface finishing.....	16
Figure 21. Labeling of Batch 13 Pot No. 5.....	16

Figure 22. Recording of the weights of batch pots during drying.....	17
Figure 23. Drying curve of Batch 7 from the day after Pressing to the day before firing where the y-axis is the weight of the filters in kg	18
Figure 24. Firing curve of a regular RDI kiln.....	18
Figure 25. Research Kiln with temperature regulation system assembled by Reitse de Jong in 2009 (Ref: Research Kiln Instruction Report)	19
Figure 26. Stacking of the kiln using spacers	20
Figure 27. Firing curve of Batch 13	20
Figure 28. Monitoring of the kiln during firing	21
Figure 29. Silver painting.....	23
Figure 30. Refilling of the pots throughout the constant head flow rate test.....	24
Figure 31. <i>E. coli</i> result for 0.5 ml of influent sample diluted 10 times.....	25
Figure 32. <i>E. coli</i> results for 1, 10 and 100 ml duplicate effluent samples from B4 P5 without silver application (<i>E. coli</i> are purple and coliforms are blue)	25
Figure 33. UV treated rain water used in the <i>E. coli</i> test	26
Figure 34. Pumping of pond water for the long-term flow rate test.....	27
Figure 35. Filling up 20 L bottles for the long-term flow rate test.....	27
Figure 36. Set-up for the long-term flow rate test	28
Figure 37. Marking discs on the bottom section of a filter after the walls were broken down.....	29
Figure 38. Ohm Mon from RDIC helping to cut the ceramic discs.....	29
Figure 39. Ceramic discs made from B21 P6, P1, P4 and P5.....	30
Figure 40. Positioning of the ceramic disc on the support.....	31
Figure 41. Bubble level check	32
Figure 42. Gradual loading of the lever plate with steel weights	32

Figure 43. Influence of the amount of rice husk on the flow rate of the pot. The two series of batches are produced with different rice husk.....	35
Figure 44. average flow rates of filters of different porosities before and after silver application	37
Figure 45. LRV's of <i>E. coli</i> versus flow rates for filters of different porosities from the first batch series.....	38
Figure 46. Box-and-whisker plots of LRV's for filters from RDI and the first batch series with increased quantity of rice husk in the clay mix.....	39
Figure 47. LRV's of <i>E. coli</i> versus flow rates for the second batch series (increasing the quantity of rice husk in the clay mix).....	40
Figure 48. Box-and-whisker plots of LRV's versus flow rates for filters from RDI and the second batch series with increased quantity of rice husk in the clay mix	41
Figure 49. Box-and-whisker plots of the MOR for pots of different porosities.....	43
Figure 50. The maximum firing temperature influences pore size and therefore flowrate too.	45
Figure 51. LRVs of <i>E. coli</i> versus flow rates for maximum firing temperature variation experiments without silver	46
Figure 52. Box-and-whisker plots of the LRV's of <i>E. coli</i> of pots fired at different maximum firing temperatures.....	47
Figure 53. MOR versus maximum firing temperature.....	48
Figure 54. LRVs versus flow rates for rice husk size variation experiments.....	50
Figure 55. Box-and-whisker plots of LRVs for pots with different rice husk particle sizes	51
Figure 56. Box-and-whisker plots of the MOR's of pots with different rice husk particle sizes	52
Figure 57. Long-Term Flow Rate results using very turbid pond water of turbidity 12.9 to 199 NTU.....	53
Figure 58. Long-Term Flow Rate results using well water of turbidity 2.84 to 27.1 NTU54	

Figure 59. Maximum throughput before flow rate becomes less than 1 LPH and the pot has to be scrubbed..... 56

Figure 60. Particle size analysis of the rice husk samples from RDI Cambodia taken in January and May 2011 58

Figure 61. Representative diagrams of the pore size distribution (vol.%) of the G and V bricks with respect to T (deg. C) (Cultrone et al. 2003) 60

Figure 62. Pug mill donated to RDIC in November 2010..... 63

List of Tables

Table 1. Description of batches made for the three sets of experiments.....	31
Table 2. Average flow rates for the first batch series	34
Table 3. Average flow rates for the second batch series.....	35
Table 4. Comparison of flow rates pre versus post silver nitrate application	36
Table 5. LRV's for the first batch series.....	37
Table 6. Statistical Summary Table for LRV's for filters from the first batch series	39
Table 7. LRVs for the second batch series.....	40
Table 8. Statistical Summary Table for LRV's for filters from the second batch series .	41
Table 9. LRV's of pots from the second batch series before and after silver nitrate application	42
Table 10. Strength testing results for filters with different porosities	43
Table 11. Flow rates for filters fired at different maximum firing temperatures	44
Table 12. Statistical summary of the LRV (<i>E. coli</i>) results for pots without silver fired at different maximum firing temperatures	45
Table 13. Statistical Summary Table for LRV's of filters fired at different maximum firing temperatures	47
Table 14. Strength testing summary results for filters with different maximum firing temperatures	48
Table 15. Flow rates for filters with rice husk of different sizes	49
Table 16. LRV's of <i>E. coli</i> for filters with different rice husk sizes.....	50
Table 17. Statistical Summary (LRV versus rice husk particle size).....	51
Table 18. Flow rates right after scrubbing events.....	55
Table 19. Rough particle size analysis of the rice husk samples pre- and post-April	57
Table 20. Comparison of the flow rates for triplicate batches 9, 13 and 25.....	61

Table 21. Comparison of the flow rates for triplicate batches 7, 22 and 23.....	61
Table 22. Strength test summary results for all three sets of pots.....	62
Table. Rice husk from May 2011	V

1.0 Introduction

1.1 Background

A ceramic pot filter is simple, potentially life-saving point-of-use water treatment system. The most important aim is to remove pathogens from the feed water. From a recent meta-study (Hunter, 2009), the ceramic pot filter appeared to be the most efficient household water treatment system out of four evaluated systems, especially on the long term. Worldwide, 22 factories produce ceramic filter pots. It is a relatively simple production process:

1. Preparation of raw materials (sieving < 1 mm)
2. Mixing of clay components (10 mins dry and 15 mins wet)
3. Forming of clay cubes for pressing
4. Pressing of clay cubes into ceramic filter form
5. Surface finishing and labeling of pressed filters
6. Drying of pressed filters (longer in the wet season than in the dry season)
7. Firing and cooling in kiln

The porous pot is currently filtering water at a rate of 1-3 liters per hour. Brown (2006) and Lantagne (2001a, 2001b) reported that microbial removal efficiencies of 2 to 6 log, 0.5 to 2 log and 4 to 6 log can be achieved for bacteria, virus and protozoa, respectively. However, in the field, Brown et al. (2007) observed an average of only 1.7 log (98 %) reduction in *E. coli*. This low reduction was likely attributable to post-treatment contamination in the treated water storage containers (Brown et al., 2007; Murphy *et al.*, 2007).

The need to improve access to safe quality water is widely recognized, however the problem of a lack of sufficient quantities of safe drinking water also deserves attention. If a family or community decides to invest their resources into a water treatment system, it is important that they not only get water that is free of harmful bacteria and disease-causing pathogens but that is also available in sufficient quantities to meet their needs. A water treatment system that provides suitable drinking water is virtually useless if there is not enough water. People will have to resort back to unsustainable practices or unsafe sources such as purchasing water or drinking untreated water (Klarman, 2009).

From The Ceramics Manufacturing Working Group's (2011) literature review, many results can be found on the performance of the ceramic water filter. Considerable reduction in flow rates due to clogging has been noted in laboratory (Lantagne 2001a; Fahlin 2003; van Halem 2006) and field studies (Lantagne 2001b). Although scrubbing has been shown to temporarily increase the flow rate (Lantagne 2001b), in the laboratory, filters did not return to their original flow rate after scrubbing and flow rates continued to decrease over time to less than 0.5 L/hr, which is insufficient to meet a

family's drinking water needs (van Halem 2006). Fahlin (2003) found that clogging impeded his research into the hydraulic conductivity of filters. However, in some field investigations users have reported that filters provided enough water for additional uses (Roberts 2004) and only 5% of filter disuse was attributed to reduced flow rate (Brown and Sobsey 2006).

Although ceramic filters are a promising household water treatment and safe storage (HWTS) option, many challenges and critical research questions still need to be addressed, especially as there are contradictory findings and continuing debate regarding the relative importance of the various mechanisms of action on the effectiveness of the filter. Little is known about the hydraulic properties of the filter and pore size investigations have documented variation by country of manufacture. Flow rate is presently relied upon as an indicator of production consistency as it is easy and inexpensive to measure locally.

There are different ways of increasing the flow rate of the filters:

1. increasing the quantity of rice husk in the clay mix (Bloem 2009; Klarman 2009);
2. using a different type of burn-out material (rice husks, coffee grounds, sawdust, and others) (Klarman 2009);
3. increasing the size of the burn-out material (Klarman 2009);
4. increasing the quantity of laterite or sand in the clay mix (Bloem 2009); and
5. optimizing the maximum firing temperature.

Studies investigating the relationship between flow rate and microbiological removal efficiency have had contradictory findings (Bloem et al. 2009; Klarman 2009); therefore, more research is needed on this matter.

1.2 Project Aims

The objectives of this research were to:

1. investigate a number of critical factors in the production process of CWFs and develop a better understanding of the production and use of these filters as a proven method for domestic water purification world-wide, ideally leading to an international certification process being identified; and
2. investigate ways to increase the flow rate so that the ceramic water filter can cater the drinking water needs of a typical Cambodian household on the long term without compromising the water quality and strength of the filter.

1.3 Research Scope

The research project was set up and carried out in the grounds of a well-established water filter factory of a local organization called Resource Development International Cambodia (RDI). The RDI team is driven by compassion to help reduce poverty by developing and implementing unique resources and appropriate technologies such as ceramic water filters to empower communities towards sustainable change (RDI, 2003). RDI is located on Royal Brick Road, Preak Thom Village, Kbal Kaoh Commune, Kean Svay District, Kandal Province, Cambodia (Figure 1)

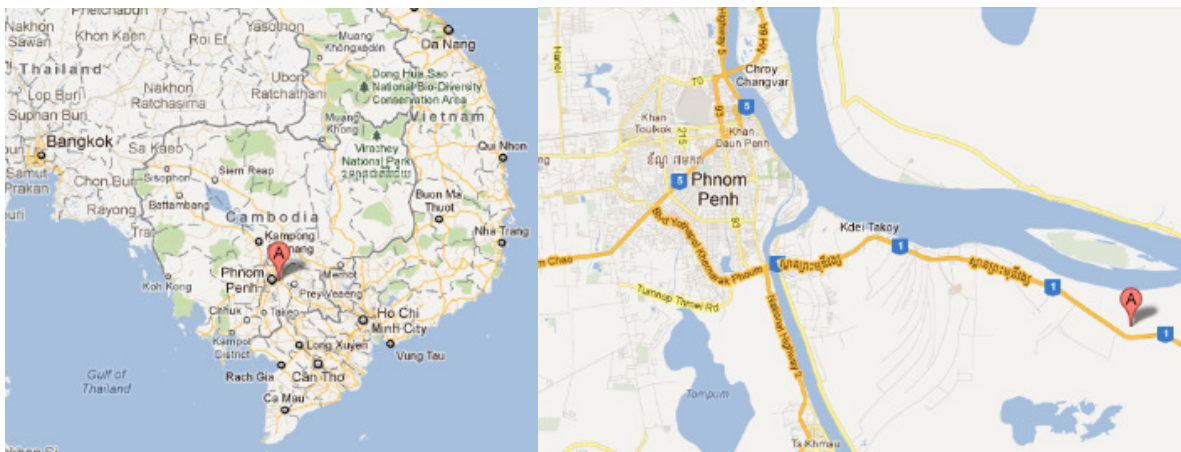


Figure 1. Location of RDI where the research project was based

The scope of this project is described below.

1.3.1 Set up and test the research production line (Stage 1)

- The research production line was set up in the grounds of the RDI ceramic water filter factory (Figures 2 and 3). The water and electricity facilities were installed and equipment such as the mixer and hydraulic press ordered and tested (Figures 4 and 5).



Figure 2. Planning of the layout of the research unit and facilities in early August 2010



Figure 3. Roof of the shed in the process of being built in late August 2010



Figure 4. Water and power connection completed and all necessary equipment purchased in November 2010



Figure 5. Necessary research equipment (including buckets, tarpaulin and so on) was purchased in November 2010

- The gas kiln (Figure 6) was improved by: (1) adding insulation to the kiln walls and chimney; (2) extending the chimney to improve draft and circulation of hot air in the kiln chamber; and (3) changing the temperature regulating system (Figure 7) in such a way that one gas bottle is connected to one burner and the second gas bottle is connected to the other burner through the regulation system.



Figure 6. Upgraded kiln ready for firing



Figure 7. Temperature regulation system for the gas-operated research kiln

1.3.2 Test reproducibility of RDI filters by mimicking RDI processes from mixing to firing and cooling (Stage 2)

- The temperature curve in the RDI operational kilns was recorded at 3 to 4 locations (near the bottom, in the middle, near the top and next to the pyrometric cones).
- The same curve was attempted to be mimicked in the research kiln by setting the kiln programmer equivalently by: (1) firing 2 batch of filters made and pressed by RDI and checking that the flow rates are in the standard range of 2 to 3 LPH; (2) firing at the set firing curve from (1) a batch of pots made in the research facilities using the same composition as the RDI standard production and fired in the research kiln, and checking that the flow rates are in the standard range; and (3) doing adjustments by trial and error until pots with the same flow rates and LRVs as RDI pots are produced.

1.3.3 Make the first series of batches of filters (dry season) (Stage 3)

- Five batches of filters with increased porosities were made by increasing the quantity of rice husk in the clay mix from the RDI standard of 9.7 kg (Batch 7) to 11 kg (Batch 18), 12 kg (Batch 13), 13 kg (Batch 4) and 14 kg (Batch 17). The quantities of clay (30 kg) and laterite (1 kg) were kept constant for the series.
- The batches were tested for flow rates and LRVs of *E. coli* without silver
- The batches were painted with silver, and two filters per batch were tested for long-term flow rate tests under turbid influent conditions while the rest of the filters were sent to the TU Delft for further testing (including virus testing and long term flow rate and *E. coli* testing).

1.3.4 Make the second series of batches of filters (wet season) (Stage 4)

- Two batches of filters were made with RDI-like composition and fired at different maximum firing temperatures: 800 deg. C (Batch 20) and 950 deg. C (Batch 19).
- The batches were tested for flow rates and LRVs of *E. coli* without silver.
- The batches were then painted with silver and tested for flow rates and LRVs of *E. coli*.

1.3.5 Make a batch with rice husks of larger particle sizes (wet season) (Stage 5)

- One batch of filter was made with the same quantity of rice husks as RDI but sieved so that only the particles greater than 0.5 mm and no larger than 1 mm were retained. The batch (Batch 12) was then fired at the standard firing curve.
- The batch was tested for flow rates and LRVs of *E. coli* without silver.
- The batches were then painted with silver and tested for flow rates and LRVs of *E. coli*.

1.3.6 Strength tests and Quality control tests (stage 6)

- Samples of filters with different pore sizes were sent to TU Delft to precisely measure for pore size by mercury intrusion porosimetry.
- Three pots per batch were broken down into 12 discs cut from the bottoms of the pots (4 discs could be made from one pot). These discs were tested for strength at the clay testing facilities of *Groupe Energies Renouvelables Environnement Solidarité* (GERES)
- Some triplicate batches were made and fired to check reproducibility of flow rates and LRVs: B22 and B9 have 9.7 and 12 kg of rice husks, respectively.

2.0 Methodology

2.1 Sourcing of the Raw Materials

2.1.1 Rice husk

RDIC uses ground rice husks (Figure 8) as the organic burn-out material in their ceramic filters. Rice husks are a waste product from rice production in Cambodia and are easily available. The rice husks are bought from a local supplier and are provided in rice bags pre ground. In November 2011, RDI started sieving its ground rice husk at a particle size of 1 mm or less as part of their quality control process.



Figure 8. Rice husk sample from RDIC

2.1.2 Clay and laterite

RDIC is situated near a brick factory where clay is mined locally and extruded into bricks before drying. RDIC uses unfired extruded bricks (Figure 9) for convenience. They are easy to transport, cheap and the extrusion process enhances the plasticity of the clay material. Clay plasticity is greatly influenced by the clay's particle size, water content and aging. A rule of thumb for determining how plastic a clay is is to make a coil of the clay and then wrap it around a finger. A plastic clay will not crack or break.



Figure 9. Clay bricks used at RDIC

Since 2005, RDIC has been adding laterite (Figure 10), a soil containing iron oxide, to the clay. Laterite is said to bind and inactivate viruses (Hagan *et al.*, 2009) but Bloem's 2008 studies found no difference in virus removal with laterite.



Figure 10. Laterite sample from RDIC

Stichting Technisch Centrum voor de Keramische Industrie (TCKI) in the Netherlands analyzed and investigated the characteristics of samples of clay and laterite taken from

RDIC. TCKI determined the particle size distribution (percentage of fine particles and concentration of coarse and fine sand) of both materials, as well as the specific surface area and chemical composition of the clay. The analysis can be found in Appendix I.

2.1.3 Water

Rain water harvested from the roof of the research shed was used in the filter making process (Figure 11).



Figure 11. Freshly constructed rainwater harvesting concrete tanks

2.2 Filter Making Procedure

The filter making procedure has 9 main steps from the preparation of raw materials to firing and cooling. These steps are described as follow.

2.2.1 Preparing raw materials

RDIC's same clay, rice husks and laterite were used for this research project. The clay bricks into pieces using "elephant feet" and the clay pieces are then hammer milled into a fine powder (Figure 12).



Figure 12. hammer mill used for grinding the clay and laterite

2.2.2 Weighing raw materials

All raw materials (clay, rice husk and laterite) were sieved through a 1 mm mesh sieve (Figure 13) and measured for the desired quantities using an accurate scale. RDI's standard recipe for 6 pots is 30 kg of clay, approx. 10 kg of rice husk, 1 kg of laterite and 14.5 L of water (Figure 14).



Figure 13. Sieving of the raw materials



Figure 14. Weighing of the raw materials

2.2.3 Mixing

The clay, rice husks and laterite were mixed dry for 10 minutes. Then, the measured volume of water was added through a funnel and evenly distributed into the mixer through a sprinkler system. The raw materials were mixed wet for 15 minutes (Figure 15). The mixer used for this purpose was designed and built identical to RDIC's. RDIC uses an automatic water spray system for consistent and uniform water distribution; but for this research, a manual system was more appropriate given that the required volume of water changed depending on the quantity of rice husk used. The more rice husk in the clay mix, the more water is needed to get satisfactory consistency for pressing.



Figure 15. Mixing of the clay mixture after water is added

2.2.3 Forming clay cubes for pressing

The clay from the mixer was emptied onto a clean tarpaulin (Figure 16). The wet clay mixture was formed into cubes for pressing. The cubes were turned and thrust against the tarpaulin (Figure 17) to remove air bubbles in the mix prior to pressing - and therefore to reduce imperfections in the clay. It is better to have excess weight in these blocks due to slight losses in the moulding process as clay is squeezed out the top. Excess material ensures that air bubbles will be pressed out of the walls of the filter in the moulding press.



Figure 16. Extraction of the wet mixture on the tarpaulin



Figure 17. Formation of cubes for pressing

2.2.4 Pressing

The cubes were pressed into ceramic water filter shapes (Figures 18 and 19). This process was mechanized by using a hydraulic press fitted with male and female moulds (which were covered with plastic bags to prevent sticking) to manufacture consistent filter elements. The filters were fully pressed between a male and female mould. The hydraulic press incorporates a fixed plate in the bottom mould which pushes the pressed mould out as the mould opens up.



Figure 18. Cubic block ready for pressing



Figure 19. Cubic block turned into a pot shape

2.2.5 Surface Finishing

After pressing, the filters were carefully carried to the polishing table, with the plastic bowl in place and using the metal plate as support (Figure 20). The filter elements were slid off the metal plate onto the drying tarpaulin and the plastic bowl was removed. The inside plastic bag was removed and the filter rim was wetted with water using a brush.



Figure 20. Surface finishing

2.2.6 Labeling

Each filter was marked with a serial number (batch and pot number, e.g. B13 P5, see Figure 21). A database was used to track the filters and keep all filter information. This database included the filters' manufacturing date and weights during the drying period and visual observations such as surface cracks or signs of any other signs of defect.



Figure 21. Labeling of Batch 13 Pot No. 5

2.2.7 Polishing

The freshly pressed filters were left on the table under shelter (with tarpaulin down) for 3 – 4 hours (or overnight) to harden. It is important they are left in the shade and not in the sun to ensure a more uniform drying process. Afterwards, the filters were polished further by hand, using a piece of plastic with a soft edge to remove irregularities on the inside surface. A wet cloth was used to wipe the rim of all the filters to reduce the likelihood of cracks. The filter elements were left in the shade to harden further until the following day, when they were hard enough to be placed upside down to polish the bottom of it.

2.2.8 Drying

The pots were left on table as per Figure 22 to dry in the research shed and the pot weights were recorded daily to estimate when the batch was dry enough to fire.



Figure 22. Recording of the weights of batch pots during drying

Filters should be as dry as possible before stacking the kiln. The dryness of a filter could be determined by plotting the drying curve (Figure 23): the pots were assumed to be dry enough when the curve reached a plateau (after an average of 10 days).

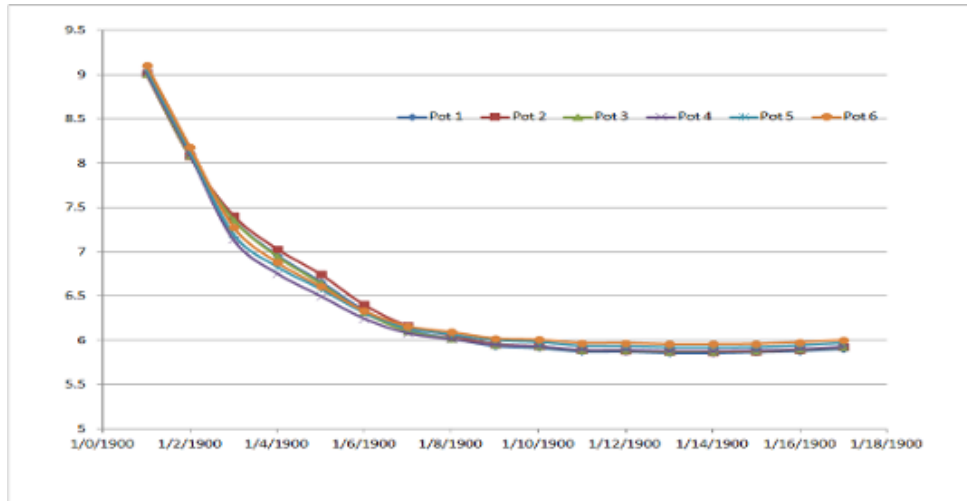


Figure 23. Drying curve of Batch 7 from the day after Pressing to the day before firing where the y-axis is the weight of the filters in kg

2.2.9 Firing and Cooling

Prior to making filters for the research, the temperature curve of the RDI kilns was surveyed using 3 thermocouples at 3 different height locations. The average maximum temperature was approximately 885 deg. C. (Figure 24)

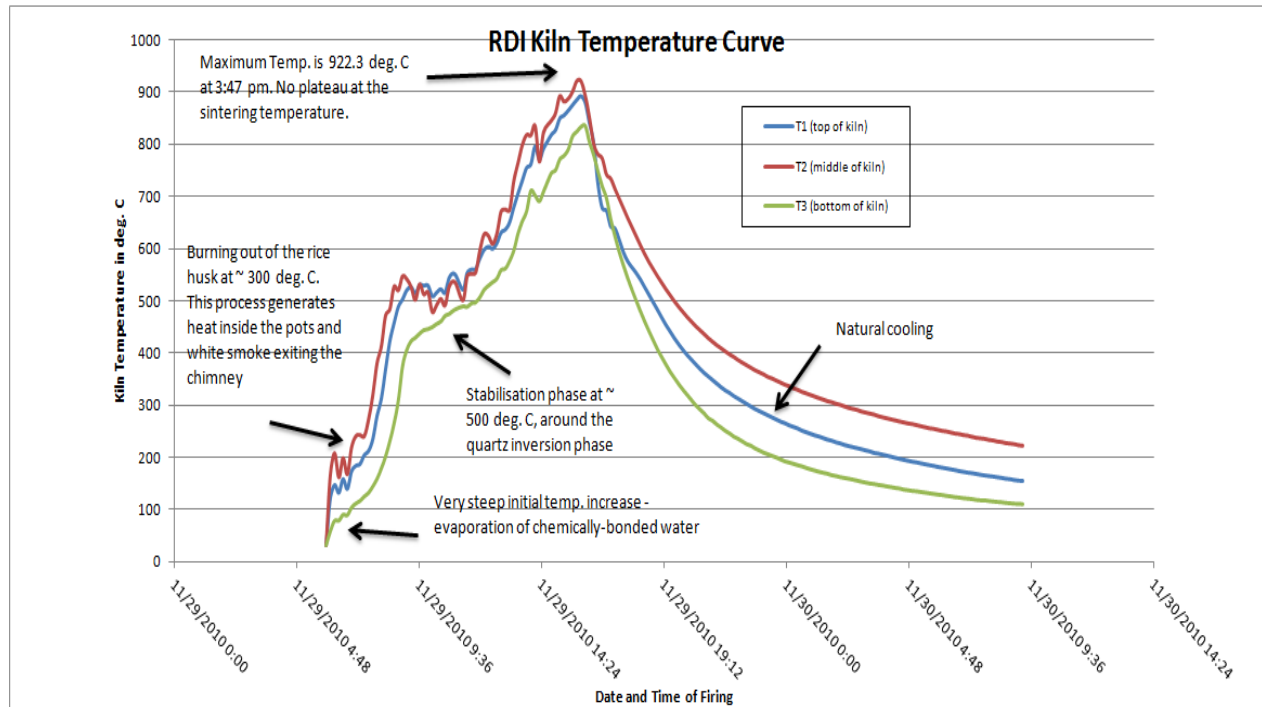


Figure 24. Firing curve of a regular RDI kiln

The research kiln has a maximum capacity of 6 pots, thereby limiting the batch sample size to only 6 pots. The configuration of the kiln can be seen in Figure 25.

There is a total of 5 thermocouples to record the temperatures at various locations inside the kiln throughout the firing process: 4 K-type thermocouples are next to 4 pots and the fifth thermocouple is directly connected to the temperature regulation system.

Before stacking the kiln, the pots are inspected for cracks. The filters are not placed directly on the kiln floor but on spacers and the filters on top sit on the filter below mouth to mouth with spacers in between to allow circulation (Figure 26).

The standard program is set to:

1. fire up to 520°C at the rate of 100°C/hour
2. plateau at 520°C for one hour
3. continue firing at the rate of 100°C until the maximum temperature (885°C for RDI-like filters) is reached; and
4. close the gas bottles, shut the kiln when the maximum temperature is reached and let the filters cool down naturally

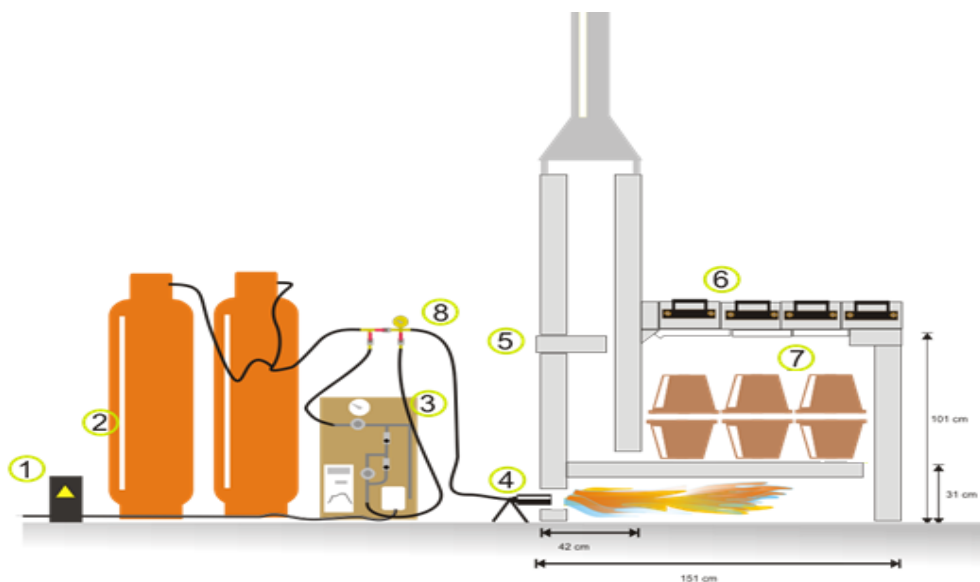


Figure 1

1. Power stabilizer
2. Gas bottles
3. Regulating system attached to wooden board
4. Burners
5. Chimney regulator
6. Roof parts
7. Internal floor.
8. Switch manual-automatic regulation.

Figure 25. Research Kiln with temperature regulation system assembled by Reitse de Jong in 2009 (Ref: Research Kiln Instruction Report)



Figure 26. Stacking of the kiln using spacers

The firing (and cooling) curve is recorded every 10 minutes using dataloggers connected to the 4 ceramic-coated thermocouples positioned near the filters (Figures 27 and 28).

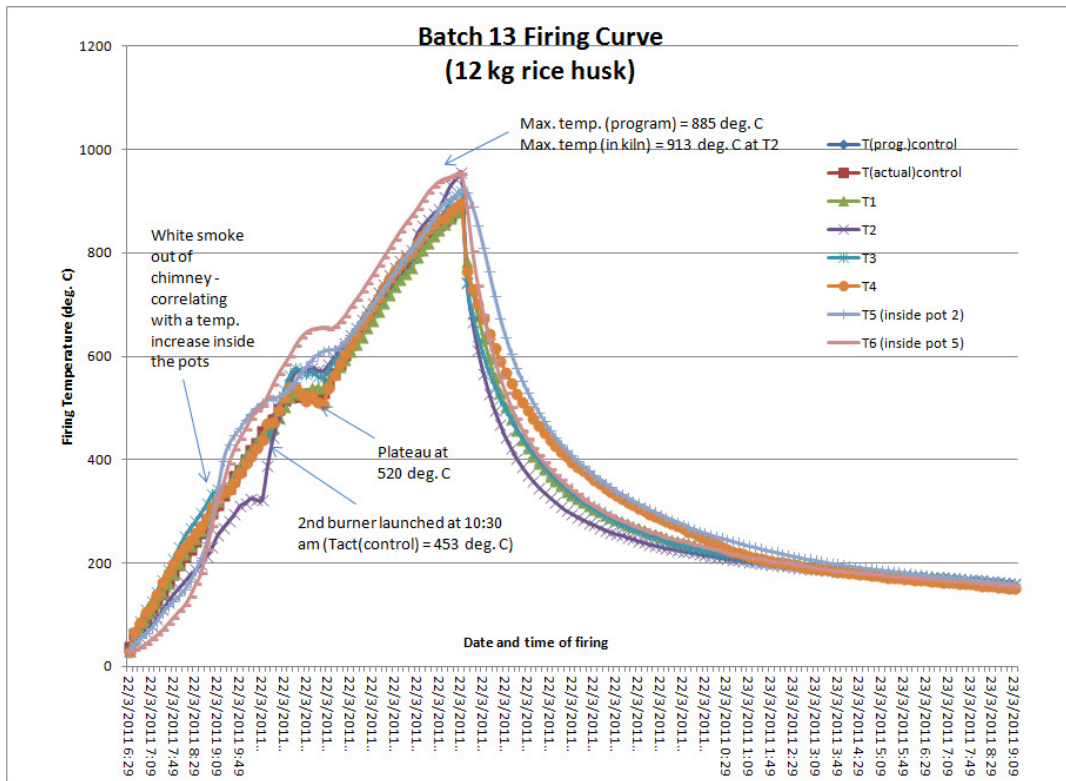


Figure 27. Firing curve of Batch 13



Figure 28. Monitoring of the kiln during firing

The firing / cooling takes approximately 10 hours, throughout which take place the following processes (The Ceramics Manufacturing Working Group, 2011):

1. **Water smoking (20°-120°C):** the pore water remaining in the filters due to atmospheric humidity evaporates and turns to steam.
2. **Decomposition (120°-350°C):** at about 200 °C, vegetable matter remaining in the clay breaks down.
3. **Combustion of Burn-out Material (350°-450°C):** the volatiles in the burn-out material will vaporize and a lot of smoke will come out of the chimney.
4. **Ceramic Change (350°-700°C):** the clay becomes ceramic. At around 600 °C, the clay particles are sintered together which results in very slight shrinkage. For this reason, the firing is maintained at 520 °C for an hour for stabilisation. (After 600 °C, there is no danger of damaging filters by heat variations.)
5. **Vitrification (800°C+):** this is when the sodium and potassium oxides start to flux with the free silica. During this stage, the body contracts as the clay particles are welded together with glass, thus providing strength. The ideal level of vitrification will be a balance between the desired strength and the desired porosity of the final product. A minimum amount of strength; however, is needed to withstand the shock of the quartz inversion during cooling.
6. **Cooling:** the kiln is left to cool naturally for 24 hours.

2.2.10 Application of Silver Solution

The silver nitrate solution is prepared in the RDIC laboratory by:

1. adding 100g of AgNO₃ crystals (RDIC purchases crystalline AgNO₃ of around 99.8% purity) to 500 ml of deionised water and mix well;
2. adding a further 1000 ml of deionised to the solution and mix for one minute;
3. storing this silver solution concentrate in a light proof plastic container; and
4. making up silver solution, taking 100 ml of the silver solution concentrate and place it in a light proof container. Eighteen L of distilled water are then added and mixed. 18.1 L makes enough solution for approximately 60 filter elements (Hagan et al. 2009)

The method for silver painting is the same as RDI's: the filters are painted with a silver nitrate solution manually.

1. ~ 47 mg or approximately 200 ml of solution are applied to the inside of the filter using a paint brush. ~ 23 mg or 100 ml of solution are applied to the outside of the filter
2. Take a cup with markings at 300ml, and 100ml
3. Pour 300 ml of silver nitrate solution into the cup (the top marker). Paint 200ml onto the inside of the filter - the silver nitrate solution will now be down to the bottom marker
4. Paint the remaining 100ml onto the outside of the filter (Figure 29)
5. Once the filters have been painted, leave them to dry for a short time



Figure 29. Silver painting

2.3 Flow rate testing

The filters were flow rate tested using a constant head method described as follows:

1. The filters are soaked in bacteria-free (UV treated rain) water for 24 hours.
2. The next day, the dry receptacles (that will contain the filtrates) are weighed individually and the weight $W(\text{dry receptacle})$ is written on the receptacle for future reference.
3. The soaked filters are placed inside their receptacles. A mark is made with a permanent marker inside the filter at 18 cm from the bottom of the filter.
4. The first filter is filled up with water up to the mark and the stop-watch is started. The next filter is then filled up to the mark and the time from the stop-watch taken note of. This procedure is continued for the rest of the filters.
5. The filters are kept on being re-filled to the mark for one hour (Figure 30).
6. After one hour, the filters are removed from their receptacles and the weights of the receptacles with filtrate inside are recorded as $W(\text{wet receptacle})$.
7. The net flow rate is $W(\text{wet receptacle}) - W(\text{dry receptacle})$.



Figure 30. Refilling of the pots throughout the constant head flow rate test

2.4 E. coli testing with and without silver

The *E. coli* test was done at the RDIC Resource Laboratory facilities. Membrane filtration was used to determine the *E. coli* concentration of the in and effluent samples of the filters. *E. coli* serves as an indicator for bacteria. Non-pathogenic *E. coli* (strain B) was used.

Samples were filtered in duplicates through 47 mm diameter and 0.45 μm pore size cellulose ester filters of Millipore. The membranes were incubated on agar for 16 to 24 hours at 37 deg. C. RAPID *E. coli* 2 Agar of BIO-RAD is used.

Influent samples were diluted 10 to 1000 times (depending on initial spiking) and 100 μl to 1000 μl of the diluted sample was filtered in duplicates through the membrane filter (see Figure 31 for an example of results).



Figure 31. *E. coli* result for 0.5 ml of influent sample diluted 10 times

Samples of 100 ml of the effluent from the filters with silver were filtered through the membrane filter (see Figure 32 for an example of results), while only 1 ml going up to 10 ml was filtered from the filters without silver.



Figure 32. *E. coli* results for 1, 10 and 100 ml duplicate effluent samples from B4 P5 without silver application (*E. coli* are purple and coliforms are blue)

More information on the *E. coli* testing methodologies used can be found in Appendices II and III.

The *E. coli* testing procedure used for the first batch series (B4 to B18) was adapted for the second batch series as technical problems arose.

Well water was initially used for the *E. coli* testing and it was passed through a UV-disinfection system was used (Figure 33) to provide bacteria-free water. Problems started at the beginning of the monsoon season when the well water became highly contaminated from the surface water entering the well. To overcome this problem, rain water (passing through the UV-disinfection system) was then used instead of well water.



Figure 33. UV treated rain water used in the *E. coli* test

Another issue was that, as the number of pots to be tested increased, the volume of influent increased too (sometimes up to 110 L) and was spiked with still small volumes (3 to 5 ml) of concentrated *E. coli* suspended in Tryptic Soya Broth (TSB) and was mixed for at least 15 minutes. Eight liters of this influent volume was poured in each filter to be tested, but the *E. coli* concentration was not well/evenly distributed, resulting in too different influent *E. coli* concentrations. For the second set of batches (B23 to B26), the *E. coli* was re-suspended in water or 0.1 % peptone water and the concentration of bacteria estimated by spectrophotometry. This estimation of 1 OD being proportional to a concentration of 1E8 cfu/ml is not very accurate; and, as a result the spiked influents varied in concentration between 1E3 (or 1000) and 1E4 cfu/ml; but results seem to indicate that influent *E. coli* concentrations are not correlated to LRVs.

2.5 Long-term Test

A long term flow rate test was done over the course of two months. The aim of this test was to investigate the rate of clogging of filters of five different porosities. Flow rate testing was done on a daily basis (except for weekends) on two same-batch filters of the first batch series (i.e. 2xB7, 2xB18, 2xB13, 2xB4 and 2xB17). All filters were painted with silver nitrate. To emulate field conditions, the filters were loaded with 20 L/day of locally available turbid water. Pond water was used for the first 400 L and (less turbid) well water was used for the next 360 L. The filters were scrubbed when the flow rate fell below 1 L/hr.

The pond water was fetched from a nearby pond (Figure 34), pumped into a 500 L vessel and transported back to the testing facilities for the week.



Figure 34. Pumping of pond water for the long-term flow rate test

For the long-term flow rate test, pond water was transferred from the vessel into 20 L bottles (Figure 35) and the turbidity recorded. Turbidity values can vary a lot depending on how much it rained before sampling. Well water is available at the testing facilities via pipeline and pumping.



Figure 35. Filling up 20 L bottles for the long-term flow rate test

The 20 L bottles are placed on each filter as shown in Figure 36 and the flow rate is measured by: (1) opening the taps at all ten receptacles; (2) recording the weights of 10 empty buckets; (3) when water starts coming out of the faucets, the empty buckets are placed under them, starting to collect the filtrate while starting the stop-watch. After one hour, all faucets are closed and the buckets are weighed. The flow rate is the weight of the wet bucket minus the weight of the empty bucket.



Figure 36. Set-up for the long-term flow rate test

2.6 Strength test

The aim of this protocol is to find the modulus of rupture of a sample, which is an inherent characteristic of the material. It doesn't depend on the form of the sample, only on the material. The first step is to put a localized charge on a cylindrical sample until it breaks, and the raw data is the load when break point is reached. The second step is to insert all the data about the sample, the test and the break load (in Newton) into an equation which leads to the modulus of rupture, in MPa (Mega Pascal).

This particular test is designed only for ceramic and cylindrical samples. If a sample cannot be broken with the maximum load, another sample can be made with a lower thickness. The variable tested is the break load. It is the load in Newton that can be put on the center of a sample before it breaks. It can be easily deduced from the mass added to break the sample.

For this test it is important to protect your eyes (the face if possible) and the body. Indeed when samples break small fragments are cast around at high speed. Facial mask or at least glasses, and a lab coat are very important. The equipment is composed of the mechanical test device and the steel weights.

The experimental steps are as follow:

1. Four discs are cut from the bottom of the filter and half a batch (i.e. 3 filters) were sacrificed for this test in order to have a sample size of 12 (Figure 37 and 38).



Figure 37. Marking discs on the bottom section of a filter after the walls were broken down



Figure 38. Ohm Mon from RDIC helping to cut the ceramic discs

- The discs are labeled (Batch No. / Pot No. / Sample No.) and brought to the GERES facilities (Figure 39). Using a caliper, two perpendicular diameters and four thicknesses were precisely measured and recorded in an Excel spreadsheet, and the center of the disc was marked to help position the load cylinder in the middle of the sample.



Figure 39. Ceramic discs made from B21 P6, P1, P4 and P5

A total of nine batches of samples were tested at GERES:

- The first 5 batches (B23, B24, B25, B21 and B26) were all been fired up to 885°C but varied in the ratio rice husk to clay, and therefore in porosity (the higher the rice husk content the higher the porosity).
- The next 3 batches (B14, B20 and B19) all contain 9.7kg of rice husks per 30kg of clay but were fired up to different maximum temperatures.
- The last batch (B12) contain 9.7kg rice husk per 30kg clay, has been fired at 885C, but contain only rice husk particles between 0.5 and 1mm, instead of all particles below 1mm. 2 samples cut out from normal RDIC water filters have been tested as a control test.

A description of the batches is summarized in Table 1 below.

Table 1. Description of batches made for the three sets of experiments

	Batch code	Number of samples	Description
<i>Rice husk quantity variation</i>	B23/B22	16	9.7kg rice husk/30kg clay
	B24	12	11kg rice husk/30kg clay
	B25/B9	12	12kg rice husk/30kg clay
	B21/B8	20	13kg rice husk/30kg clay
	B26	8	14kg rice husk/30kg clay
<i>Maximum firing temperature variation</i>	B14	4	Fired up to 685C
	B20	8	Fired up to 800C
	B19	8	Fired up to 950C
<i>Rice husk size variation</i>	B12	8	0.5mm<Particles size<1mm
<i>Control sample</i>	RDIC	2	Samples from regular RDIC filters

3. A support is put under the long lever to facilitate the next stage when the sample is put on the three little balls so that the charging module is exactly in the middle of the sample (figure 40)

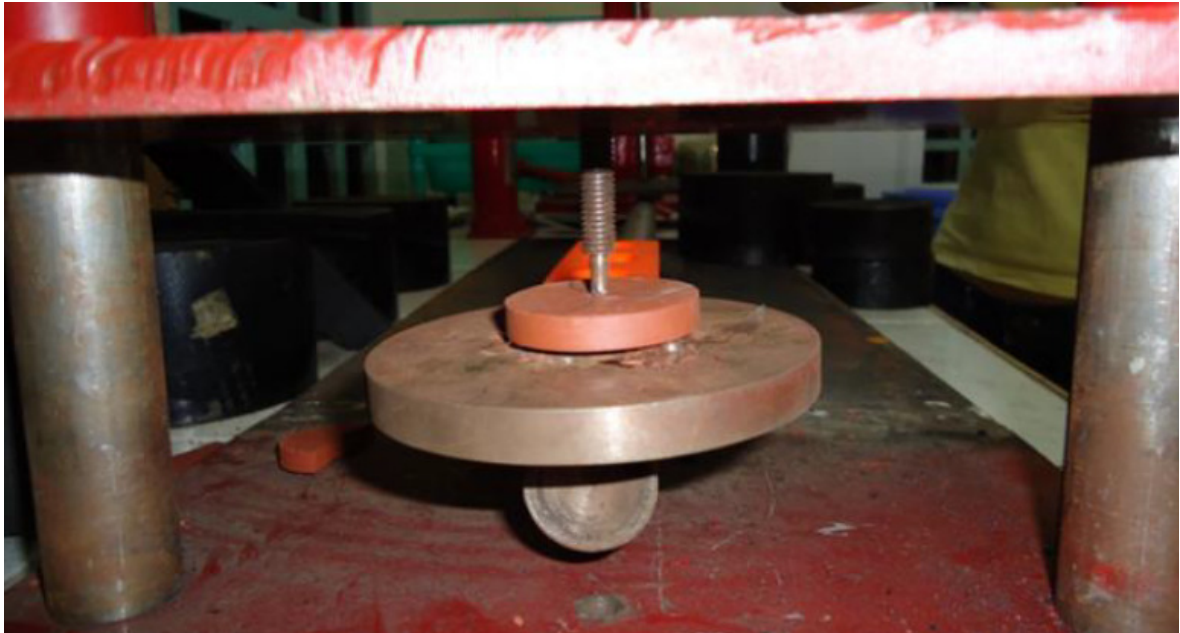


Figure 40. Positioning of the ceramic disc on the support

4. Using the bubble level, the horizontality of the lever is checked (Figure 41).



Figure 41. Bubble level check

5. The steel weights are put on the plate (Figure 42), little by little (500g. step size), until the last one added make the sample break (the lighter the last weight is, the more precise the measurement will be).



Figure 42. Gradual loading of the lever plate with steel weights

6. Note the final load in kg, and then convert it into Newton. Remove the charge from the plate and then clean the pieces of broken sample for the next test.

7. The variable measured in this test is the Modulus of Rupture (MOR), which is an inherent characteristic of the material, i.e. it does not depend on the sample shape. A specific device is used to apply a 4-point flexural strength to the sample until failure. The mass applied at failure point is recorded and the MOR of each sample is calculated using this mass as well as parameters of the sample (diameter and thickness) and of the device (loading pin diameter and supporting pins spacing). For each batch, the average MOR of all samples is calculated.

The modulus of rupture can then be calculated as per the following equation:

$$\sigma = \frac{3F}{4\pi e^2} \left\{ (1-\nu) \left[1 + \ln\left(\frac{a}{\Theta}\right)^2 + \left(\frac{a}{\Theta}\right)^2 \right] - (1+\nu) \ln\left(\frac{b}{\Theta}\right)^2 - \left(\frac{1-\nu}{2}\right) \left(\frac{b}{\Theta}\right)^2 \right\}$$

With:

$F=9.8*(\text{final charge in kg} * 5 + 25.6)$

F: break charge in N.

ν : Poisson coefficient (no unit, usually 0.3 for ceramics).

Θ : Diameter of the cylindrical sample in mm.

a: Diameter of inferior support (given by the 3 little balls) in mm (32 mm).

b: Diameter of charge zone in mm (3 mm).

e: Thickness of the cylindrical sample in mm.

σ : Modulus of rupture in MPa

The seeked value is σ , which is an inherent characteristic of the material, and never depends on dimensions.

The Coefficient of Variation (COV= Standard Deviation / Average) gives an idea of the precision of the results. It should be lower than 20% for the results to be reliable.

3.0 Results

The effect of (1) increasing the rice husk quantity in the clay mix, (2) increasing the size of rice husk particles, and (3) changing the maximum firing temperature on flow rate, log-reduction of bacteria (with and without silver nitrate application) and strength was investigated

3.1 Rice husk quantity variations

Six standard (RDI-recipe) pots were made from 9.7 kg rice husk, 30 kg of clay and 1 kg of laterite. In this research the rice husk concentration was increased to 11, 12, 13 and 14 kg in order to increase the porosity of the pots. For every batch, six pots were mixed, pressed and fired. The combination of these six pots are called a batch (same composition, same firing curve). One set of batches (30 pots), the first batch series, was made in the dry season and another (duplicate) set of batches, the second batch series, was made in the wet season. The results are compared in this section.

The raw data for this set of experiments can be found in Appendices IV, V and VI.

3.1.1 Flow rates of the first and second batch series

The flow rates for the first batch series without silver are shown in Table 2.

Table 2. Average flow rates for the first batch series

First batch series					
kg rice husk per batch	Batch	Average flow rate (LPH)	Min. (LPH)	Max. (LPH)	St. dev. (LPH)
9.7	B7	2.997	2.397	3.293	0.334
11	B18	7.836	6.615	9.161	0.963
12	B13	11.453	10.365	12.425	0.728
13	B4	14.463	13.658	15.758	0.724
14	B17	16.861	14.111	18.969	1.682

Pots with increased rice husk in their clay mix have consistently higher flow rates; indeed, pots with 1.23 times more rice husk (12 kg) than standard pots (9.7 kg) have flow rates 3.8 times higher on average than standard pots, and pots with 1.44 times more rice husk (14 kg) than standard pots (9.7 kg) have flow rates 5.6 times higher on average than standard pots.

The flow rates for the second batch series without silver are shown in Table 3.

Table 3. Average flow rates for the second batch series

Second batch series					
kg rice husk per batch	Batch	Average flow rate (LPH)	Min. (LPH)	Max. (LPH)	Standard deviation
9.7	B23	7.361	7.172	7.455	0.146
11	B24	10.833	9.942	11.815	0.729
12	B25	18.583	14.440	22.313	3.582
13	B21	18.720	16.522	21.485	2.269
14	B26	22.840	21.542	24.742	1.381

It is interesting to note that the average flow rates of the second set of batches are consistently higher than the first set by 58 % on average (see Figure 43). This could be due to a number of reasons such as different rice husk quality (particle size distribution) and water uptake.

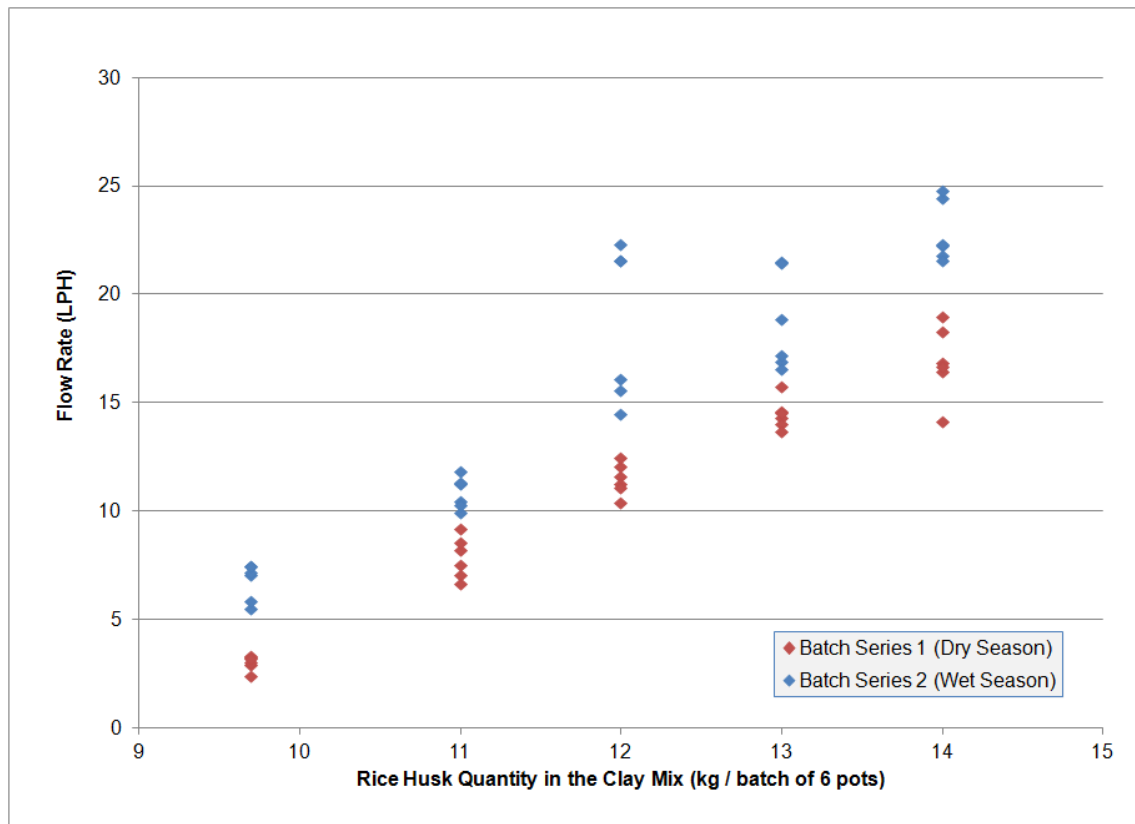


Figure 43. Influence of the amount of rice husk on the flow rate of the pot. The two series of batches are produced with different rice husk. Batch series 2 were made using rice husks having a larger proportion of larger particle sizes compared to Batch series 1.

Pots from the second batch series were painted with silver nitrate and tested for flow rate a few days after the silver impregnated pots had dried. The results are presented in Table 4.

Table 4. Comparison of flow rates pre versus post silver nitrate application

Pot ID	kg rice husk per batch	Flow rate pre Ag app.	Flow rate post Ag app.	Percentage difference
B23 P5	9.7	7.172	5.948	-17.1
B23 P6	9.7	7.455	6.199	-16.8
Average (B23)	9.7	7.314	6.074	-16.950
B24 P1	11	10.453	9.134	-12.6
B24 P2	11	11.243	9.542	-15.1
B24 P3	11	11.312	11.628	2.8
B24 P4	11	11.815	10.293	-12.9
B24 P5	11	9.942	9.400	-5.4
B24 P6	11	10.235	10.418	1.8
Average (B24)	11	10.833	10.069	-6.900
B25 P5	12	16.055	11.280	-29.7
B25 P6	12	22.313	10.782	-51.7
Average (B25)	12	19.184	11.031	-40.700
B21 P1	13	16.868	13.840	-18.0
B21 P3	13	21.485	13.805	-35.7
B21 P4	13	18.814	15.070	-19.9
B21 P5	13	21.451	17.965	-16.3
B21 P6	13	17.178	14.361	-16.4
Average (B21)	13	19.159	15.008	-21.260
B26 P5	14	24.742	19.706	-20.4
B26 P6	14	21.542	20.254	-6.0
Average (B26)	14	23.142	19.980	-13.200

After silver nitrate application, the pots have lower flow rates. From Table 3, flow rates of pots with silver are 17 % lower on average than without silver (Figure 44). It is possible that the lower flow rates after silver application are due to the silver solution clogging the surface pores.

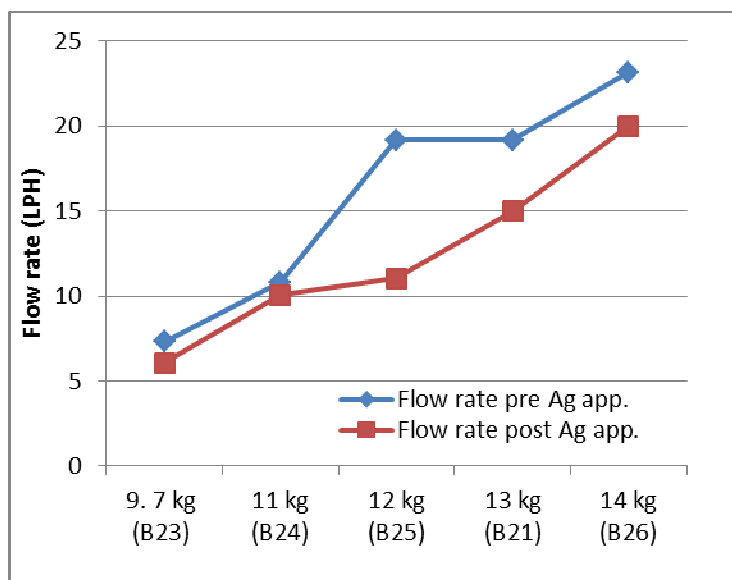


Figure 44. average flow rates of filters of different porosities before and after silver application

3.1.2 LRV's of *E. coli* of the first and second batch series with and without silver

The LRV's of bacteria (*E. coli*) for the first set of batches without silver are shown in Table 5.

Table 5. LRV's for the first batch series

First batch series						
kg rice husk per batch	Batch	n	Average	Min.	Max.	St. dev.
9.7	B7	4	2.985	2.123	4.181	0.951
11	B18	3	4.374	4.003	5	0.545
12	B13	4	4.006	3.631	4.296	0.295
13	B4	3	3.167	2.881	3.47	0.295
14	B17	5	3.757	3.546	3.952	0.184

There is no obvious decrease in the *E. coli* reduction effectiveness with increasing porosity and flow rate for the first batch series (see Figure 45). Batch 13 pots (13 kg rice husk), for example, have almost the same LRV's (3.167 on average) than Batch 7 (9.7 kg rice husk) (2.985 on average).

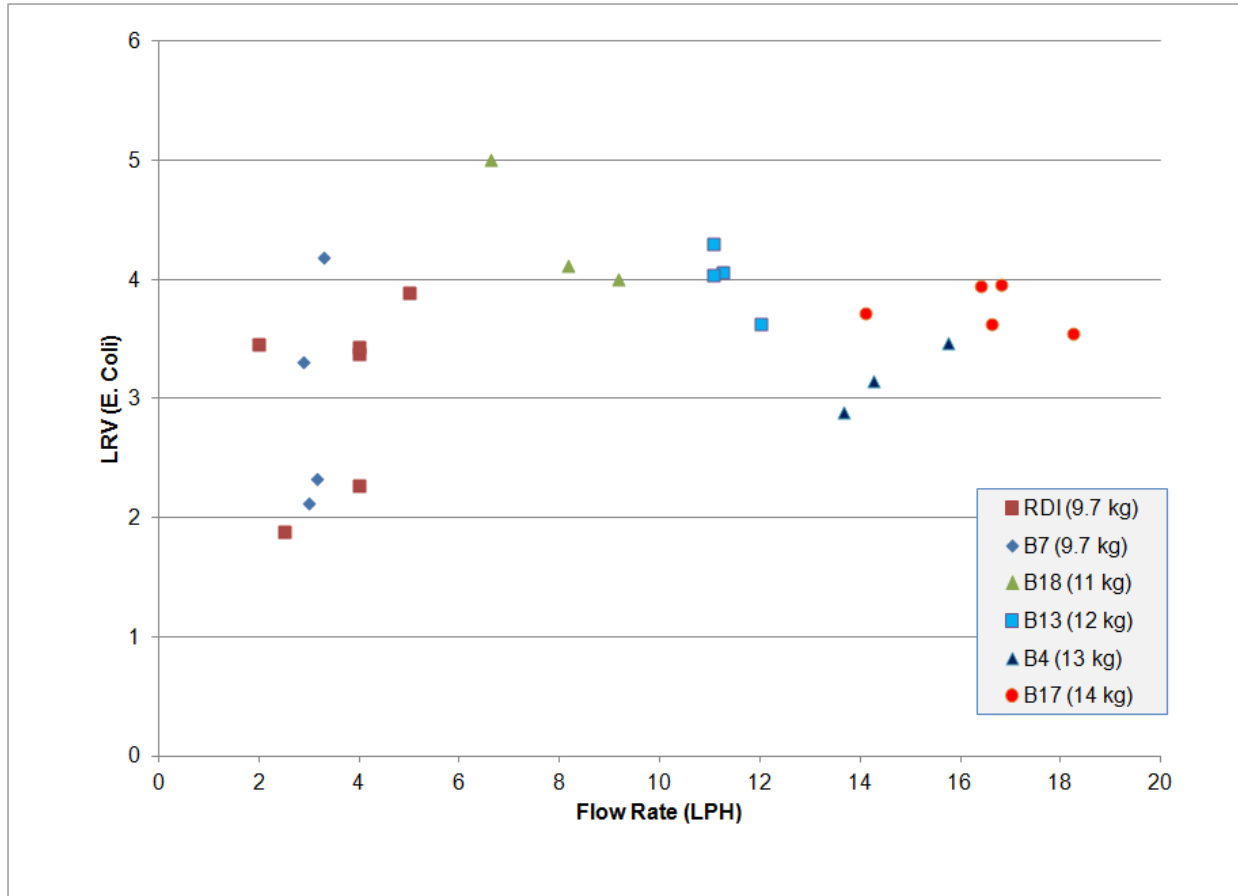


Figure 45. LRV's of *E. coli* versus flow rates for filters of different porosities from the first batch series

In order to analyze the data sets more clearly, box-and-whisker plots and statistical summary table are used (Figure 46 and Table 6)

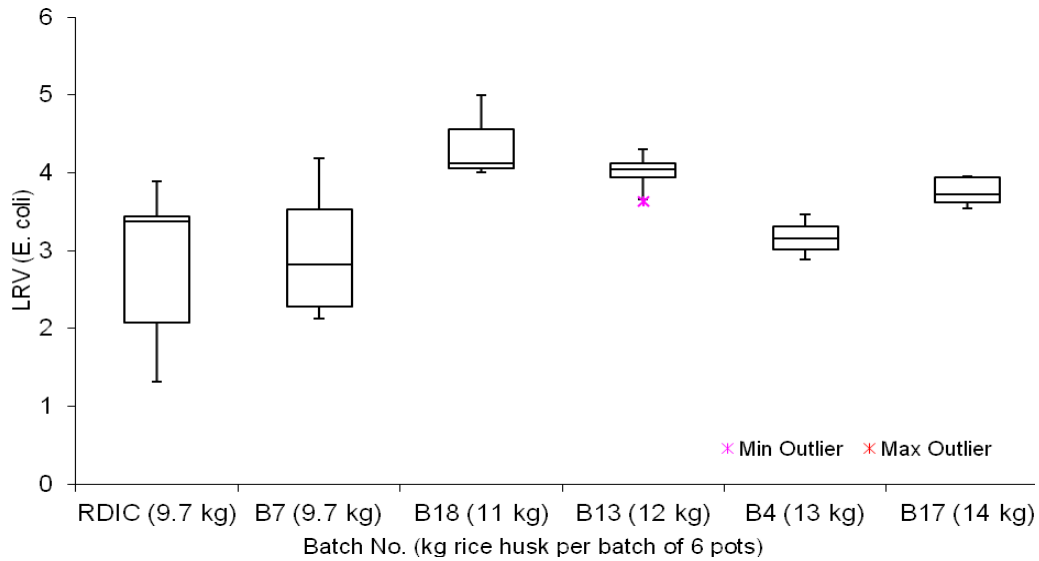


Figure 46. Box-and-whisker plots of LRV's for filters from RDI and the first batch series with increased quantity of rice husk in the clay mix

Table 6. Statistical Summary Table for LRV's for filters from the first batch series

Labels	RDIC (9.7 kg)	B7 (9.7 kg)	B18 (11 kg)	B13 (12 kg)	B4 (13 kg)	B17 (14 kg)
Min	1.311	2.123	4.003	3.631	2.881	3.546
Q ₁	2.0805	2.27525	4.061	3.9355	3.0155	3.625
Median	3.376	2.818	4.119	4.049	3.15	3.722
Q ₃	3.4435	3.52775	4.5595	4.11975	3.31	3.941
Max	3.893	4.181	5	4.296	3.47	3.952
IQR	1.363	1.2525	0.4985	0.18425	0.2945	0.316
Upper Outliers	0	0	0	0	0	0
Lower Outliers	0	0	0	1	0	0

When plotting the LRV's of *E. coli* against the quantities of rice husks used in the clay mix, there does not appear to be (linear) correlation. Indeed, the Pearson correlation coefficient, r (flow rates, LRV's), is 0.196, which is much closer to 0 than 1.

The formula for the Pearson (product moment) correlation coefficient, r , is:

$$r = \frac{\sum(x - \bar{x})(y - \bar{y})}{\sqrt{\sum(x - \bar{x})^2 \sum(y - \bar{y})^2}}$$

where x and y are the sample means AVERAGE(array1) and AVERAGE(array2). In this case, Array 1 = LRVs (*E. coli*), and Array 2 = Flow rates.

The LRVs of bacteria (*E. coli*) for the second set of batches without silver are shown in Table 7.

Table 7. LRVs for the second batch series

Second batch series						
kg rice husk per batch	Batch	n	Average	Min.	Max.	St. dev.
9.7	B23	6	2.069	1.365	3.281	0.8
11	B24	8	2.927	1.163	4.886	1.3
12	B25	4	2.192	1.272	4.231	1.4
13	B21	10	2.411	1.295	4.284	1.0
14	B26	4	2.179	1.286	3.338	1.0

As observed for the first batch series, there is also no obvious decrease in the *E. coli* reduction effectiveness (see Figure 47) with increasing porosity and flow rate for the second batch series. Batch 26 pots (14 kg rice husk), for example, have almost the same LRV's (2.179 on average) than Batch 23 (9.7 kg rice husk) (2.069 on average).

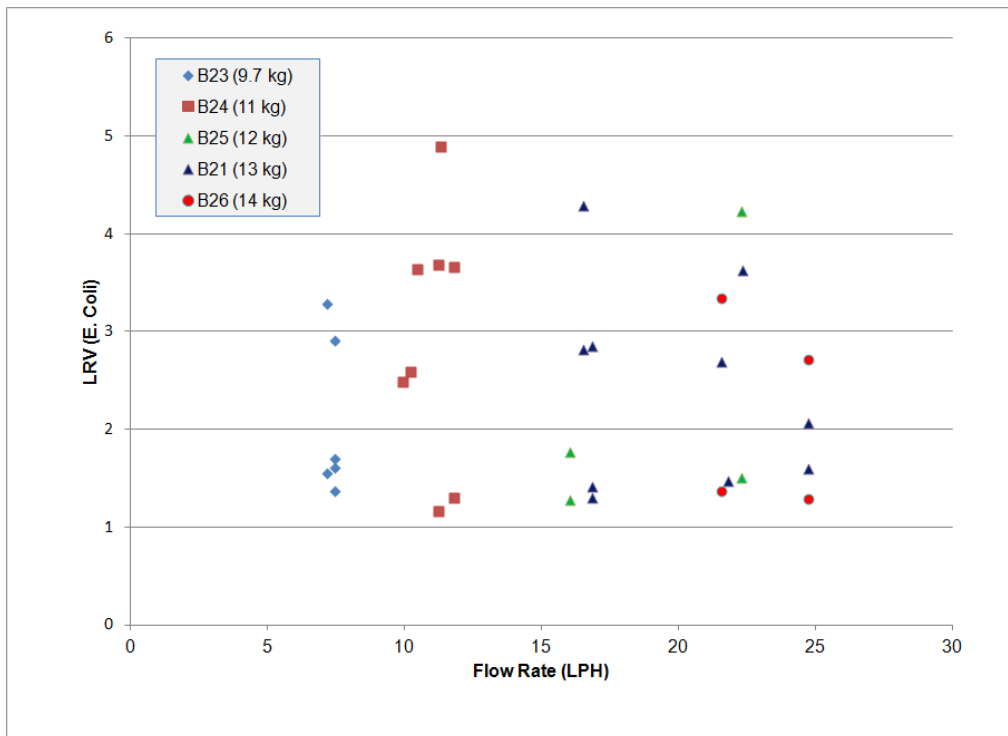


Figure 47. LRV's of *E. coli* versus flow rates for the second batch series (increasing the quantity of rice husk in the clay mix)

The box-and-whisker plots (Figure 48) and statistical summary table (Table 8) are used to show the data sets more clearly.

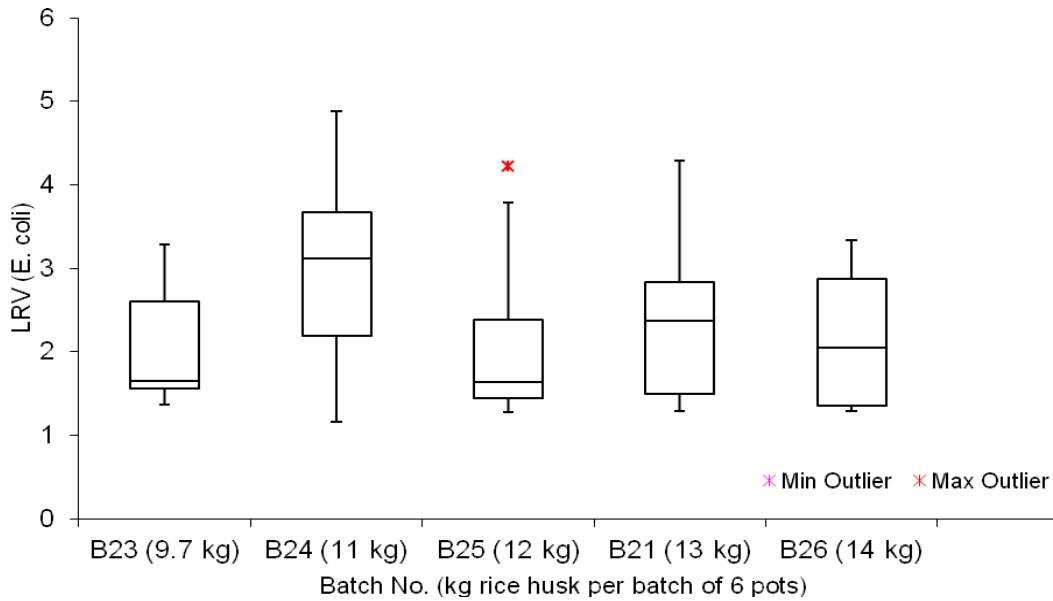


Figure 48. Box-and-whisker plots of LRV’s versus flow rates for filters from RDI and the second batch series with increased quantity of rice husk in the clay mix

Table 8. Statistical Summary Table for LRV’s for filters from the second batch series

Labels	B23 (9.7 kg)	B24 (11 kg)	B25 (12 kg)	B21 (13 kg)	B26 (14 kg)
Min	1.365	1.163	1.272	1.295	1.286
Q ₁	1.565	2.1905	1.44525	1.502	1.3505
Median	1.6535	3.1135	1.633	2.375	2.0455
Q ₃	2.60525	3.666	2.38	2.83925	2.87375
Max	3.281	4.886	4.231	4.284	3.338
IQR	1.04025	1.4755	0.93475	1.33725	1.52325
Upper Outliers	0	0	1	0	0
Lower Outliers	0	0	0	0	0

The Pearson correlation coefficient, r (flow rates, LRV’s), which is -0.056 , is very close to 0 and confirms that there is no correlation between the two datasets.

There is more variability in the LRV results for the second batch series, which could be due to the different rice husk kind and more specifically to the proportion of larger size particles. This could not be proved due to resource limitations: only two size meshes – 0.5 and 1 mm – were available for particle size distribution analysis.

A sensitivity analysis was done to determine how much error in the LRV results can be attributed in the variation in influent *E. coli* concentrations. The analysis proves that this error is very small, the average difference between possible minimum and maximum LRVs being only 0.196 LRV. The detailed calculations can be found in Appendix VII.

Some filters from the second batch series were painted with silver nitrate and tested for *E. coli*. The results are shown in Table 9.

Table 9. LRV's of pots from the second batch series before and after silver nitrate application

Pot ID	kg rice husk per batch	LRV (<i>E. coli</i>) pre Ag app.	LRV (<i>E. coli</i>) post Ag app.
B23 P5	9.7	2.415	5.178
B23 P6	9.7	1.895	> 7 (0 cfu/100 ml)
B24 P4	11	2.482	5.604
B24 P1	11	3.639	6.954
B24 P2	11	2.425	> 7 (0 cfu/100 ml)
B25 P5	12	1.518	> 7 (0 cfu/100 ml)
B25 P6	12	2.867	> 7 (0 cfu/100 ml)
B21 P1	13	1.853	> 7 (0 cfu/100 ml)
B21 P4	13	1.471	> 7 (0 cfu/100 ml)
B21 P3	13	3.627	> 7 (0 cfu/100 ml)
B26 P5	14	2.003	6.324
B26 P6	14	2.179	> 7 (0 cfu/100 ml)

Pots without silver have an average LRV of *E. coli* of 2.328 whereas the same filters impregnated with silver have much higher LRVs, i.e. higher than 7.2 (and might be even higher). These results support the theory that silver nitrate does indeed play an important role in improving the filter efficacy.

3.1.3 Strength test results for the second batch series with silver

The summarized results for silver-impregnated filters from the second set of batches are introduced in Table 10.

Table 10. Strength testing results for filters with different porosities

Batch ID	Quantity of rice husks in clay mix (kg)	No. of samples (n)	Average MOR (MPa)	Coefficient of variation (%)
B23	9.7	16	2.4	21
B24	11	11	1.78	17
B25	12	12	1.59	8
B21	13	17	1.3	9
B26	14	4	1.27	29

The box-and-whisker plots (Figure 49) show that there is a clear correlation between the increasing quantity of rice husks in the clay mix and the decreasing modulus of rupture (MOR) values.

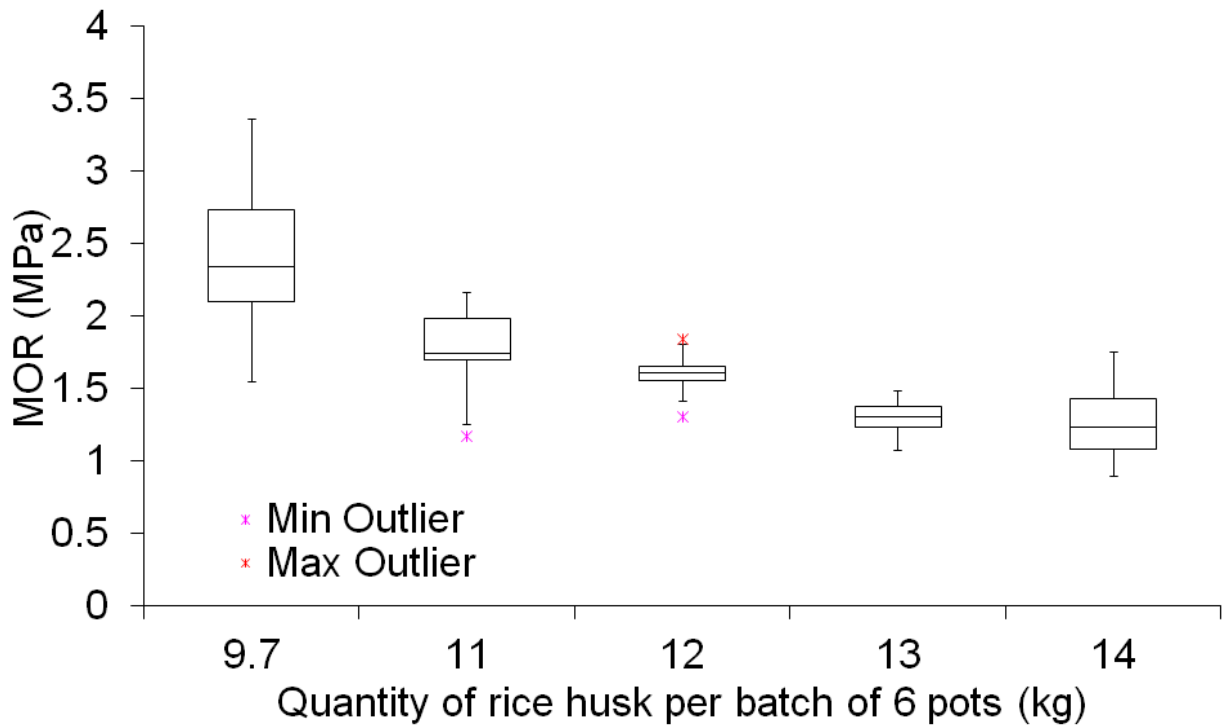


Figure 49. Box-and-whisker plots of the MOR for pots of different porosities

This strong correlation is confirmed by the Pearson correlation coefficient, r (MOR, quantity of rice husk), which is -0.957, very close to -1.

3.2 Maximum firing temperature variations

Changing the maximum firing temperature shows what happens when changing the pore size distribution instead of the porosity of the filter. Three batches of pots were made of the same composition as RDIC pots (30 kg of clay, 9.7 kg of rice husk, 1 kg of laterite and water per batch) and fired up to three different maximum firing temperatures: 685; 800 and 950 deg. Celsius. The flow rate, LRV of *E. coli* and strength results are presented in this section.

The raw data for this set of experiments can be found in Appendix VIII.

3.2.1 Flow rates

The flow rates of the filters (without silver) fired at different maximum temperatures are shown in Table 11.

Table 11. Flow rates for filters fired at different maximum firing temperatures

Batch	Max. firing temp. (deg. C)	Average flow rate (LPH)	Min. (LPH)	Max. (LPH)	St. Dev. (LPH)
B14	685	2.324	2.033	3.035	0.411
B20	800	3.760	2.440	5.431	1.226
B23	885	6.735	6.076	9.681	0.862
B19	950	8.004	5.485	7.455	1.449

Figure 50 shows that there is a strong correlation between maximum firing temperature and flow rate after 800 deg. C.

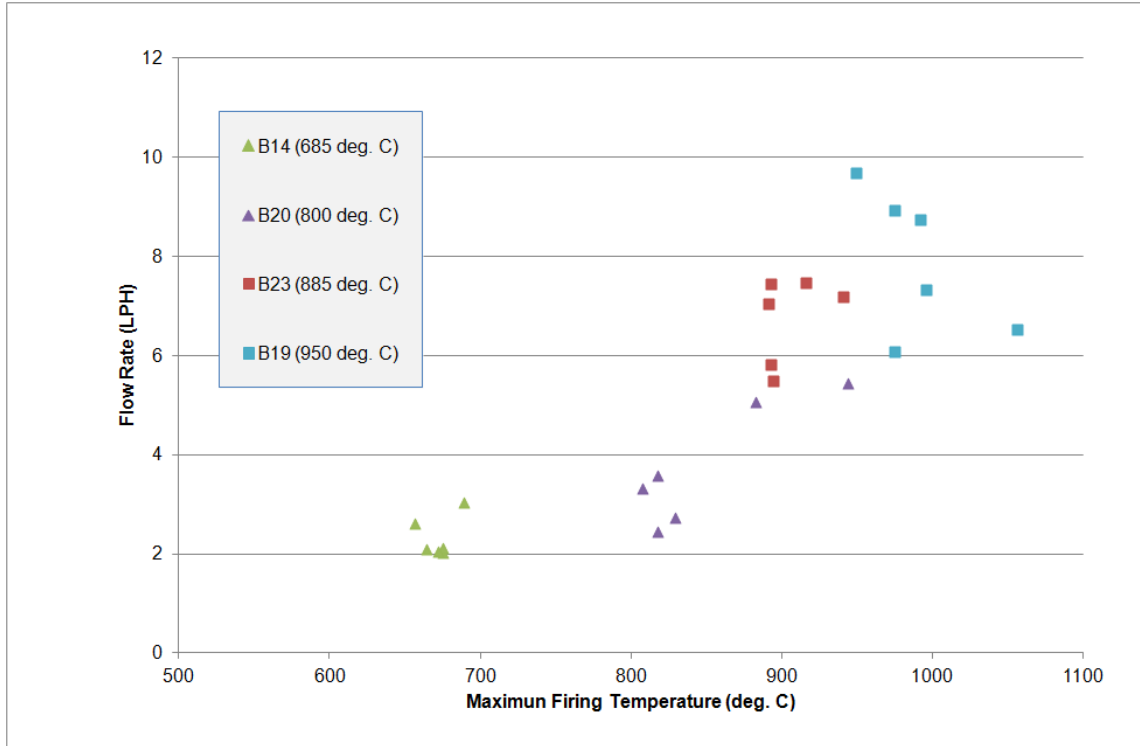


Figure 50. The maximum firing temperature influences pore size and therefore flowrate too.

When increasing the maximum firing temperature from 800 to 950 deg. C., the average rate of the pot increases from 3.8 to 8.0 LPH.

3.2.2 LRVs of *E. coli* for filters fired at different maximum firing temperatures

The LRVs of *E. coli* are presented in Table 12 and are plotted against flow rate values in Figure 51.

Table 12. Statistical summary of the LRV (*E. coli*) results for pots without silver fired at different maximum firing temperatures

Batch	Max. firing temp. (deg. C)	n	Average LRV	Min. LRV	Max. LRV	St. Dev. (LRV)
B20	800	9	2.251	1.095	4.974	1.287
B23	885	6	2.069	1.365	3.281	0.811
B19	950	11	1.890	0.779	3.192	0.908

Filters fired up to 800, 885 and 950 deg. C. have average LRVs of *E. coli* of 2.251, 2.069 and 1.890, respectively.

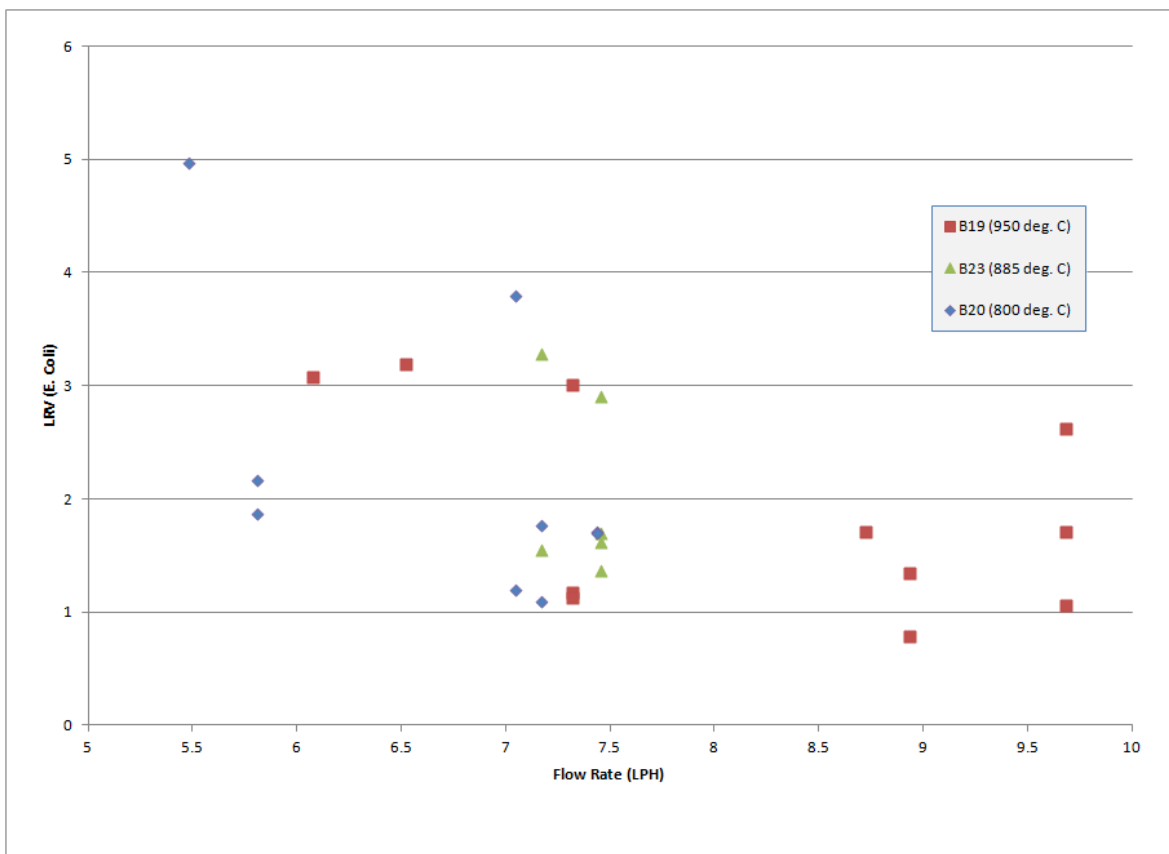


Figure 51. LRVs of *E. coli* versus flow rates for maximum firing temperature variation experiments without silver

Results indicate that increasing flow rates by increasing the maximum firing temperature (hence the pore sizes) from 800 to 1000 deg. C. has a slight tendency to negatively affect the bacterial removal efficacy: the average LRV's for B20 (800 deg.C), B23 (885 deg.C) and B19 (950 deg.C) are 2.251, 2.069 and 1.890, respectively. However, this is not very clear from Figure 52 and Table 13. The Pearson correlation coefficient r is -0.454.

The mean pore diameters of the filter samples were measured in the Technical University of Delft in the Netherlands by mercury intrusion porosity (MIP) tests. The mean effective pore sizes for batches 20 (fired up 800 deg. C.), 23 (fired up to 885 deg. C.) and 19 (fired up to 950 deg. C.) are 27.76 μ m, 28.91 μ m and 30.63 μ m, respectively. Those results show a small increase in the filter's pore size with increasing maximum

firing temperatures, resulting in the higher flow rates. Detailed MIP results can be found in Appendix IX.

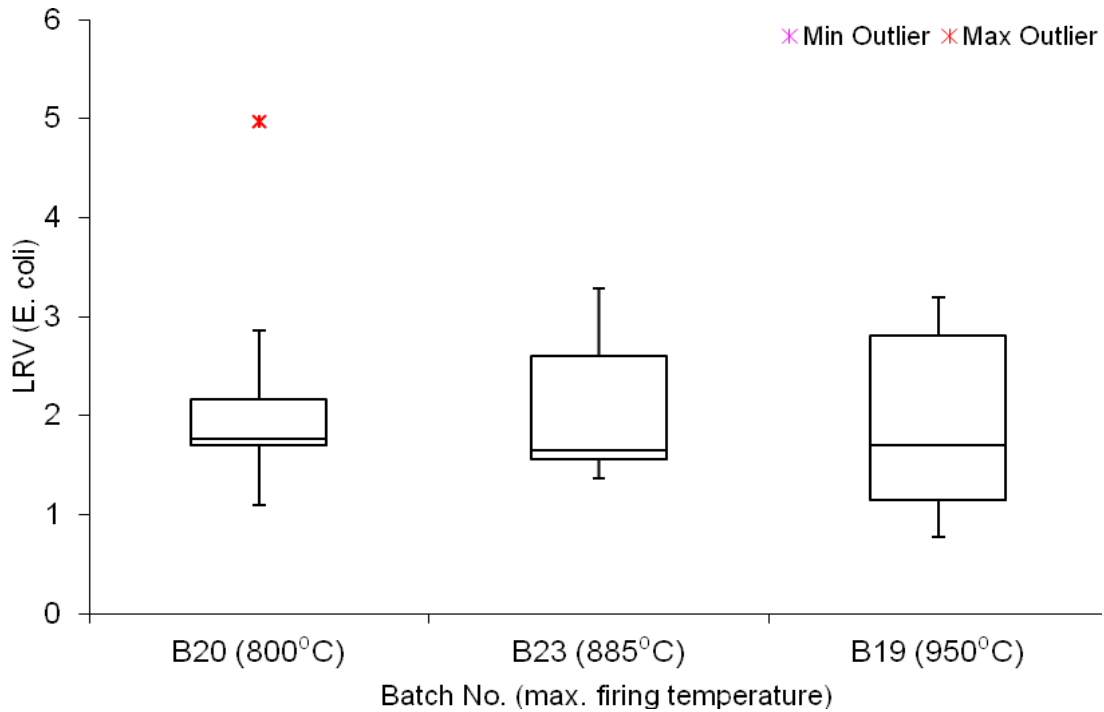


Figure 52. Box-and-whisker plots of the LRV's of *E. coli* of pots fired at different maximum firing temperatures

Table 13. Statistical Summary Table for LRV's of filters fired at different maximum firing temperatures

Labels	B20 (800°C)	B23 (885°C)	B19 (950°C)
Min	1.095	1.365	0.779
Q ₁	1.702	1.565	1.147
Median	1.764	1.6535	1.707
Q ₃	2.165	2.60525	2.811
Max	4.974	3.281	3.192
IQR	0.463	1.04025	1.664
Upper Outliers	2	0	0
Lower Outliers	0	0	0

3.2.3 Strength test results of the filters with silver

The summarized strength test results for the second set of batches are introduced in Table 14 (see detailed results in Appendix X).

Table 14. Strength testing summary results for filters with different maximum firing temperatures

Batch ID	Max. firing temp. (deg. C.)	Number of samples (n)	Average modulus of rupture (MPa)	Coefficient of variation (%)
B14	685	6	1.08	18
B20	800	3	1.86	10
B23	885	16	2.40	21
B19	950	7	2.81	20

The strength results can be plotted against the maximum firing temperature (Figure 53).

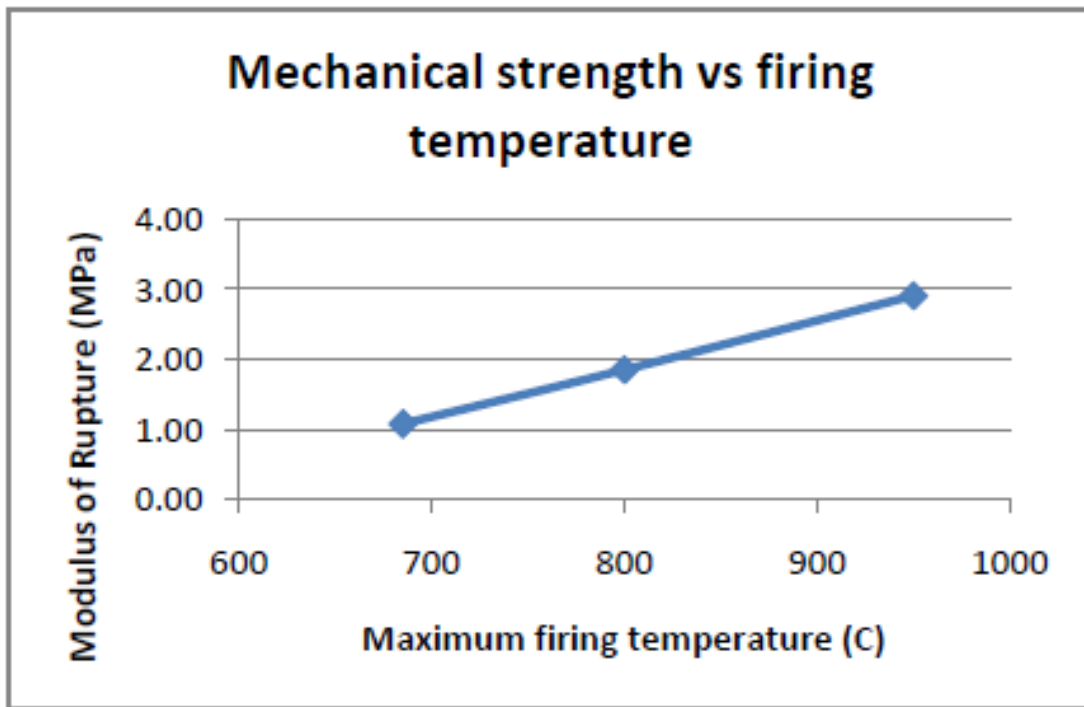


Figure 53. MOR versus maximum firing temperature

Increasing the maximum firing temperature between 800 and 950 deg. C. increases the strength of the filter.

3.3 Rice husk particle size variations

In this section, three batches are compared. The quantity of rice husk is the same for all three batches, resulting in the same porosity. Batch 7 was manufactured during the first series with the lower flow rates. Batch 23 was fired during the second series. Batch 12 was produced with rice husks of 0.5 to 1 mm in size. This rice husk size was obtained after an extra sieving step with a sieve of 0.5 mm. The remaining rice husk on the sieve was used and the fines (< 0.5 mm) were discarded.

The raw data for this set of experiments can be found in Appendix XI.

3.3.1 Flow rates for filters with various rice husk particle sizes

The flow rates of the pots with different rice husk particle sizes are shown in Table 15.

Table 15. Flow rates for filters with rice husk of different sizes

Batch	Rice husk quantity and size	Average flow rate (LPH)	Min. (LPH)	Max. (LPH)	St. dev. (LPH)
B12	9.7 kg [0.5 - 1 mm]	10.106	12.288	9.303	1.2
B23	9.7 kg < 1 mm (wet season)	6.735	5.484	7.455	0.3
B7	9.7 kg < 1 mm (dry season)	2.997	2.397	3.293	0.9

The flow rate can clearly be increased by increasing the size of the burn-out material particles in the clay mix. Indeed, Batches 7 and 23 (made of 9.7 kg of rice husk of particle size below 1 mm) have an average flow rate of 2.997 LPH (in the dry season) and 6.735 LPH (in the wet season), whereas Batch 12 (made of 9.7 kg of rice husk of particle size between 0.5 and 1 mm), the average flow rate is increased to 10.106 LPH.

The mean pore diameters of the filter samples were measured in the Netherlands by mercury intrusion porosity (MIP) tests. Increasing the rice husk particle size from [0-1] mm (Batch 23) to [0.5-1] mm (Batch 12) increased the mean effective pore sizes from 28.91µm to 32.28 µm.

In the next section, the effect of this increase in the rice husk particle size (thus pore size) on the LRV's of *E. coli* will be examined.

3.3.2 LRV's of *E. coli* for filters with various rice husk particle sizes

The LRV's of *E. coli* for filters of B12, 7 and 23 are presented in Table 16 and Figure 54.

Table 16. LRV's of *E. coli* for filters with different rice husk sizes

Batch	Rice husk quantity and size	Average LRV	Min. LRV	Max. LRV	St. dev.
B12	9.7 kg [0.5 - 1 mm]	0.720	0.585	1.074	0.17
B23	9.7 kg < 1 mm (wet season)	1.668	0.811	3.281	0.92
B7	9.7 kg < 1 mm (dry season)	2.985	2.123	4.181	0.95

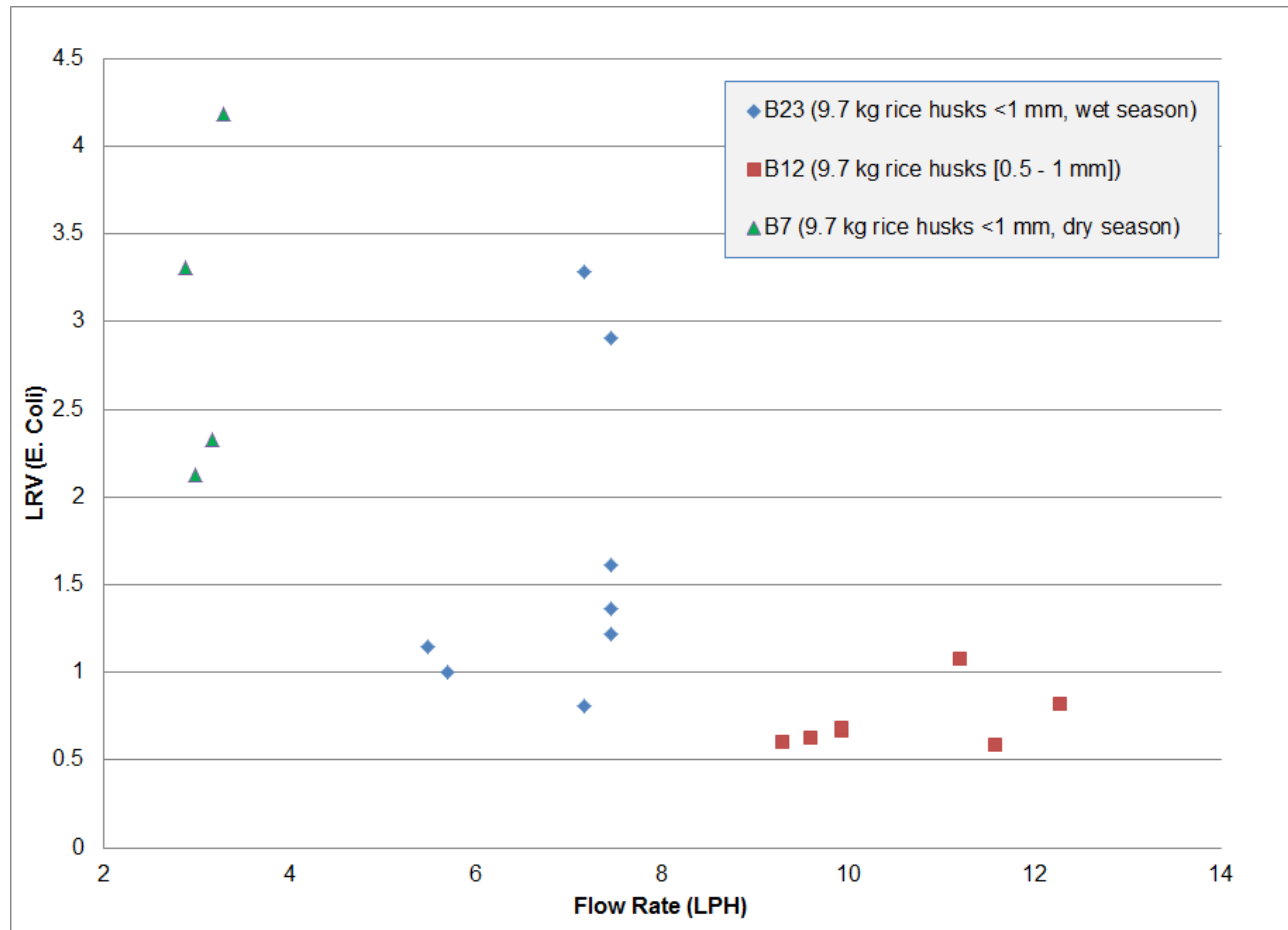


Figure 54. LRVs versus flow rates for rice husk size variation experiments

The larger rice husk particles result in larger pores in the clay wall and therefore in higher flow rates. Unfortunately, the disinfection capacity of the pot filter is decreasing with increasing the proportion of bigger pores. Indeed, the average LRV falls from 2.985 (for Batch 7) and 1.668 (for Batch 23) to 0.720 (for Batch 12).

The Box-and-whisker plots and statistical summary are shown in Figure 55 and Table 17.

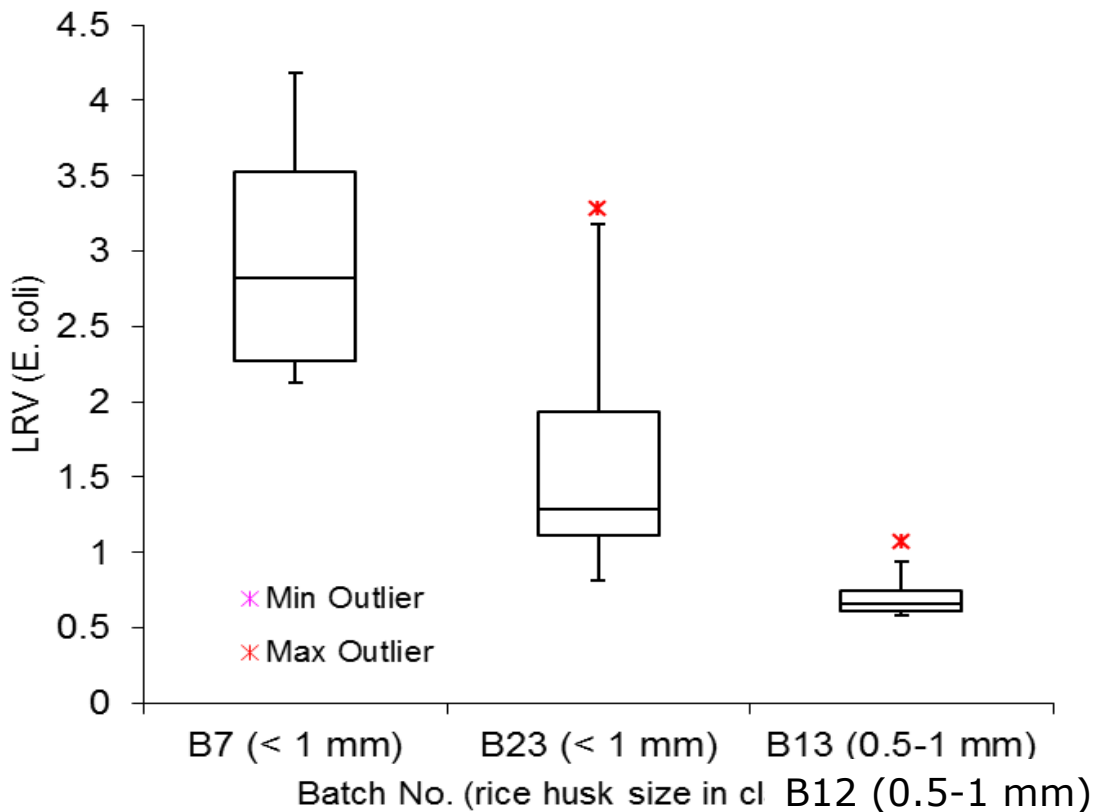


Figure 55. Box-and-whisker plots of LRVs for pots with different rice husk particle sizes

Table 17. Statistical Summary (LRV versus rice husk particle size)

Labels	B7 (< 1 mm)	B23 (< 1 mm)	B12 (0.5-1 mm)
Min	2.123	0.811	0.585
Q ₁	2.27525	1.1095	0.613
Median	2.818	1.291	0.662
Q ₃	3.52775	1.937	0.745
Max	4.181	3.281	1.074
IQR	1.2525	0.8275	0.132
Upper Outliers	0	1	1
Lower Outliers	0	0	0

The Pearson correlation coefficient $r(\text{LRV of } E. coli, \text{ flow rate})$ value of -0.998 being very close to -1 confirms the indication that the two data sets are very strongly correlated. Increasing the flow rate by increasing the rice husk particle size negatively affects the filter's ability to filter out bacteria.

It was suspected that the difference in flow rates between the wet and dry seasons might be due to the different rice husk quality since RDIC ordered their rice husks from a different provider. Samples of rice husks from the dry and wet seasons were analyzed in the laboratory in the Netherlands. Results show a difference in the particle size distribution curves. The details of the analysis can be found in Appendix XII.

3.3.3 Strength test results for filters with silver

Results show that the MOR decreases when the size of the rice husk used in the clay mix is increased. B12 pots (having particle sizes between 0.5 and 1 mm) have an average MOR of 1.34 MPa whereas B23 / B22 pots (particle size less than 1 mm) have an average MOR of 2.40 MPa, almost twice higher than B12.

In Figure 56, the results are shown in the form of a statistical summary.

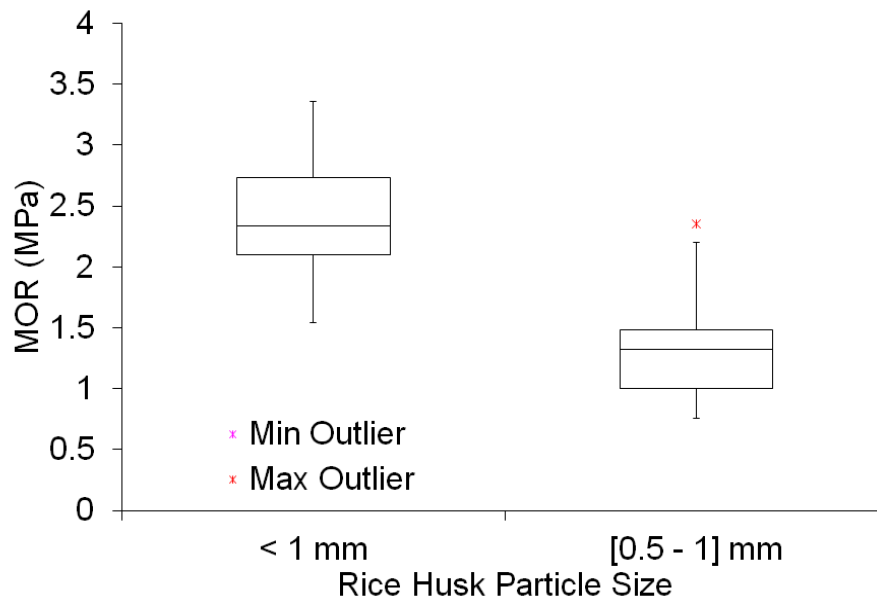


Figure 56. Box-and-whisker plots of the MOR's of pots with different rice husk particle sizes

There is a clear correlation between the distribution of the rice husk particle sizes and the MOR. The larger the rice husk used in the clay mix, the weaker the filter.

3.4 Long-Term Flow Rate Testing

A long-term (two-month) flow rate test was done on two same-batch filters for all the first batch series (B7 to B17). In the first month, very turbid pond water was first used as feed water. In the second month, the feed water was changed to less turbid well water. The pots were scrubbed when the flow rate fell below 1 L/hr.

The raw data for this set of experiments can be found in Appendices XIII and XIV.

3.4.1 Highly turbid feed water

From the 28th of June to the 31st of July 2011, very turbid pond water was used as influent. The turbidities for this water source ranged from 12.9 to 199 NTU (with an average of 67.1 NTU). Flow rate results over time are shown in Figure 57.

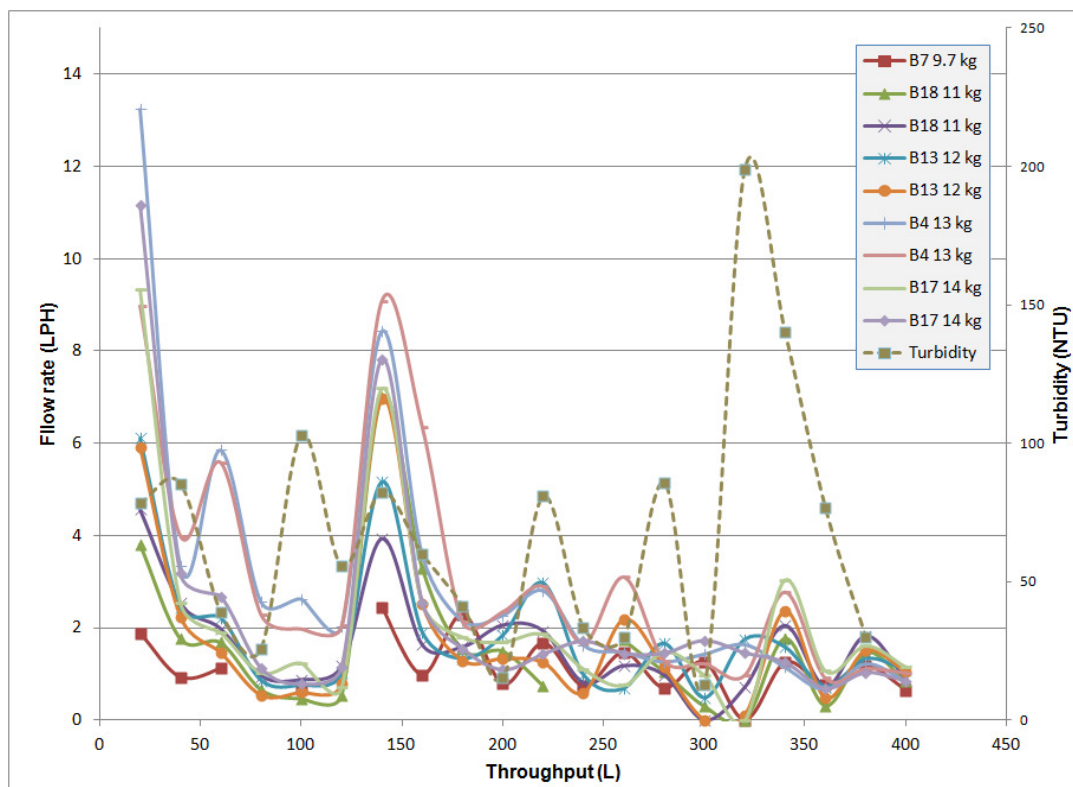


Figure 57. Long-Term Flow Rate results using very turbid pond water of turbidity 12.9 to 199 NTU

As expected, the higher the turbidity of the feed water, the faster the rate of clogging. The flow rates of all filters decreased very rapidly when the pot were fed with very turbid

water, and within a week, the flow rates of pots with 9.7 to 12 kg of rice husk fell below 1 LPH while the flow rates of pots with 13 to 14 kg of rice husks stayed just above 1 LPH.

Rapid clogging is not desirable because the user will have to scrub the filter to restore flow rates and is likely to contaminate or break the filter in this process. The less the pots are handled the better since, as Murphy, Sampson, McBean and Farahbakhsh (2008) demonstrated, contamination of water storage containers occurs through inappropriate household practices (e.g. improper cleaning and moving of the filter).

For this reason, the experiment was reset. All filters were scrubbed and thereafter filled with less turbid (well and pond) water (with turbidity no higher than 30 NTU) on a daily basis, as described in the next sub-section.

3.4.2 Less turbid feed water

From the 1st of August to the 1st of September, less turbid well water was used as influent. The turbidities (shown in the dotted line in Figure 58) for this water source ranged from 2.84 to 27.1 NTU (with an average of 11.697 NTU). Flow rate results over time are shown in Figure 58.

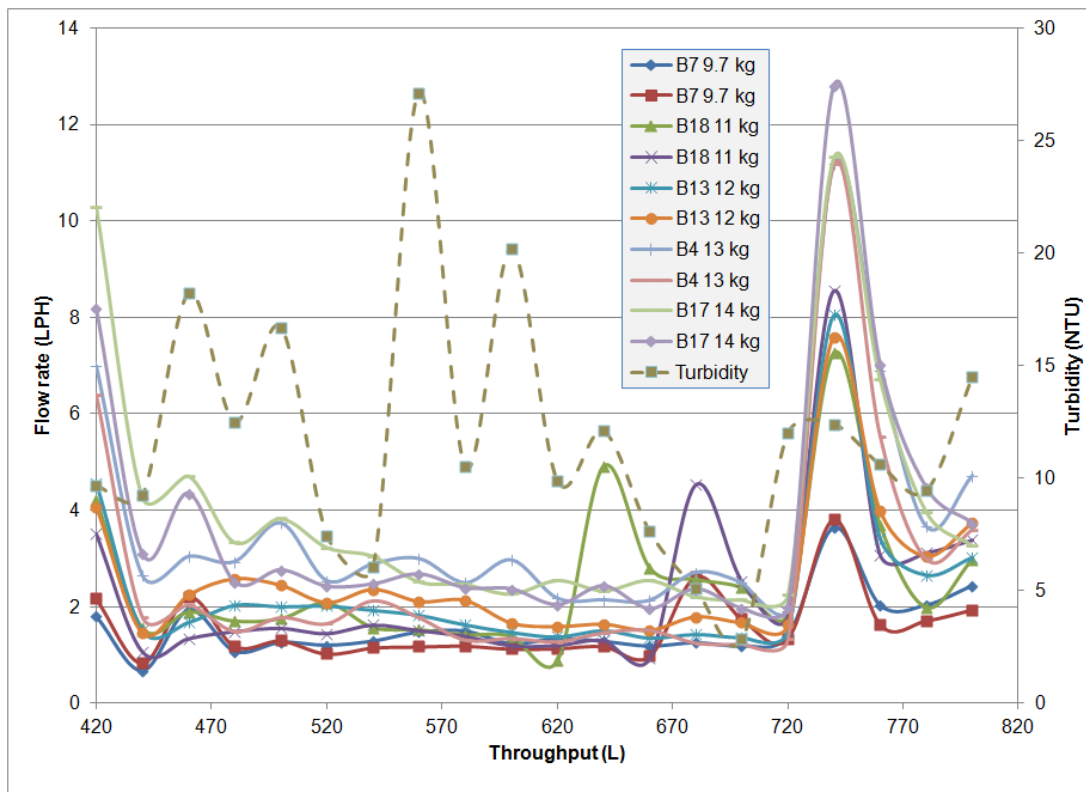


Figure 58. Long-Term Flow Rate results using well water of turbidity 2.84 to 27.1 NTU

Figure 58 shows that the clogging rate is not as steep as in Figure 57. After about a month of feeding the filters almost every day, the flow rate of pots with 9.7 to 12 kg of rice husk falls below 2 LPH while the flow rate of pots with 13 and 14 kg of rice husk is still maintained above 2 LPH.

Table 18 compares flow rates after scrubbing events. After scrubbing all filters for the first time about a week after silver nitrate was applied, the high flow rates were restored (5/7/2011). However, the second scrubbing event (1/8/2011) seems to indicate that the inner pores were partially clogged as the flow rates were lower than previously.

Table 18. Flow rates right after scrubbing events

Date	28/06/11 (initial flow rate after silver app.)	5/7/2011 (after scrubbing)	1/8/2011 (after scrubbing)	15/9/2011 (after scrubbing)
Feed water	Pond water	Pond water	Well water	Well water
B7 (9.7 kg)	1.13	4.079	1.8	3.651
B7 (9.7 kg)	0.928	2.445	2.168	3.812
B18 (11 kg)	1.77	6.996	4.208	7.261
B18 (11 kg)	2.535	3.942	3.512	8.555
B13 (12 kg)	2.43	5.171	4.564	8.048
B13 (12 kg)	2.24	6.969	4.073	7.594
B4 (13 kg)	3.341	8.434	6.993	11.191
B4 (13 kg)	3.993	9.086	6.399	11.194
B17 (14 kg)	2.547	7.189	10.29	11.321
B17 (14 kg)	3.174	7.816	8.171	12.802
Turbidity	85.4	82.4	9.7	12.4

At the end of the two-month test period, no biofilm was observed on the filter surfaces. It is possible that the silver nitrate application helped by inhibiting biological growth.

When using less turbid well water ($2.7 < \text{NTU} < 27.1$), pots with 9.7 – 11 kg already had flow rates less than 2 LPH to start with. Pots with 12 – 13 kg of rice husks maintained flow rates > 2 LPH throughout the second month testing period and only had to be scrubbed 2 times. Pots with 14 kg of rice husks always managed to maintain flow rates > 2 LPH throughout the whole month.

From Figure 59, it is clear that the higher the porosity of the pot, the lower the rate of clogging. Pots with 13 and 14 kg of rice husks only had to be scrubbed twice in the one month testing period whereas pots with 9.7, 11 and 12 kg of rice husks had to be scrubbed six, five and four times, respectively.

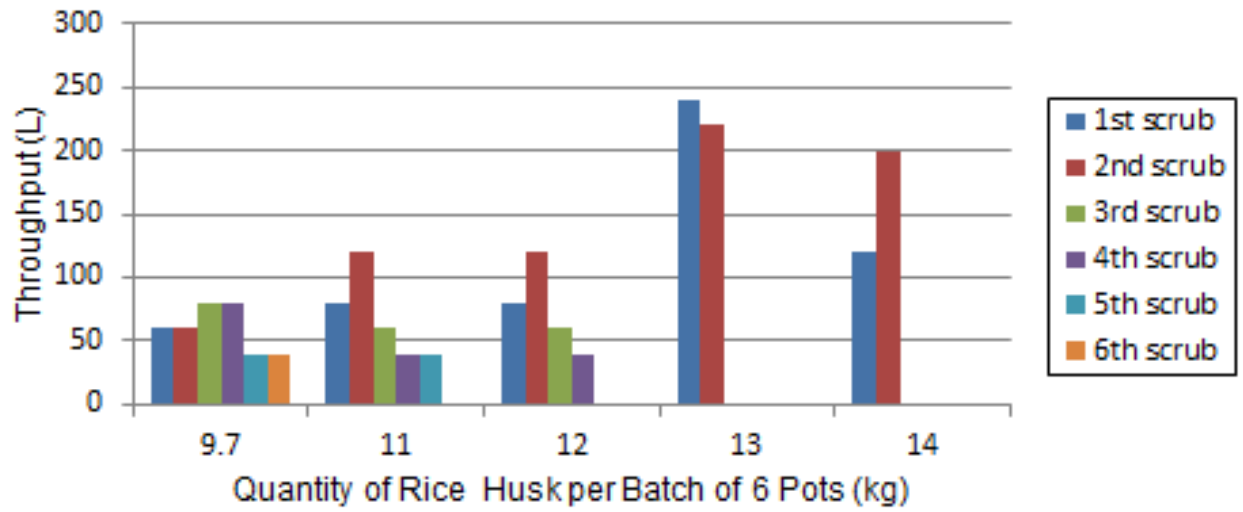


Figure 59. Maximum throughput before flow rate becomes less than 1 LPH and the pot has to be scrubbed

4. Discussion

This chapter aims to provide a discussion of results obtained from this study.

4.1 Raw Material Characteristics

4.1.1 Clay and Laterite (TCKI)

Samples of the clay and laterite from RDIC used for the research were sent to TCKI in order to investigate their characteristics. The analysis can be found in Appendix I. TCKI determined the particle size distribution (percentage of fine particles and concentration of coarse and fine sand) of both materials as well as the specific surface area and chemical composition of the clay.

4.1.2 Rice husk

RDIC changed rice husk provider in April, so the first series of batches (B7 to B17) used the rice husk kind from before April 2011 whereas the second series (B23 to B26) used the rice kind from after April 2011. A rough particle size distribution of the rice husk pre- and post-April was done for comparison and understanding of how it could affect flow rates and filtration effectiveness. The results (see Table 19 below) show that there is a small decrease in the proportion of particles less than 0.5 mm (or a small increase in the proportion of particles in the range [0.5 – 1] mm).

Table 19. Rough particle size analysis of the rice husk samples pre- and post-April

	<0.5 mm	[0.5 - 1] mm	< 1 mm	> 1 mm	Total
Before April 2011	0.6	0.394	0.994	0.006	1 kg
	60	39.4	99.4	0.6	100 %
After April 2011	0.569	0.428	0.997	0.003	1 kg
	56.9	42.8	99.7	0.3	100 %
Percentage difference	-0.031	0.034	0.003	-0.003	kg
	-3.1	3.4	0.3	-0.3	%

It is possible that the large difference in flow rate between the first batch series and the second batch series is due to a different rice husk quality and, more specifically, to a larger proportion of larger rice husk particles (e.g. a larger proportion of particles just

below 1 mm). A more accurate particle size analysis of the rice husk samples was performed in the Netherlands (see Appendix XII) and the curves are compared in Figure 60 below. Surprisingly enough, it appears that, although the rice husks sample from May 2011 has more lower-size particles, it also has less bigger-size particles. It was expected that the larger fractions in rice husks are better represented in May than in January, but in fact the opposite was found.

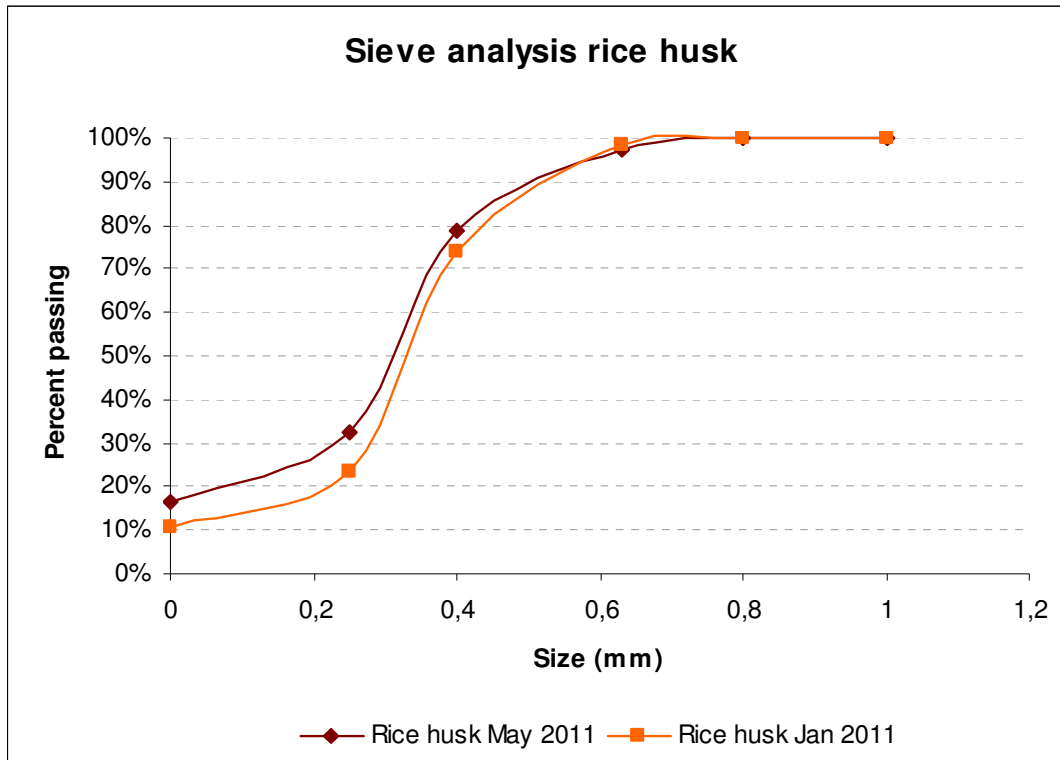


Figure 60. Particle size analysis of the rice husk samples from RDI Cambodia taken in January and May 2011

4.2 Rice Husk Quantity Variations

In theory, the LRV of bacteria is expected to stay the same at higher porosities (Bloem, 2008), and the results are supporting this theory. At the same maximum firing temperature, the pore size is assumed to be the same, but the number of pores is increased, thereby increasing the flow rate per pot (while the flow rate per pore is still the same).

After application of silver, there are no countable bacteria in 100 ml of raw effluent samples. This test needs to be continued in a long-term study to ensure that such high flow rate pots are safe to be used throughout their lifetime.

The biggest concern is that there could be direct pathway via cracks, increasing the probability of having direct routes or passageways through the filter cross-section. For the highest flow rate pots, however, this was not remarked in this research so far. Eventually, control measures can be put in place, for example, by setting a safe flow rate range (e.g. 18 – 19 LPH for pots made of 12 kg of rice husk per batch).

4.3 Maximum Firing Temperature Variations

When the maximum firing temperature is increased (between 800 and 1000 deg. C.), the pore size increases and so the flow rate also increases. But this increase of the flow rate results in a small decrease of the LRV of bacteria.

When the maximum firing temperature is increased, the shape and size of the pores in the clay matrix and clay texture undergo such changes that the clay pores can no longer filter out bacteria as effectively. Van Halem (2006) mentioned that only the interconnected pores contribute to the flow rate; however, the unglazed clay is not completely impervious (the terracotta is porous as well) and isolated and open ended pores will also contribute to the flow rate (but to a smaller extent).

From TCKI's clay analyses (see Appendix I), the clay used in this research is predominantly siliceous and lacking in carbonates, i.e. 59 % SiO₂ and 21 % Al₂O₃ (incl. CaO). It has a higher concentration of phyllosilicates (i.e. clay minerals) than clays rich in carbonates (calcite and dolomite with a micritic and sparitic texture) (Van Wijck 2011). Figure 61 below extracted from a study of the Influence of mineralogy and firing temperature on the porosity of bricks refers to this clay type as Type G (Cultrone et al. 2003), supports these research results and the theory that, from 800 and 1000 deg. C.), the percentage of larger pores in the clay matrix increases, thereby letting more bacteria pass through the filter.

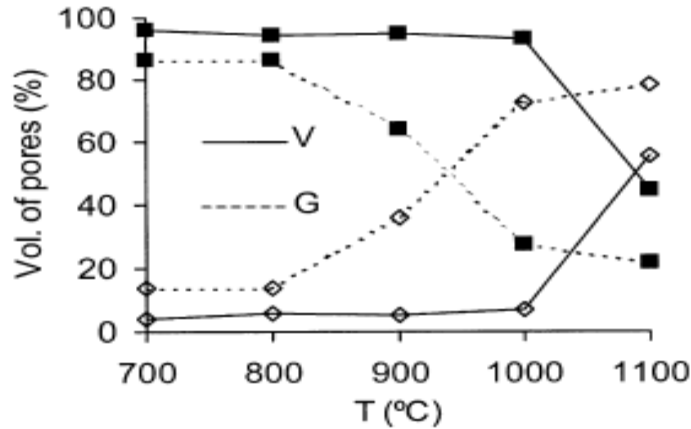


Figure 61. Representative diagrams of the pore size distribution (vol.%) of the G and V bricks with respect to T (deg. C). Legend: dark squares =<1 mm pore radius; white diamonds =>1 mm pore radius. (Cultrone et al. 2003)

The pore sizes of the clay matrix (and flow rates) increase up to about 1000 deg. C. and then decrease when the clay reaches the stage of vitrification whereby the spaces between refractory particles become completely filled up with glass, fusing the particles together and making the clay body impervious to water. This observation is confirmed by the set of figures in Appendix XV (taken from Cultrone et al. 2003), i.e. the clay porosity and pore interconnectivity increases up to 1000 deg. C. and then decreases as the process of vitrification starts.

4.4 Rice Husk Particle Size Variations

There appeared to be a strong correlation between the size of the rice husks used in the clay mix and the bacteria filtration effectiveness. The increase in pore size results in higher flow rates and lower LRV's.

The flow rate is very sensitive to the pore sizes of the filter. Indeed, for laminar, non-pulsatile fluid flow through a uniform straight pipe, the flow rate F (volume per unit time) is proportional to the fourth power of the pore radius. This is given by Poiseuille's Equation:

$$F = \Delta P \pi r^4 / 8 \eta l$$

where r is the inner radius of the tube (or the pore radius in the case of the filter), ΔP is the pressure difference between the two ends of the tube ($P_1 - P_2$), η is the coefficient of viscosity of the fluid and l is the length travelled.

4.5 Reproducibility

Two triplicate batches were made to check reproducibility of the flow rates:

- B9 (dry season), B13 (dry season) and B25 (wet season) were made of 12 kg of rice husks per batch; and
- B7 (dry season), B22 (wet season) and B23 (wet season) were made of 9.7 kg of rice husks per batch.

The flow rates of B9, B13 and B25 pots are compared in Table 20.

Table 20. Comparison of the flow rates for triplicate batches 9, 13 and 25

12 kg RH	Flow rates of B9 (LPH) (dry season)	Flow rates of B13 (LPH) (dry season)	Flow rates of B25 (LPH) (dry season)
P1	11.022	11.562	21.566
P2	10.294	10.365	14.440
P3	12.138	11.264	21.545
P4	11.396	12.026	15.580
P5	8.593	11.073	16.055
P6	12.39	12.425	22.313
Average	10.972	11.453	18.583

The flow rates of B7, B22 and B23 pots are compared in Table 21.

Table 21. Comparison of the flow rates for triplicate batches 7, 22 and 23

9.7 kg RH	Flow rates of B7 (LPH) (dry season)	Flow rates of B22 (LPH) (wet season)	Flow rates of B23 (LPH) (wet season)
P1	2.882	5.485	6.862
P2	2.397	5.812	5.484
P3	3.257	7.435	5.690
P4	2.985	7.05	5.073
P5	3.293	7.172	Broken pot
P6	3.168	7.455	5.875
Average	2.997	6.735	5.797

The average flow rates of the second set of batches from the wet season were higher than the first set. This could be due to a number of reasons such as different rice husk quality (particle size distribution) as discussed before.

This difference in flow rates between the wet and dry seasons was also thought to be caused by the moisture content of the rice husks. As the rice husks have higher moisture content in the wet season, the weight (density) is higher. As a result, less burn-out material is added to the mixture during the wet season. This seems an important quality control issue; however, the results from this study indicated the opposite, i.e. that flow rates from filters manufactured in the wet season (second batch series) had higher flow rates than the ones manufactured in the dry season (first batch series).

4.6 Clogging test

This two-month flow rate test was useful to get an idea of the effect of the rate of clogging of the pots when fed with water of different levels of turbidity; however, it is recommended that further testing be done to evaluate the long-term effectiveness of silver-painted pots of higher porosity in terms of bacteria reduction and flow rates. In order to perform this test adequately, the filters would need to be re-filled every single day, including in the weekends, in order to emulate field conditions.

4.7 Strength test

The strength test results for all three sets of experiments are introduced in Table 22.

Table 22. Strength test summary results for all three sets of pots

	Batch code	Average Modulus of Rupture (MPa)	<i>Coefficient of Variation</i>
<i>Rice husk quantity variation</i>	B23/B22	2.40	21%
	B24	1.78	17%
	B25/B9	1.59	8%
	B21/B8	1.30	9%
	B26	1.27	29%
<i>Maximum firing temperature variation</i>	B14	1.08	18%
	B20	1.86	10%
	B19	2.91	20%
<i>Rice husk size variation</i>	B12	1.34	39%
<i>Control sample</i>	RDIC	4.55	21%

Several remarks can be made from these results:

- It can be concluded from the MOR of the five first batches of samples that the higher the porosity of a sample, the lower its mechanical resistance.

- On the other hand, the result of the three last batches show that the higher the firing temperature, the higher the MOR. It can therefore be concluded that porosity diminishes the mechanical resistance of ceramic samples while a high firing temperature will increase it.

The Coefficient of Variation of most batches is high, which indicates a lack of homogeneity between the samples of a batch. It can be explained by the fact that samples given varied widely in shape and dimensions, and that some samples had large cracks on their sides, which may result in accelerated failure and can be a source of error. Moreover, the number of samples given for some batches was limited; a minimum of 10 samples is generally required to give a precise enough value. Results therefore have to be used warily, mainly for a comparative purpose. More standard samples would have given more homogenous and precise results.

It is interesting to see that RDIC filter samples were much stronger (MOR = 4.55 MPa) than filter samples of the same composition made for the research (MOR = 2.40 MPa). In Dr. Derek Chitwood's recent (2011) studies, the pug mill was also able to increase cracking point to about 9% increase over normal operation. It is assumed that the pug mill (Figure 62) is able to compress and remove air pockets from the clay cubes before pressing much better than manually.



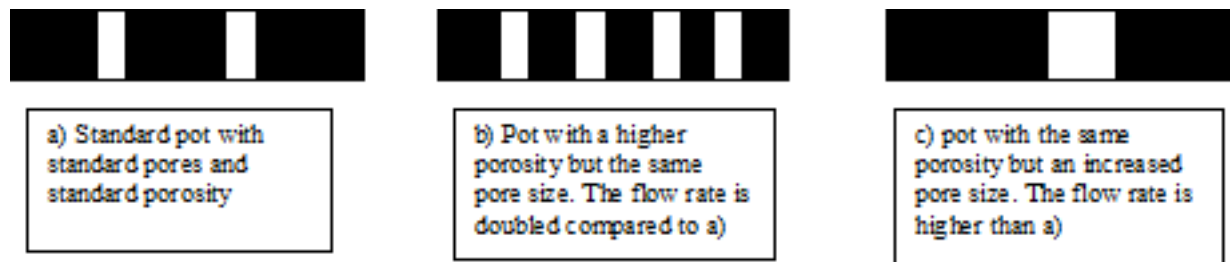
Figure 62. Pug mill donated to RDIC in November 2010

5.0 Conclusions

It appeared that the flow rate of the pot could be increased in two ways: (1) by increasing the porosity of the filter, by increasing the quantity of burn-out material (rice husk in this case) in the clay mix; and (2) by increasing the pore size. The pore size can be changed by either changing the particle size distribution of the burnout material or by changing the maximum firing temperature.

A higher flow rate is of course beneficial because of the larger water production, especially because the pot filters are clogging during use (the clogging rate depending on the water quality). A higher initial flow rate can prolong the operational lifetime of the pot before cleaning.

According to theory, a higher flow rate achieved by increasing porosity does not result in a decrease in the bacteria removal effectiveness, but larger pore sizes can have a negative effect on the filtering quality. The difference is explained in the figure below, where the flow rates of b) and c) are both increased compared to a); but in the case of the increased pore size c), the disinfection capacity of the filter pot is in danger.



Increasing flow rates by increasing maximum firing temperatures (at the same clay mix composition) seems to result in some small reduction in the *E. coli* reduction effectiveness; however increasing the quantity of rice husks in the clay mix (keeping the maximum firing temperature constant) does not seem to correlate in a drop in the *E. coli* reduction effectiveness. This observation confirms Sophie Bloem's 2008 results.

Increasing the size of rice husk particles also increases flow rate but at the expense of the water quality. The main conclusion of this study is that the most critical parameter for effective water filtration appears to be the pore size (either achieved by increasing the maximum firing temperature or the rice husk particle size).

6.0 Recommendations for future research

The durability of pots with higher porosities needs to be investigated under field conditions. Indeed, more research needs to be done, especially long-term studies, to determine whether it is safe to use a filter with increased porosity (and thus increased flow rate) throughout its operational lifetime (at least two years). This recommended long-term study should emulate the field conditions as much as possible, for example, by re-filling the filters every day, including in the weekends, to keep the pot wet.

References

- Bloem, S.C., Halem, D. van, Sampson, M.L., Huoy L., Heijman S.G.J. (2009). "Silver Impregnated Ceramic Pot Filter: Flow Rate versus the Removal Efficiency of Pathogens". Proceedings of the International Ceramic Pot Filter Workshop, WEF Disinfection conference, Atlanta, February 28th 2009.
- Brown, J. 2007 Effectiveness of Ceramic Filtration for Drinking Water Treatment in Cambodia. PhD Thesis, University of North Carolina, Chapel Hill.
- Brown, J., Sobsey, M. D. & Proum, S. (2007). Improving Household Drinking Water Quality: Use of Ceramic Water Filters in Cambodia. Water and Sanitation Program (WSP) field note. World Bank, Phnom Penh, Cambodia.
- Brown, J., Proum, S. & Sobsey, M. D. (2009). Sustained use of a household-scale water filtration device in rural Cambodia. *Water Health* 7(3), 404-412.
- Cultrone, G., Elert, E., de la Torre, M., Cazalla, O., Navarro, C. (2004). Influence of mineralogy and firing temperature on the porosity of bricks, *Journal of the European Ceramic Society*, Volume 24, Issue 3, March 2004, Pages 547-564.
- Fahlin, C.J. (2003) Hydraulic Properties Investigation of the Potters For Peace Colloidal Silver Impregnated, Ceramic Filter. Unpublished Thesis, University of Colorado at Boulder, Boulder, CO, USA.
- Klarman, M. (2009) Investigation of Ceramic Pot Filter Design Variables. Unpublished Thesis, Emory University, Rollins School of Public Health, USA.
- Hagan, J.M., Harley, N., Pointing, D., Sampson, M., Smith, K., and Soam, V. (2009). Resource Development International - Cambodia Ceramic Water Filter Handbook -, Version 1.1, Phnom Penh, Cambodia.
- Halem, D van, Laan, JG van der, Heijman, SGJ, Dijk, JC van, Amy, GL (2009). Assessing the sustainability of the silver-impregnated ceramic pot filter for low-cost household drinking water treatment. *Physics and chemistry of the earth*, 34, 36-42.
- Hunter, P.R. (2009). Household Water Treatment in Developing Countries: Comparing Different Intervention Types Using Meta-Regression. School of Medicine, Health Policy and Practice, University of East Anglia, Norwich U.K. Received June 30, 2009. Accepted October 15, 2009.
- Influence of mineralogy and firing temperature on the porosity of bricks (Giuseppe Hunter, P.R. (2009), Household Water Treatment in Developing Countries: Comparing Different Intervention Types Using Meta-Regression, *Environ. Sci. Technol* (accepted October 2009)
- Lantagne. D. (2001) Investigation of the Potters for Peace Colloidal Silver Impregnated Ceramic Filter—Report 1: Intrinsic Effectiveness. Alethia Environmental, Allston, Massachusetts.
- Lantagne, D. (2001). Investigation of the Potters for Peace Colloidal Silver Impregnated Ceramic Filter-Report 2: Field Investigations. Alethia Environmental. Allston, Massachusetts.

- Murphy, H. M., Sampson, M., McBean, E., & Farahbakhsh, K. (2008). Influence of Household Practices on the Performance of Clay Pot Water Filters in Rural Cambodia.
- Roberts, M. (2004) Field Test of a Silver-Impregnated Ceramic Water Filter. People-Centred Approaches to Water and Environmental Sanitation. Vientiane, Lao PDR, WEDC.
- The Ceramics Manufacturing Working Group (2011). Best Practice Recommendations for Local Manufacturing of Ceramic Pot Filters for Household Water Treatment, Ed. 1. Atlanta, GA, USA: CDC.

Appendices

APPENDIX I: Analysis of the Raw Materials (by TCKI)

Samples of the clay and laterite from RDIC used for the research were sent to TCKI in order to investigate their characteristics. TCKI determined the particle size distribution (percentage of fine particles and concentration of coarse and fine sand) of both materials as well as the specific surface area and chemical composition of the clay.

The particle size distribution was determined by a combination of techniques, i.e. via the use of sieves and sedimentation of the fine particles in water. Sieves with a mesh of 250 μm and 63 μm were used to separate, dry and weigh the coarse and fine sand fractions respectively. Using the weight originally found for the dried clay, it is then possible to calculate the weight percentages for both these fractions. The actual clay minerals were found in the fraction composed of particles smaller than 10 μm . Clay minerals have a plate shaped structure; the thickness is much smaller than the length and width. This structure gives clays their mouldable characteristics after addition of suitable amount of water.

Particles smaller than 10 μm cannot be retained on a sieve. This fraction is determined on the basis of their sedimentation speed in water, after all the individual particles have been separated from each other and no longer coagulate. After a specific sedimentation time, the density of the suspension is determined at a specific depth. This density will be higher than the density of pure water, depending on the amount of particles smaller than 10 μm present in the suspension. In combination with the original weight of the dried clay, this information is then used to calculate the quantity of particles smaller than 10 μm . This concentration is referred to as the concentration of fine particles in the clay.

The specific surface area of a clay is defined as the total surface area (in m^2) of all the individual particles present in one gram of the clay. The specific surface area increases rapidly as the quantity of granular particles decreases and is replaced by an increasing quantity of plate shaped particles (i.e. clay minerals). In addition, there are various types of clay minerals which each have a different specific surface area: kaolinite, illite and montmorillonite. The specific surface area of these clay minerals increases (rapidly) in the order listed here.

The percentage of fine particles provides information about the quantity of clay minerals present. If we also consider the specific surface area, we also obtain additional insight into the nature of the clay minerals (and therefore also into its mouldability, moisture retention capacity and the manner in which the clay becomes vitrified).

The specific surface area is determined on the basis of the amount of moisture which binds to the surface of all the particles under conditions of equilibrium at a fixed temperature and relative humidity.

The chemical composition of all the types of minerals present and their relative contributions to the total mass. This is determined via x-ray fluorescence for the sample

being analyzed is melted into a glass bead. The surface of the bead is then subjected to x-ray radiation. Each chemical element reflects its own characteristic x-ray radiation, the intensities of which are then scanned and used to calculate the contribution of each element to the total mineral mass. The loss of ignition is then added to this total to calculate the original total mass. The loss of ignition is the loss of weight that takes place as the sample is heated from 100 deg. C to 1000 deg. C. This loss is due, for example, to the combustion of organic components and the evaporation of physically and chemically bound water.

If we consider the particle size distribution, it is clear that the clay consists almost exclusively of particles smaller than 10 μ . The largest part of the clay mass consists of clay minerals that are not linked to each other. This results in a very high degree of mouldability after the addition of an adequate amount of water. It also results in a high moisture retention capacity, without the addition of additives, which means that it will be very difficult to dry this clay without any cracking taking place.

The (broken) laterite material that was also investigated has a very different particle structure. The percentage of fine particles here is only 25%. This material also contains a fine sand fraction of 28% and a coarse sand fraction of 36%. This material can be characterized as a mixture of sand and fine particles. It can be used quite effectively to reduce the percentage of very fine particles in a clay, thereby making the clay somewhat less plastic and less susceptible to cracking during drying.

The specific surface area of the clay is 121 m^2/g . Although this value for the specific surface area is quite high (which is not surprising considering the high percentage of clay minerals present), it is still relatively low in relation to the quantity of fine particles present (i.e. a ratio of 1.2 to 1.3). This indicates that the relative share of montmorillonite clay minerals (clay minerals that can swell quite strongly and bind a great deal of moisture) is limited and that the share of kaolinite clay minerals (which bind smaller amounts of moisture) present in the sample is larger.

The chemical composition also reflects the presence of a large quantity of clay minerals, in particular of the kaolinite type (with a high aluminium concentration and loss on ignition). The high concentration of potassium also indicates that there is a relatively large fraction of illite clay minerals present. The iron concentration is also high and will give the product a red colour after firing.

In addition to the main elements, several trace elements were also analyzed and found to be present. No abnormally high values were discovered relative to clay.

In addition to these trace elements, an analysis was also carried out for arsenic. However, this value has not been reported, as a validation of the analysis indicated that the result was not completely reliable. The result of this insufficiently reliable analysis indicated that the concentration of arsenic was below our detection limit of 0.006 % As_2O_3 .

In order to optimize the day recipe, consideration should be given to further reducing the concentration of very fine particles present. The laterite material analyzed can serve as an excellent material for doing so. However, before being used, the latter should be sufficiently homogeneous in nature and sufficiently broken down or crushed (or sieved).

In order to reduce the risk of cracking upon drying and increase the permeability to water of the final filter pot product, a maximum amount of laterite should be added to the

recipe. We would expect that this laterite could certainly comprise 30% and perhaps as much as 40% of the recipe (based on the dry weight of the clay and laterite). However, it needs to be mixed into the clay in such a manner as to ensure that the resulting mixture is as homogeneous as possible. If this is not realized or is not possible, the product will actually be increasingly susceptible to cracking during the drying process.

Mixing in this fine laterite material will increase the percolation speed of the fired liter pot. However, its influence on the purifying effect of the filter pot also needs to be carefully considered. The firing temperature will also affect the pore structure of the fired material and therefore also the percolation speed and purifying effect. In principle, one would expect that an increase in firing temperature (e.g. from 800°C to 1000°C) would lead to an increase in pore diameter and a greater percolation speed. However, if the firing temperature is increased even further (above 1050°C or 1100°C?), the pores will become constricted and the percolation speed will actually decrease. In this regard, it would be advisable according to TCKI to determine the optimum firing temperature in terms of percolation speed and purifying effect.

APPENDIX II: Initial *E. Coli* Testing Procedure (First Batch Series)

Day 1:

- **Autoclave** glassware, water (same volume as bouillon) and filters (separately from liquids).
- **The glass plates should be sterilized at 250 deg. C for 20 mins in the little oven on the bench.**
- Melt TSA in bain-marie for making **plastic plates** (to the mark, but thicker is better than too thin)
- Prepare the **TSA Agar solution** as per instructions to grow *E. coli* and make sure the culture is pure (non-selective medium). 12g in 300 mL is enough for 12 plates.
- Inoculate **pure *E. coli* B** on 2 TSA plates (rich medium) from the older sealed culture plate in fridge. Don't forget to sterilize the oese in between lines (do it in 4 directions) (check the purity of the *E. coli* B cultures, RDI's *E. coli* B stock is NOT pure!).
- Prepare the **bouillon Tryptic Soya Broth** (6 g in 200 mL is more than enough)--> autoclave. The 100 mL sterilized bouillon will be used for (1) 1 X 25 mL conical flask with bin and (2) 10 tubes with 9 mL pure bouillon/water (50:50) (50 mL of sterile bouillon and 50 mL sterilized water in 250 mL conical flask)
- Prepare **Rapid Agar** (selective medium) as per instructions. 18.5 g in 500 mL is enough for at least 60 plates.
- Prepare sterilized plates of Rapid Agar (7 mL per plate) - For 4 pots, need 50 plates of rapid agar (400 mL of rapid agar in total) (need 6 plates for 1 sample, for every effluent pot sample need 12 plates).

Day 2:

- **Prepare inoculation of bouillon of *E. coli* B** (9 am) - take **one individual separate colony** of (hopefully) pure *E. coli* B and put it in sterile bouillon (25 mL in sterile flask with sterile magnetic bar) (scrape the *E. coli* on the glass of the flask and swirl well. Stir it in 37 deg. C incubation for 8 hours while sitring (so that bacteria multiply in the bouillon) while stirring (magnetic stirrer inside incubator).

Important note: After used the *E. coli* plate, put the plate in the fridge (with label: date, name and what it is) but well sealed with Parafilm. It can then be reused within the next 6 weeks to make a fresh culture for new bouillon inoculation. Don't forget to write the date and expiry date on the plate!

- 4 or 5 pm: **Membrane filtration for the bouillon dilutions -6, -7 and -8 of rapid agar in duplos.** Dilution -5 is not necessary. Do the dilutions sterile (autoclaved) water and bouillon (50:50 mix). Take 50 mL sterile bouillon and 50 mL sterile

water. Mix well in the flask. Put 9 mL of this mix in each universal tube (9 tubes in total): -1, -2, -3, -4, -5, -6, -7, -8 and control/blank (bouillon/water)

1. 8 universal tubes with 9 mL of water sterilized in autoclave
 2. Take 1 mL from bouillon and put into first universal tube (dilution -1)
 3. Take 1 mL from first universal tube and put into second universal tube (dilution -2), etc.
 4. Membrane filtration
 5. Put the dilution duplicate plates to incubate upside down at 37 degrees for 16 hours.
 6. **Put the 9 universal tubes in the frigidaire** to keep the *E. coli* concentration stable at 4 degrees C as we need to know exactly which concentration is needed for influent spiking.
 7. For dilutions -5, -6 and -7, take 0.1 mL (or 100 microL) directly into TSA plate and use the Ineke's blue spreader so that it spreads on the whole plate. This is to check that the culture is pure. If not pure, make a new one (quality control!). Put the 2 TSA plates in the incubator upside down ~16 hours.
 8. (the concentration of the bouillon dilutions -6, -7 and -8 (-5 not necessary) will be defined the next morning)
- **Rinse the filters** using UV water treated water and **soak the filters for 24 hours in UV treated water** (in 2 X 100 L buckets)
 - **Rinse the receptacles** with UV water 3 times and bring inside to **disinfect them with alcohol**

Important note: The UV lamp is a hazard, so always wear safety goggles. The instructions for using the UV lamp is as follow: Open tap gently and not all the way open (with valve always half open!), then open the UV lamp. keep the water pressure low in the system. When finished, close the UV lamp but let the water run through it for 15 mins to cool the UV tube down, and then turn the tap off, but NOT the valve. In case the UV tube explodes, don't reach to the valve if feet are soaking in water. Climb on a bench and use a wooden stick to not get electrocuted.

Day 3:

- First thing in the morning: check purity of the culture on the 2 TSA plates (no need to count). Then, count Rapid Agar plates and calculate the influent concentration of *E. coli* from bouillon. Use Ineke's program (tab '1 ML') to calculate the number of mL needed for the influent for a total influent volume of 50 L (for 4 pots). So, if 3.2×10^{-1} , need to put in 3.2 mL of the first dilution (-1) into the 50 L influent volume. We want an **influent concentration of 1,000 cfu (*E. coli* B)/mL in order to have countable results**. (If log removal is higher than expected, make the influent concentration higher, say 10 times higher, so 10,000 cfu/mL (for example if use silver).

Important note: When finished counting the plates, scoop out the contaminated media into a black bag to incinerate in the rubbish kiln and put the plates in a bucket in the sink with bleach to soak for 30 minutes, and then rinse off and dry. Also, don't forget to clean the filters before autoclaving them.

- Autoclave the filters (and water separately if needed) for the membrane filtration of samples at the end of the day.
- Set up the receptacles and filters inside (delicately, **holding them only by the rim** and taking all the soaking water out of them).
- Rinse the clean red 125 L bucket using UV treated water and put 40 L of UV treated water in it (8L X 4 pots = 32 L, so 40L just to be safe). Also rinse the blue 8 L bucket for scooping influent from the 125 L container to the filters.
- Preparation of influent (spike UV water at last minute, **when everything else is ready (and record time at which the influent was spiked)**. Stir the 50 L with a long spoon for 10 mins in the 125 L vessel
- **While waiting for sampling, prepare everything for membrane filtration, have all the material ready, all the plates labeled (USE STICKERS!) and so on.**
- Rinse the 250 mL sampling bottles well (at least 3 times with UV treated water) and shake the water out
- **Sampling procedure: 1 blanco, 3 influents and 4 effluents = total of 8 sampling bottles**
 - Blanco (start) sample from influent without *E. coli* B spiking. Record time.
 - Influent (start) straight in cooler
 - Influent (half-way) – sample at start but put in cooler half-way through the experiment
 - Influent (end) – sample at start but put in cooler half-way through the experiment
 - Put bleach in the 125 L red bucket to disinfect
 - Discard the first 2L of effluent from all pots using the graduated beaker and dispose of it in the 125 L bucket containing bleach. Record time.
 - When there is enough effluent to sample for all pots, collect sample, but don't forget to discard the first 100 mL before taking the sample. Record the sampling time.
- Rinse the filters and receptacles and leave them to dry outside (but do not leave them right under the sun!)
- **Membrane filtration of the samples at end of day – always use duplos!**
 - Clean up the work bench with alcohol before starting
 - **EFFLUENT: 24 plates**
 - sample 1: 2 X 1 mL, 2 X 10 mL and 2 X 100 mL --> 6 plates
 - sample 2: 2 X 1 mL, 2 X 10 mL and 2 X 100 mL --> 6 plates
 - sample 3: 2 X 1 mL, 2 X 10 mL and 2 X 100 mL --> 6 plates
 - sample 4: 2 X 1 mL, 2 X 10 mL and 2 X 100 mL --> 6 plates
 - **INFLUENT: 14 plates**
 - 2 influent at start (0.5 mL and 1 mL at -1) --> 4 plates

- 2 influent half-way (0.5 mL and 1 mL at -1) --> 4 plates
- 2 influent at end (0.5 mL and 1 mL at -1) --> 4 plates
- 2 blanks (influent w/o spiking, 100 mL) --> 2 plates
- Incubate the plates **upside down** (always) for 16 hours

Important notes: To make the -1 dilution, take the spiked influent sample and take 1 mL of it into a sterilized tube containing 9 mL of autoclaved water. Shake well (let the bubble go up and down to stir). Take 0.5 mL and 1 mL from this tube.

Another important note: For one sample, go from low dilution to high of want to use the same filter.

- Filter 1 – 2 X Blanks
- Filter 2 – Influent (start): 0.5 mL, 1 mL
- Filter 3 – Influent (half-way): 0.5 mL, 1 mL
- Filter 4 – Influent (end): 0.5 mL, 1 mL
- Filter 5 – Effluent 1: 2 X 1 mL, 2 X 10 mL, 2 X 100 mL
- Filter 6 – Effluent 2: 2 X 1 mL, 2 X 10 mL, 2 X 100 mL (use metal filter)
- Filter 7 – Effluent 3: 2 X 1 mL, 2 X 10 mL, 2 X 100 mL (use metal filter)
- Filter 8 – Effluent 4: 2 X 1 mL, 2 X 10 mL, 2 X 100 mL (use metal filter)

Clean up everything at the end of the day!

APPENDIX III: Adapted *E. Coli* Testing Procedure (Second Batch Series)

Day 1:

1. Incubate (at 37 deg.) 1 *E. coli* colony in 5 mL of TSB overnight (16 hours: 5 pm to 8 am the next day). 12 to 18 hours is OK.
2. Soak the well scrubbed pots in bacteria-free water (UV-treated rain water is OK for me).
3. Clean all filtrate receptacles with bacteria-free water, wipe them with 70% alcohol, and leave them inside the lab overnight to let the alcohol evaporate.
4. Prepare enough rapid agar for membrane filtration: 500 ml for 90 plates

Day 2:

5. At 8 am, take 0.1 mL of the concentrated *E. coli* broth into 10 mL of TSB and incubate (at 37 deg.) for 3 or 4 hours.
6. Take 5 mL of the concentrated *E. coli* broth in a tube and centrifuge for 10 minutes at 3000 rpm (place a similar tube of the same weight on the opposite side of the centrifuger for balance). Discard the supernatant and resuspend the pellet in 5 ml of peptone water (0.1% peptone). Re-centrifuge for 10 minutes. Discard the supernatant again. Re-suspend the pellet in 5 ml of peptone water (0.1% peptone). The peptone (dilluent) does not cause the bacteria to clump like Tryptic Soya Broth.
7. Estimate the concentration of the *E. coli* broth by spectrophotometry, using the calibration curve OD (absorbance) versus [*E. coli*]: 1 OD α 1E9 cfu/ml (at wavelength 600 nm). Use peptone (0.1 %) as the blank.

(To make the calibration curve: Take the *E. coli* in 4 ml of peptone. Take 1 ml to measure OD . Make OD 1 (normally 1E9 cfu/ml). Take 1 ml to plate: 1ml at -6, -7, -8 and -9. There is 2 ml left. Add 2 ml of peptone water in the tube to dilute twice. Take 1 ml to measure OD. Make OD 0.5. Take 1 ml to plate: 1ml at -6, -7 and -8. There is 2 ml left. Add 2 ml of peptone water in the tube to dilute twice. Take 1 ml to measure OD. Make OD 0.25. Take 1 ml to plate: 1ml at -4, -5 and -6.

There is 2 ml left. Add 2 ml of peptone water in the tube to dilute twice. Take 1 ml to measure OD. Make OD 0.1. Take 1 ml to plate: 1ml at -4 and -5.)

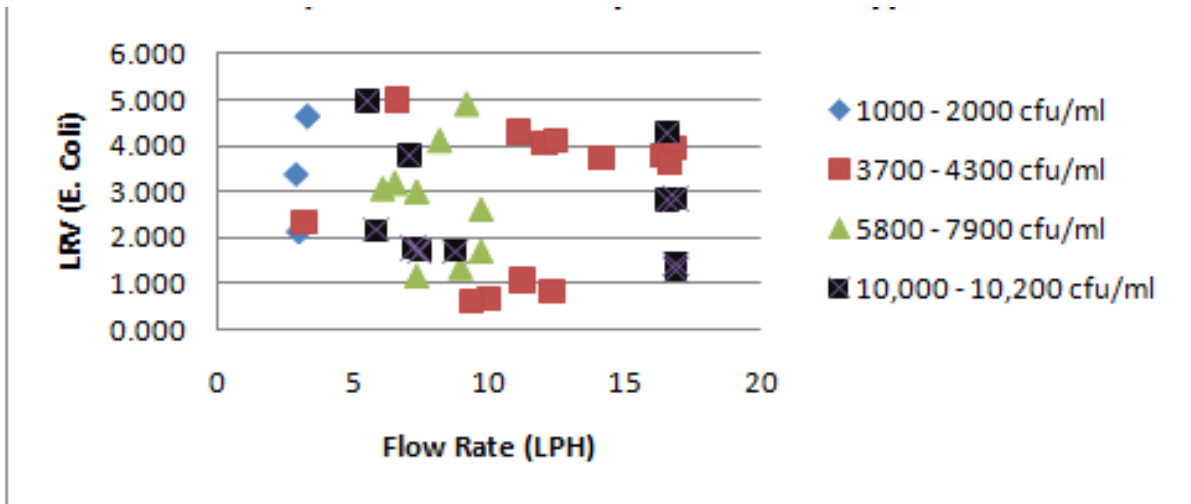
8. Prepare one set of dilution tubes per filter **without silver** to test. Put 1 ml of the concentrated *E. coli* broth into a dilution tube (dilution -1) containing 9 ml of sterile DI water and mix well. Put 1 ml of the dilution -1 into 99 ml of sterile DI

water in 125 ml conical flask to make dilution -3 (1E6 cfu/ml). The *E. coli* concentrate should be 1E9 cfu/mL. The desired concentration for the spiking solution is 1E6 cfu/ml for filters painted with silver and 1E3 cfu/ml for filters without silver.

9. The total volume of bacteria-free water to be spiked **per filter** is 8 L. Use a 10 or 15 L bucket with spout to make sure that the influent does not spill into the clean receptacle. If the bucket is not already graduated, fill it up to 8 L using a measuring cylinder and make a mark at the 8 L line using a permanent marker.
10. Take a sample of the bacteria-free water before spiking. Take the sample in a 250 ml sterile or autoclaved bottle and keep in a cooler (at 4 deg. C.)
11. Spike each 8 L water bucket with (a) 8 mL of the dilution -3 (1E6 cfu/ml)) for filters **without silver**; or (b) with 8 mL of the concentrated *E. coli* broth (1E9 cfu/ml) for filters **with silver**.
12. Take a sample of each spiked influent using 250 ml bottles. I use 500 ml water bottles that only contained pure drinking water.
13. Place a 2 L beaker under each outlet, and discard the first 2 L of effluent for all filters.
14. Before taking all effluent samples, discard the first 100 ml.
15. Test all influent and effluent samples by **membrane filtration** (this method is standard). For effluent samples, mix the sample bottle well and test 1 ml, 10 ml and 100 ml for each sample. For influent samples, mix the sample bottle well and make duplicate series of dilutions of the sample by taking 1 ml of the water sample into the first dilution tube of the first dilution series and then taking 1 ml of the water sample into the first dilution tube of the second (duplicate) dilution series.
 - a. For filters **with** silver, make two sets of 5 dilutions (we expect to count approximately 10 cfu in the -5 dilution) and **test 1 ml of the 2 duplicate dilutions -5, 0.5 ml and 1 ml of the 2 duplicate dilutions -4, 0.1 ml of the 2 duplicate dilutions -3, and 1 ml of the original water sample** (to ensure it is TNTC (too numerous to count)).
 - b. For filters **without** silver, make two sets of 2 dilutions (we expect to count approximately 10 cfu in the -2 dilution) and **test 0.5 ml and 1 ml of the 2 duplicate dilutions -2, 0.1 ml of the 2 duplicate dilutions -1, and 1 ml of the original water sample** (to ensure it is TNTC (too numerous to count)).

Note: throughout the period of testing, there is variability in the influent *E. coli* concentrations (see Figure 3); but, influent concentrations do not seem to be correlated to LRVs. For the first set of batches (B7 to B17), a large influent volume (70 to 100 L)

was spiked with a small volume (3 to 5 ml) of concentrated *E. coli* suspended in TSB) and mixed for at least 15 minutes. Eight liters of this influent volume was poured in each filter to be tested, but the *E. coli* concentration was not well/evenly distributed, resulting in very different (often too low) influent *E. coli* concentrations. For the second set of batches (B23 to B26), the *E. coli* was re-suspended in water or 0.1 % peptone water and the concentration of bacteria estimated by spectrophotometry. This estimation of 1 OD being proportional to a concentration of 1E8 cfu/ml is not very accurate; and, as a result the spiked influents varied in concentration between 1E3 (or 1000) and 1E4 cfu/ml. Figure below shows that there is no correlation between influent *E. coli* concentrations (between 1000 and 10,000 cfu/ml) and LRVs, so the variability in the influent *E. coli* concentrations is not problematic in the interpretation of the LRV results.



APPENDIX III: Raw and Calculated Data (First Batch Series)

Batch	Pot	kg rice husk / 6 pots	kg clay / 6 pots	kg laterite / 6 pots	Firing temp (deg. C)	Flow rate (LPH)	LRV (<i>E. Coli</i>)	[<i>E. coli</i>] inf. (cfu/ml)
7	1	9.7 (< 1 mm)	30 (< 1 mm)	1 kg (< 1 mm)	877	2.882	3.310	1062.5
7	2	9.7 (< 1 mm)	30 (< 1 mm)	1 kg (< 1 mm)	883	2.397		
7	3	9.7 (< 1 mm)	30 (< 1 mm)	1 kg (< 1 mm)	883	3.257		
7	4	9.7 (< 1 mm)	30 (< 1 mm)	1 kg (< 1 mm)	888	2.985	2.123	925.0
7	5	9.7 (< 1 mm)	30 (< 1 mm)	1 kg (< 1 mm)	944	3.293	4.181	1062.5
7	6	9.7 (< 1 mm)	30 (< 1 mm)	1 kg (< 1 mm)	908	3.168	2.326	402.5
18	1	11 (< 1 mm)	30 (< 1 mm)	1 kg (< 1 mm)	873	7.043		
18	2	11 (< 1 mm)	30 (< 1 mm)	1 kg (< 1 mm)	873	6.615	4.898	197.5
18	3	11 (< 1 mm)	30 (< 1 mm)	1 kg (< 1 mm)	873	7.472		
18	4	11 (< 1 mm)	30 (< 1 mm)	1 kg (< 1 mm)	874	8.164	4.119	197.5
18	5	11 (< 1 mm)	30 (< 1 mm)	1 kg (< 1 mm)	916	8.561		
18	6	11 (< 1 mm)	30 (< 1 mm)	1 kg (< 1 mm)	890	9.161	4.003	402.5
13	1	12 (< 1 mm)	30 (< 1 mm)	1 kg (< 1 mm)	879	11.562		
13	2	12 (< 1 mm)	30 (< 1 mm)	1 kg (< 1 mm)	884	10.365		
13	3	12 (< 1 mm)	30 (< 1 mm)	1 kg (< 1 mm)	884	11.264		
13	4	12 (< 1 mm)	30 (< 1 mm)	1 kg (< 1 mm)	889	12.026	5.207	402.5
13	5	12 (< 1 mm)	30 (< 1 mm)	1 kg (< 1 mm)	943	11.073	3.631	545.0
13	5	12 (< 1 mm)	30 (< 1 mm)	1 kg (< 1 mm)	943	11.073	4.296	197.5
13	6	12 (< 1 mm)	30 (< 1 mm)	1 kg (< 1 mm)	910	12.425	4.037	545.0

			mm)	mm)				
4	1	13 (< 1 mm)	30 (< 1 mm)	1 kg (< 1 mm)	906	14.263	3.150	402.5
4	2	13 (< 1 mm)	30 (< 1 mm)	1 kg (< 1 mm)	900	14.590		
4	3	13 (< 1 mm)	30 (< 1 mm)	1 kg (< 1 mm)	900	13.980		
4	4	13 (< 1 mm)	30 (< 1 mm)	1 kg (< 1 mm)	894	15.758	3.470	13000.0
4	5	13 (< 1 mm)	30 (< 1 mm)	1 kg (< 1 mm)	1009	13.658	2.881	13000.0
4	6	13 (< 1 mm)	30 (< 1 mm)	1 kg (< 1 mm)	947	14.529		
17	1	12 (< 1 mm)	30 (< 1 mm)	1 kg (< 1 mm)	873	16.412	3.941	545.0
17	2	13 (< 1 mm)	30 (< 1 mm)	1 kg (< 1 mm)	870	14.111	3.722	197.5
17	3	13 (< 1 mm)	30 (< 1 mm)	1 kg (< 1 mm)	870	18.969		
17	4	13 (< 1 mm)	30 (< 1 mm)	1 kg (< 1 mm)	868	16.808	3.952	402.5
17	5	13 (< 1 mm)	30 (< 1 mm)	1 kg (< 1 mm)	954	18.235	3.546	402.5
17	6	13 (< 1 mm)	30 (< 1 mm)	1 kg (< 1 mm)	911	16.633	3.625	402.5

APPENDIX V: Raw E. coli Data (First Batch Series)

Experiment date: 16/03/2011

sample type	dilution	mL	Duplo 1	Duplo 2	average	cfu/mL	LRV
Influent	10	0.5	43	46	44.5	925.000	
	10	1	90	102	96		
Effluent - B1 P4 (RDIC pot fired on research kiln)		1	1	2	1.5	1.225	2.878
		10	13	10	11.5		
		100	97	108	102.5		
Effluent - B2 P4 (RDIC pot fired on research kiln)		1	2	2	2	2.975	2.493
		10	35	44	39.5		
		100		TNTC	TNTC		
Effluent - B7 P4		1	9	5	7	6.975	2.123
		10	64	75	69.5		
		100		TNTC	TNTC		
Effluent - B10 (RDI) P4		1	0	0	0	0.100	3.966
		10	1	1	1		
		100	6	0	3		
Effluent - B8 P4 (13 kg rice husk) (big crack inside, but not outside)		1	0	0	0	0.060	4.188
		10	2	0	1		
		100	6	6	6		

Experiment date: 17/03/2011

sample type	dilution	mL	Duplo 1	Duplo 2	average	cfu/mL	LRV
Influent - start	10	0.5	24	41	32.5	865.000	
Influent - start	10	1	84	91	87.5		
Influent - end	10	0.5	127	63	95	1260.000	
Influent - end	10	1	127	-	127		
					[influent]avg	1062.500	
BLANCO (influent without spiking)			0	0	0	0.000	
Effluent - B7 P1		1	1	0	0.5	0.520	3.310
		10	4	6	5		
		100	52	44	48		
Effluent - B7 P5 (minor crack all along the height of pot)		1	0	0	0	0.070	4.181
		10	0	0	0		
		100	6	7	6.5		

Experiment date: 23/03/2011

sample type	dilution	mL	Duplo 1	Duplo 2	average	cfu/mL	LRV
Influent - start	10	0.5	647	650	650	13000	
Influent - start	10	1	TNTC	TNTC			
Influent - half-way	10	0.5	TNTC	TNTC			
Influent - half-way	10	1	TNTC	TNTC			
Influent - end	10	0.5	TNTC	TNTC			
Influent - end	10	1	TNTC	TNTC			
Average [influent]					[influent]avg	13000	
Effluent - B8 P1 (13 kg rice husk)		1	6	1	3.5	3.85	3.528
		10	32	45	38.5		
		100	TNTC	TNTC	TNTC		
Effluent - B8 P5 (13 kg rice husk)		1	0	0	0	0.03	5.637
		10	0	1	0.5		
		100	3	3	3		
Effluent - B4 P5 (superficial crack)		1	22	21	21.5	17.1	2.881
		10	128	126	127		
		100	TNTC	TNTC	TNTC		
Effluent - B4 P4 (superficial crack)		1	3	6	4.5	4.4	3.470
		10	42	44	43		
		100	TNTC	TNTC	TNTC		

Experiment date: 28/03/2011

sample type	dilution	mL	Duplo 1	Duplo 2	average	cfu/mL	LRV
Influent Blanco (UV water before spiking)	10	100	0	0	0	545	
Influent Start	10	0.1	4	10	7		
Influent Start	10	0.5	25	36	30.5		
Influent Start	10	1	49	47	48		
Influent halfway	10	0.1	4	12	8	572.5	
Influent halfway	10	0.5	23	31	27		
Influent halfway	10	1	50	71	60.5		
Influent End	10	0.1	8	5	6.5	310	
Influent End	10	0.5	28	22	25		
Influent End	10	1	48	51	49.5		
Average [influent]							
Effluent - B13 P5		1	0	0	0	0.1275	3.631
		10	1	2	1.5		
		100	7	14	10.5		

		1	0	0	0		
		10	1	0	0.5		
Effluent - B13 P6		100	0	0	0	0.05	4.037
		1	0	0	0		
		10	2	0	1		
Effluent - B17 P1 (superficial crack)		100	4	1	2.5	0.0625	3.941
		1	0	0	0		
		10	3	0	1.5		
Effluent - B17 P5 (superficial crack)		100	20	12	16	0.155	3.546

Experiment date: 04/05/2011

sample type	dilution	mL	Duplo 1	Duplo 2	average	cfu/mL	LRV
Influent Blanco (UV water before spiking)		100	0	0	0		
Influent Start	10	0.1	1	1	1		
Influent Start	10	0.5	7	10	8.5		
Influent Start	10	1	13	23	18	175	
Influent half-way	10	0.1	1	1	1		
Influent half-way	10	0.5	5	5	5		
Influent half-way	10	1	13	16	14.5	122.5	
Influent End	10	0.1	0	2	1		
Influent End	10	0.5	7	3	5		
Influent End	10	1	17	8	12.5	112.5	
Average [influent]						136.7	
		1	0	0	0		
		10	0	1	0.5		
Effluent - RDI pot 1		100	6	7	6.5	0.0575	3.376
		1	0	0	0		
		10	0	1	0.5		
Effluent - RDI pot 2		100	4	4	4	0.05	3.437
		1	0	0	0		
		10	0	0	0		
Effluent - RDI pot 3		100	3	4	3.5	0.0175	3.893
		1	9	6	7.5		
		10	48	69	58.5		
Effluent - RDI pot 4 (cross-contamination?)		100	TNTC	TNTC	TNTC	6.675	1.311

Experiment date: 07/05/2011

sample type	dilution	mL	Duplo 1	Duplo 2	average	cfu/mL	LRV
Influent Blanco (UV water before spiking)		100	0	0	0	0	
Influent Start	10	0.1	3	12	7.5	302.5	
Influent Start	10	0.5	16	16	16		
Influent Start	10	1	27	30	28.5		
Influent half-way	10	0.1	1	2	1.5	446.7	
Influent half-way	10	0.5	34	18	26		
Influent half-way	10	1	51	83	67		
Influent End	10	0.1	4	3	3.5	458.3	
Influent End	10	0.5	21	20	20.5		
Influent End	10	1	55	68	61.5		
Average [influent]						402.5	
Effluent - B8 P6		1	0	0	0	0.0025	5.207
		10	0	0	0		
		100	0	1	0.5		
Effluent - B8 P6		1	0	0	0	0.005	4.906
		10	0	0	0		
		100	1	1	1		
Effluent - B10 P4 (RDI)		1	0	0	0	0.0025	5.207
		10	0	0	0		
		100	0	1	0.5		
Effluent - B18 P6		1	1	0	0.5	0.04	4.003
		10	2	0	1		
		100	4	4	4		
Effluent - B7 P6		1	2	2	2	1.9	2.326
		10	12	24	18		
		100	TNTC	TNTC	TNTC		
Effluent - B17 P4		1	0	0	0	0.045	3.952
		10	1	0	0.5		
		100	3	6	4.5		
Effluent - B4 P1 (superficial crack)		1	1	1	1	0.285	3.150
		10	2	1	1.5		
		100	49	35	42		
Effluent - B13 P4		1	0.1	0.1	0.1	0.0025	5.207
		10	0	0	0		
		100	0	1	0.5		

Experiment date: 12/05/2011

sample type	Dilution	mL	Duplo 1	Duplo 2	average	cfu/mL	LRV
Influent Blanco (UV water before spiking)		100	0	0	0	0	
Influent Start	10	0.1	4	5	4.5		
Influent Start	10	0.5	14	11	12.5		
Influent Start	10	1	30	30	30	275.0	
Influent half-way	10	0.1	2	8	5		
Influent half-way	10	0.5	14	11	12.5		
Influent half-way	10	1	10	9	9.5	172.5	
Influent End	10	0.1	1	8	4.5		
Influent End	10	0.5	8	8	8		
Influent End	10	1	13	13	13	145.0	
Average [influent]						197.5	
Effluent - B17 P2		1	0	0	0	0.0375	3.722
		10	0	1	0.5		
		100	2	3	2.5		
Effluent - B18 P2		1	0	0	0	0.0025	4.898
		10	0	0	0		
		100	0	1	0.5		
Effluent - B18 P4		1	0	0	0	0.015	4.119
		10	0	0	0		
		100	1	2	1.5		
Effluent - B8 P1 (13 kg rice husk)		1	0	0	0	0.07	3.450
		10	0	1	0.5		
		100	6	8	7		
Effluent - B13 P5		1	0	0	0	0.01	4.296
		10	0	1	0.5		
		100	0	2	1		
Effluent - RDI (4L/hr) P4		1	0	1	0.5	1.05	2.274
		10	7	14	10.5		
		100	TNTC	TNTC	TNTC		
Effluent - B10 (RDI - 2 L/hr) P1		1	0	0	0	0.07	3.450
		10	0	0	0		
		100	5	9	7		

APPENDIX VI: Raw and Calculated Data (Second Batch Series)

Batch	Pot	kg rice husk / 6 pots	kg clay / 6 pots	kg laterite / 6 pots	Firing temp (deg. C)	Flow rate (LPH)	LRV (E. Coli)	[E. coli] inf. (cfu/ml)
23	5	9.7 (< 1 mm)	30 (< 1 mm)	1 kg (< 1 mm)	941.1	7.172	3.281	361
23	5	9.7 (< 1 mm)	30 (< 1 mm)	1 kg (< 1 mm)	941.1	7.172	1.549	4235
23	6	9.7 (< 1 mm)	30 (< 1 mm)	1 kg (< 1 mm)	916.1	7.455	2.909	1987
23	6	9.7 (< 1 mm)	30 (< 1 mm)	1 kg (< 1 mm)	916.1	7.455	1.613	4100
23	6	9.7 (< 1 mm)	30 (< 1 mm)	1 kg (< 1 mm)	916.1	7.455	1.694	4235
23	6	9.7 (< 1 mm)	30 (< 1 mm)	1 kg (< 1 mm)	916.1	7.455	1.365	5806
24	1	11 (< 1 mm)	30 (< 1 mm)	1 kg (< 1 mm)	900	10.453	3.639	7896
24	2	11 (< 1 mm)	30 (< 1 mm)	1 kg (< 1 mm)	915	11.243	3.687	1411
24	2	11 (< 1 mm)	30 (< 1 mm)	1 kg (< 1 mm)	915	11.243	1.163	3700
24	3	11 (< 1 mm)	30 (< 1 mm)	1 kg (< 1 mm)	915	11.312	4.886	1411
24	4	11 (< 1 mm)	30 (< 1 mm)	1 kg (< 1 mm)	899	11.815	1.304	5806
24	4	11 (< 1 mm)	30 (< 1 mm)	1 kg (< 1 mm)	899	11.815	3.659	7896
24	5	11 (< 1 mm)	30 (< 1 mm)	1 kg (< 1 mm)	953	9.942	2.486	361
24	6	11 (< 1 mm)	30 (< 1 mm)	1 kg (< 1 mm)	930	10.235	2.588	7896
25	5	12 (< 1 mm)	30 (< 1 mm)	1 kg (< 1 mm)	942	16.055	1.763	361
25	5	12 (< 1 mm)	30 (< 1 mm)	1 kg (< 1 mm)	942	16.055	1.272	5806
25	6	12 (< 1 mm)	30 (< 1 mm)	1 kg (< 1 mm)	921	22.313	4.231	1987
25	6	12 (< 1 mm)	30 (< 1 mm)	1 kg (< 1 mm)	921	22.313	1.503	4100
21	1	13 (< 1 mm)	30 (< 1 mm)	1 kg (< 1 mm)	912	16.868	2.846	361

			mm)	mm)				
21	1	13 (< 1 mm)	30 (< 1 mm)	1 kg (< 1 mm)	912	16.868	1.418	4100
21	1	13 (< 1 mm)	30 (< 1 mm)	1 kg (< 1 mm)	912	16.868	1.295	5806
21	2	13 (< 1 mm)	30 (< 1 mm)	1 kg (< 1 mm)	903	16.522	4.284	1411
21	2	13 (< 1 mm)	30 (< 1 mm)	1 kg (< 1 mm)	903	16.522	2.819	10100
21	3	13 (< 1 mm)	30 (< 1 mm)	1 kg (< 1 mm)	908	22.3164	3.627	1411
21	4	13 (< 1 mm)	30 (< 1 mm)	1 kg (< 1 mm)	893	21.8004	1.471	10211
21	5	13 (< 1 mm)	30 (< 1 mm)	1 kg (< 1 mm)	1029	24.7416	1.595	361
21	5	13 (< 1 mm)	30 (< 1 mm)	1 kg (< 1 mm)	1029	24.7416	2.063	7896
21	6	13 (< 1 mm)	30 (< 1 mm)	1 kg (< 1 mm)	969	21.5424	2.687	10100
26	5	14 (< 1 mm)	30 (< 1 mm)	1 kg (< 1 mm)	1029	24.7416	2.719	361
26	5	14 (< 1 mm)	30 (< 1 mm)	1 kg (< 1 mm)	1029	24.7416	1.286	5806
26	6	14 (< 1 mm)	30 (< 1 mm)	1 kg (< 1 mm)	969	21.5424	3.338	1987
26	6	14 (< 1 mm)	30 (< 1 mm)	1 kg (< 1 mm)	969	21.5424	1.372	4100

APPENDIX VII. Sensitivity Analysis (First Batch Series)

Batch Pot No.	l(min)	l(avg)	l(max)	cfu(avg)/ml	LRV(min)	LRV(avg)	LRV(max)	error(LRV) = max - min
B21P1	140.75	361.4167	681.5	0.485	2.463	2.872	3.148	0.685
B21 P5	140.75	361.4167	681.5	3.575	1.595	2.005	2.280	0.685
B24 P5	140.75	361.4167	681.5	1.190	2.073	2.482	2.758	0.685
B23 P5	140.75	361.4167	681.5	0.357	2.596	3.006	3.281	0.685
B25 P5	140.75	361.4167	681.5	2.780	1.704	2.114	2.389	0.685
B26 P5	140.75	361.4167	681.5	0.919	2.185	2.595	2.870	0.685
B23 P6	1703.333	1986.667	2165	2.580	2.820	2.887	2.924	0.104
B25 P6	1703.333	1986.667	2165	0.001	6.231	6.298	6.335	0.104
B26 P6	1703.333	1986.667	2165	0.993	3.234	3.301	3.338	0.104
B24 P3	1262.5	1410.833	1553	0.018	4.838	4.886	4.928	0.090
B21 P2	1262.5	1410.833	1553	0.073	4.236	4.284	4.326	0.090
B21 P3	1262.5	1410.833	1553	0.333	3.578	3.627	3.668	0.090
B24 P2	1262.5	1410.833	1553	0.290	3.639	3.687	3.729	0.090
B24 P6	7400	7895.833	8850	19.100	2.588	2.616	2.666	0.078
B21 P5	7400	7895.833	8850	64.000	2.063	2.091	2.141	0.078
B24 P4	7400	7895.833	8850	1.623	3.659	3.687	3.737	0.078
B24 P1	7400	7895.833	8850	1.700	3.639	3.667	3.716	0.078
B19 P1	8166.667	8800	10100	8.117	3.003	3.035	3.095	0.092
B21 P6	8166.667	8800	10100	16.800	2.687	2.719	2.779	0.092
B21 P2	8166.667	8800	10100	12.400	2.819	2.851	2.911	0.092
B20 P1	8166.667	8800	10100	0.087	4.974	5.007	5.066	0.092
B19 P2	7966.667	10055.56	11450	8.500	2.972	3.073	3.129	0.158
B19 P4	7966.667	10055.56	11450	24.167	2.518	2.619	2.676	0.158
B19 P5	7966.667	10055.56	11450	6.467	3.091	3.192	3.248	0.158
B20 P4	7966.667	10055.56	11450	1.605	3.696	3.797	3.853	0.158
B23P6	4483.333	5805.556	6817	250.667	1.253	1.365	1.434	0.182
B24P4	4483.333	5805.556	6817	288.000	1.192	1.304	1.374	0.182
B25P5	4483.333	5805.556	6817	310.667	1.159	1.272	1.341	0.182
B21P1	4483.333	5805.556	6817	294.667	1.182	1.295	1.364	0.182
B26P5	4483.333	5805.556	6817	300.667	1.174	1.286	1.355	0.182
B20 P3	7833.333	10211.11	13350	202.667	1.587	1.702	1.819	0.232
B21 P4	7833.333	10211.11	13350	345.333	1.356	1.471	1.587	0.232
B19 P6	7833.333	10211.11	13350	200.667	1.591	1.707	1.823	0.232
B19 P3	7833.333	10211.11	13350	458.000	1.233	1.348	1.465	0.232
B20 P5	3083.333	4100	4717	70.667	1.640	1.764	1.824	0.185

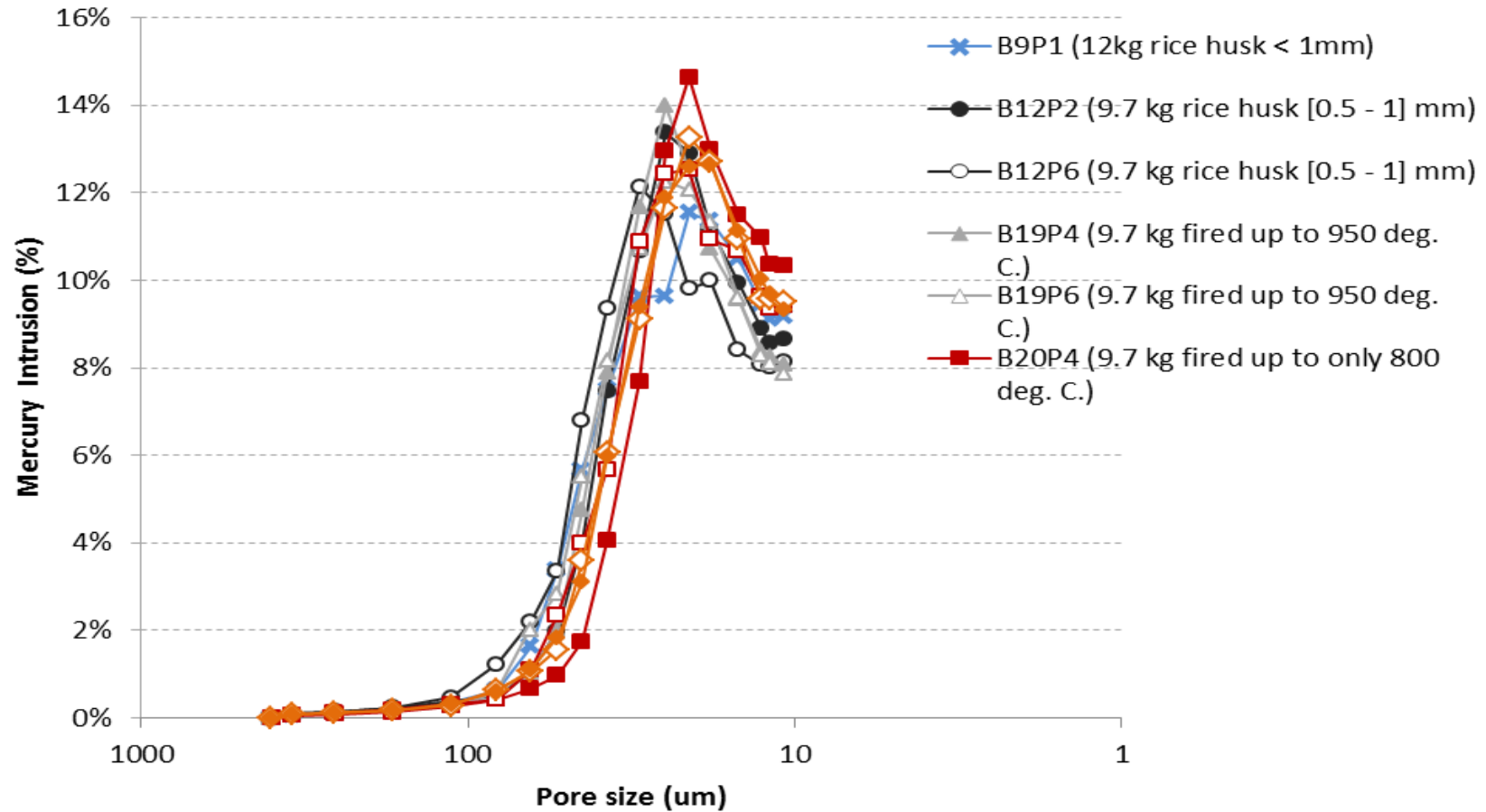
B19 P4	3083.333	4100	4717	80.000	1.586	1.710	1.771	0.185
B23 P6	3083.333	4100	4717	100.000	1.489	1.613	1.674	0.185
B25 P6	3083.333	4100	4717	128.667	1.380	1.503	1.564	0.185
B21 P1	3083.333	4100	4717	156.667	1.294	1.418	1.479	0.185
B26 P6	3083.333	4100	4717	174.000	1.248	1.372	1.433	0.185
B20 P2	2675	3700.833	3701	25.333	2.024	2.165	2.165	0.141
B20 P3	2675	3700.833	3701	72.333	1.568	1.709	1.709	0.141
RDIC	2675	3700.833	3701	48.000	1.746	1.887	1.887	0.141
B19 P1	2675	3700.833	3701	251.333	1.027	1.168	1.168	0.141
B12 P6	3990	4235	4468	357.000	1.048	1.074	1.097	0.049
B12 P5	3990	4235	4468	652.000	0.787	0.813	0.836	0.049
B12 P3	3990	4235	4468	1061.000	0.575	0.601	0.624	0.049
B12 P2	3990	4235	4468	922.000	0.636	0.662	0.685	0.049
B23 P5	3990	4235	4468	655.000	0.785	0.811	0.834	0.049
B23 P6	3990	4235	4468	257.000	1.191	1.217	1.240	0.049
B22 P3	2533.333	2983.333	3300	298.000	0.929	1.000	1.044	0.115
B22 P2	2533.333	2983.333	3300	213.000	1.075	1.146	1.190	0.115
B12 P1	2533.333	2983.333	3300	775.000	0.514	0.585	0.629	0.115
B12 P2	2533.333	2983.333	3300	628.000	0.606	0.677	0.721	0.115
B12 P4	2533.333	2983.333	3300	708.000	0.554	0.625	0.668	0.115
B20 P4	970	1391.111	1677	89.833	1.033	1.190	1.271	0.238
B20 P2	970	1391.111	1677	19.000	1.708	1.865	1.946	0.238
B20 P5	970	1391.111	1677	111.667	0.939	1.095	1.177	0.238
B22 P6	970	1391.111	1677	175.000	0.744	0.900	0.981	0.238
B22 P4	970	1391.111	1677	225.167	0.634	0.791	0.872	0.238
B19 P4	970	1391.111	1677	120.500	0.906	1.062	1.143	0.238
B19 P1	970	1391.111	1677	104.167	0.969	1.126	1.207	0.238
B19 P3	970	1391.111	1677	231.167	0.623	0.779	0.861	0.238

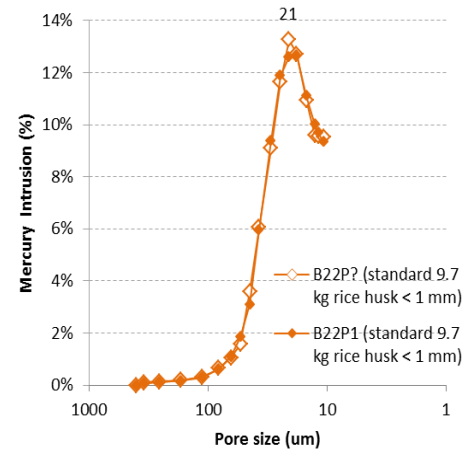
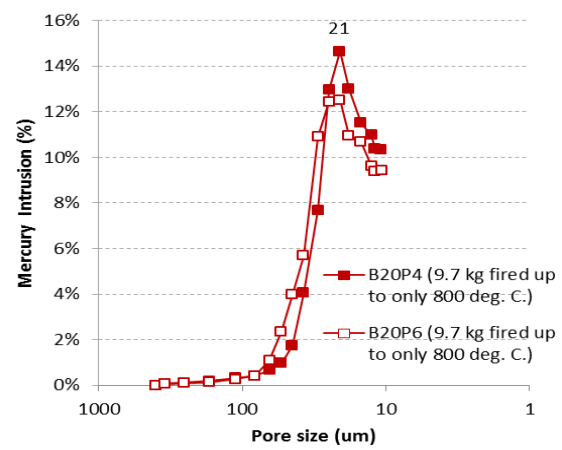
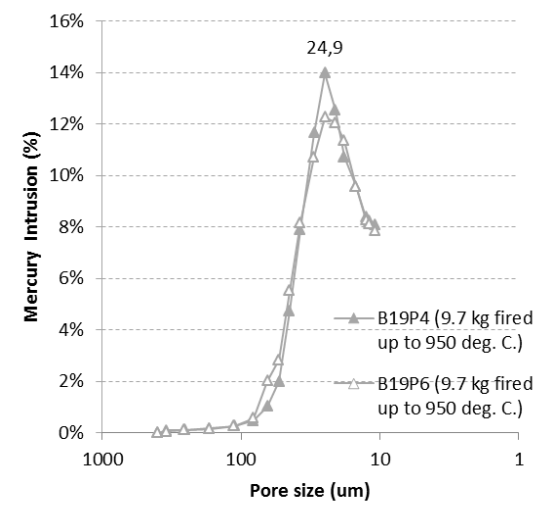
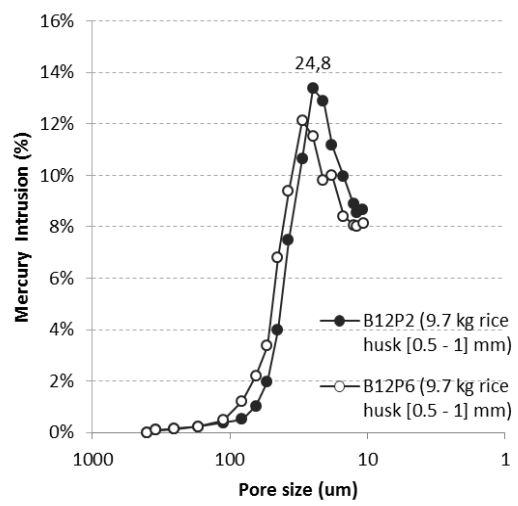
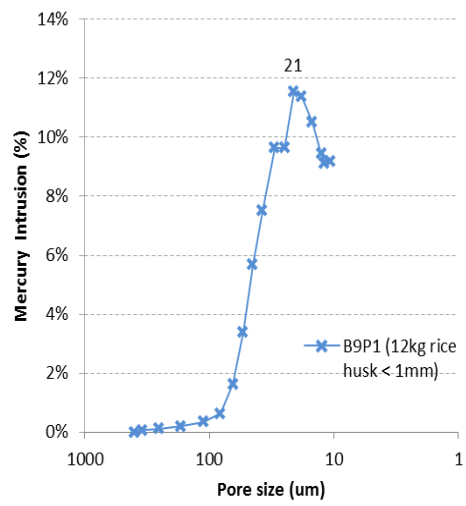
APPENDIX VIII: Raw and Calculated Data (Maximum Firing Temperature Variations)

Batch	Pot	kg rice husk / 6 pots	kg clay / 6 pots	kg laterite / 6 pots	Firing temp (deg. C)	Flow rate (LPH)	LRV (E. Coli)	[E. coli] inf. (cfu/ml)
14	1	9.7 (< 1 mm)	30 (< 1 mm)	1 kg (< 1 mm)	589	3.035		
14	2	9.7 (< 1 mm)	30 (< 1 mm)	1 kg (< 1 mm)	575	2.033		
14	3	9.7 (< 1 mm)	30 (< 1 mm)	1 kg (< 1 mm)	575	2.111		
14	4	9.7 (< 1 mm)	30 (< 1 mm)	1 kg (< 1 mm)	565	2.099		
14	5	9.7 (< 1 mm)	30 (< 1 mm)	1 kg (< 1 mm)	557	2.613		
14	6	9.7 (< 1 mm)	30 (< 1 mm)	1 kg (< 1 mm)	573	2.051		
20	1	9.7 (< 1 mm)	30 (< 1 mm)	1 kg (< 1 mm)	829	5.485	4.974	10100
20	2	9.7 (< 1 mm)	30 (< 1 mm)	1 kg (< 1 mm)	818	5.812	2.165	3700
20	3	9.7 (< 1 mm)	30 (< 1 mm)	1 kg (< 1 mm)	818	7.435	1.709	3700
20	3	9.7 (< 1 mm)	30 (< 1 mm)	1 kg (< 1 mm)	818	7.435	1.702	10211
20	4	9.7 (< 1 mm)	30 (< 1 mm)	1 kg (< 1 mm)	807.7	7.05	3.797	10056
20	5	9.7 (< 1 mm)	30 (< 1 mm)	1 kg (< 1 mm)	944.2	7.172	1.764	4100
20	6	9.7 (< 1 mm)	30 (< 1 mm)	1 kg (< 1 mm)	883			
23	5	9.7 (< 1 mm)	30 (< 1 mm)	1 kg (< 1 mm)	941.1	7.172	3.281	361
23	5	9.7 (< 1 mm)	30 (< 1 mm)	1 kg (< 1 mm)	941.1	7.172	1.549	4235
23	6	9.7 (< 1 mm)	30 (< 1 mm)	1 kg (< 1 mm)	916.1	7.455	2.909	1987
23	6	9.7 (< 1 mm)	30 (< 1 mm)	1 kg (< 1 mm)	916.1	7.455	1.613	4100
23	6	9.7 (< 1 mm)	30 (< 1 mm)	1 kg (< 1 mm)	916.1	7.455	1.694	4235

			mm)	mm)				
23	6	9.7 (< 1 mm)	30 (< 1 mm)	1 kg (< 1 mm)	916.1	7.455	1.365	5806
19	1	9.7 (< 1 mm)	30 (< 1 mm)	1 kg (< 1 mm)	996	7.319	1.168	3700
19	1	9.7 (< 1 mm)	30 (< 1 mm)	1 kg (< 1 mm)	996	7.319	3.003	10100
19	2	9.7 (< 1 mm)	30 (< 1 mm)	1 kg (< 1 mm)	975	6.076	3.073	10056
19	3	9.7 (< 1 mm)	30 (< 1 mm)	1 kg (< 1 mm)	975	8.937	1.348	10211
19	4	9.7 (< 1 mm)	30 (< 1 mm)	1 kg (< 1 mm)	949	9.683	1.71	4100
19	4	9.7 (< 1 mm)	30 (< 1 mm)	1 kg (< 1 mm)	949	9.683	2.619	10056
19	5	9.7 (< 1 mm)	30 (< 1 mm)	1 kg (< 1 mm)	1056	6.52	3.192	10056
19	6	9.7 (< 1 mm)	30 (< 1 mm)	1 kg (< 1 mm)	992	8.727	1.707	10211

APPENDIX IX: Mercury Intrusion Porosimetry Results from the Technical University of Delft in the Netherlands





	Porosity %	Porosity Mean %	Average pore diameter μm	Pore diameter Mean μm	Flow rate L/hr	Flow rate Mean L/hr	Average LRV	LRV Mean
	(pot)	(batch)	(pot)	(batch)	(pot)	(batch)	(pot)	(batch)
B9P1 (12 kg rice husk < 1 mm)	7.4074	7.41	31.05	31.05	11.022	11.02		
B12P2 (9.7 kg rice husk [0.5 - 1] mm)	8.364		30.2696		9.94	10.57	0.67	
B12P6 (9.7 kg rice husk [0.5 - 1] mm)	8.1493	8.26	34.2932	32.28	11.206	10.57	1.07	0.87
B19P4 (9.7 kg fired up to 950 deg. C.)	7.0359		30.0594		9.683	9.21	1.8	
B19P6 (9.7 kg fired up to 950 deg. C.)	6.4637	6.75	31.2025	30.63	8.727	9.21	1.71	1.75
B20P4 (9.7 kg fired up to only 800 deg. C.)	6.6456		26.7911		3.316	4.19	2.49	
B20P6 (9.7 kg fired up to only 800 deg. C.)	7.551	7.1	28.7298	27.76	5.063	4.19	1.43	1.96
B22P1 (standard 9.7 kg rice husk < 1 mm)	5.2116		28.9396					
B22P4 (standard 9.7 kg rice husk < 1 mm)	6.8235	6.02	28.8841	28.91			0.96	0.96

	Porosity %	Porosity Mean %	Average pore diameter μm	Pore diameter Mean μm	Flow rate L/hr	Flow rate Mean L/hr	LRV	LRV	Average LRV	LRV Mean
	(pot)	(batch)	(pot)	(batch)	(pot)	(batch)			(pot)	(batch)
B9P1 (12 kg rice husk < 1 mm)	7.4074	7.41	31.0500	31.05	11.022	11.02				
B12P2 (9.7 kg rice husk [0.5 - 1] mm)	8.3640	8.26	30.2696	32.28	9.940	10.57	0.662		5.62	0.87
B12P6 (9.7 kg rice husk [0.5 - 1] mm)	8.1493	8.26	34.2932	32.28	11.206	10.57	1.074		5.82	0.87
B19P4 (9.7 kg fired up to 950 deg. C.)	7.0359	6.75	30.0594	30.63	9.683	9.21	2.619	1.062	4.30	1.75
B19P6 (9.7 kg fired up to 950 deg. C.)	6.4637	6.75	31.2025	30.63	8.727	9.21	1.707		5.46	1.75
B20P4 (9.7 kg fired up to only 800 deg. C.)	6.6456	7.10	26.7911	27.76	3.316	4.19	3.797		3.99	1.96
B20P6 (9.7 kg fired up to only 800 deg. C.)	7.5510	7.10	28.7298	27.76	5.063	4.19	1.764		2.98	1.96
B22P1 (standard 9.7 kg rice husk < 1 mm)	5.2116	6.02	28.9396	28.91						0.96
B22P4 (standard 9.7 kg rice husk < 1 mm)	6.8235	6.02	28.8841	28.91			0.959		0.96	0.96

APPENDIX X: Detailed Results of the Strength Tests by GERES

<i>Batch ID</i>	<i>Sample ID</i>	ϕ (mm)	t(mm)	Mass (kg)	σ (Mpa)	
B23	P5-1	74.1	18.4	45.6	2.45	
	P5-2	75.7	18.5	50.6	2.69	
	P5-3	77.0	18.8	55.6	2.86	
	P5-4	75.5	20.5	48.1	2.07	
	P6-1	74.7	20.5	43.1	1.86	
	P6-2	73.7	19.7	33.1	1.54	
	P6-3	73.2	18.6	48.1	2.51	
	P6-4	72.9	17.9	40.6	2.28	
B22	P1-1	75.8	18.9	58.1	2.95	
	P1-2	74.2	18.1	60.6	3.36	
	P1-3	74.9	18.1	55.6	3.06	
	P1-4	75.0	19.0	45.6	2.28	
	P3-1	76.0	19.3	35.6	1.73	
	P3-2	76.6	18.7	40.6	2.11	
	P3-3	76.4	18.8	45.6	2.34	
	P3-4	77.5	19.9	50.6	2.33	
	Average					2.40
	Coefficient of Variation					21%
B24	P3-1	75.0	20.1	38.1	1.71	
	P3-2	74.7	21.5	35.6	1.40	
	P3-3	73.8	20.2	38.1	1.69	
	P3-4	73.6	19.7	38.1	1.77	
	P6-1	73.7	19.9	45.6	2.08	
	P6-2	73.0	19.5	43.1	2.04	
	P6-3	73.6	19.5	45.6	2.16	
	P6-4	74.1	19.6	43.1	2.03	
	P4-1	74.5	19.4	35.6	1.70	
	P4-2	75.7	20.0	40.6	1.85	
	P4-3	75.7	21.8	30.6	1.17	
	P4-4	75.8	21.3			
	Average					1.78
	Coefficient of Variation					17%

B25	P6-1	76.7	20.0	35.6	1.62
	P6-2	76.2	20.2	35.6	1.58
	P6-3	73.7	19.9	33.1	1.51
	P6-4	75.1	19.5	33.1	1.57
	P5-1	73.9	19.7	35.6	1.66
	P5-2	74.5	21.2	35.6	1.43
	P5-3	74.9	19.3	38.1	1.84
	P5-4	73.3	20.0	35.6	1.61
B9	P1-1	71.5	20.6	30.6	1.30
	P1-2	75.8	19.7	35.6	1.66
	P1-3	74.2	20.4	38.1	1.65
	P1-4	73.4	20.1	35.6	1.60
	Average				1.59
Coefficient of Variation				8%	
B21	P1-1	73.8	20.8		
	P1-2	74.6	20.9	31.6	1.30
	P1-3	75.0	21.0	32.6	1.33
	P1-4	73.6	20.6	34.6	1.47
	P6-1	73.9	23.0	33.1	1.13
	P6-2	75.9	20.8	30.6	1.29
	P6-3	75.0	22.1	34.6	1.28
	P6-4	76.0	20.7	34.6	1.46
	P4-1	76.6	20.8		
	P4-2	74.7	20.4	24.6	1.07
	P4-3	76.4	21.3	34.6	1.38
	P4-4	74.8	20.3	29.6	1.30
	P5-1	74.0	20.1	33.1	1.48
	P5-2	74.2	22.8	35.6	1.23
	P5-3	74.4	20.9	33.1	1.37
	P5-4	75.1	20.5	30.6	1.32
B8	P2-1	71.7	21.1	28.1	1.14
	P2-2	75.3	22.1		
	P2-3	74.8	21.8	31.6	1.20
	P2-4	73.8	21.6	34.6	1.33
	Average				1.30
Coefficient of Variation				9%	

B26	P5-1	71.8	19.7		
	P5-2	73.2	19.7	24.6	1.14
	P5-3	74.5	19.5	27.6	1.32
	P5-4	74.4	18.1	31.6	1.75
	P6-1	75.1	19.3		
	P6-2	75.8	20.4		
	P6-3	74.3	20.5		
	P6-4	73.3	20.0	19.6	0.89
	Average				1.27
	Coefficient of Variation				29%
B14	P1-1	74.4	20.0		
	P1-2	76.3	21.1	26.6	1.08
	P1-3	75.1	19.5	19.6	0.93
	P1-4	77.6	19.4	26.6	1.28
	P3-1	77.8	21.5		
	P3-2	76.1	21.1	23.6	0.96
	P3-3	75.9	18.9	26.6	1.35
	P3-4	77.7	20.1	19.6	0.88
	Average				1.08
	Coefficient of Variation				18%
B20	P6-1	74.0	18.9	40.6	2.05
	P6-2	74.3	20.3	38.1	1.68
	P6-3	74.7	21.1		
	P6-4	75.8	20.0	40.6	1.84
	Average				1.86
Coefficient of Variation				10%	
B19	P6-1	75.9	17.7	63.1	3.65
	P6-2	74.9	19.2	55.6	2.72
	P6-3	73.0	20.6	55.6	2.37
	P6-4	75.6	19.6	53.1	2.50
	P3-1	75.2	19.8		
	P3-2	74.1	18.8	63.1	3.23
	P3-3	75.7	21.1	55.6	2.26
	P3-4	76.0	18.7	70.6	3.65
	Average				2.91
	Coefficient of Variation				20%

B12	P6-1	76.1	20.1			
	P6-2	78.2	18.7	44.6	2.31	
	P6-3	73.8	22.3	25.6	0.93	
	P6-4	74.8	21.6	19.6	0.76	
	P3-1	74.9	20.5	30.6	1.32	
	P3-2	75.6	19.5	33.1	1.58	
	P3-3	76.0	21.1	26.1	1.07	
	P3-4	75.3	19.7	29.6	1.38	
	Average					1.34
	Coefficient of Variation					39%
RDIC	RDIC2	78.4	14.2	58.1	5.23	
	RDIC1	77.0	14.2	43.1	3.87	
	Average					4.55
	Coefficient of Variation					21%

Red cells indicate samples which broke before putting any mass on the plate, and therefore cannot be taken into account in the calculation of the Modulus of Rupture.

APPENDIX XI: Raw Data (Rice Husk Size Variations)

Batch	Pot	kg rice husk / 6 pots	kg clay / 6 pots	kg laterite / 6 pots	Firing temp (deg. C)	Flow rate (LPH)	LRV (<i>E. Coli</i>)	[<i>E. coli</i>] inf. (cfu/ml)
7	1	9.7 (< 1 mm)	30 (< 1 mm)	1 kg (< 1 mm)	877	2.882	3.310	1062.5
7	2	9.7 (< 1 mm)	30 (< 1 mm)	1 kg (< 1 mm)	883	2.397		
7	3	9.7 (< 1 mm)	30 (< 1 mm)	1 kg (< 1 mm)	883	3.257		
7	4	9.7 (< 1 mm)	30 (< 1 mm)	1 kg (< 1 mm)	888	2.985	2.123	925.0
7	5	9.7 (< 1 mm)	30 (< 1 mm)	1 kg (< 1 mm)	944	3.293	4.181	1062.5
7	6	9.7 (< 1 mm)	30 (< 1 mm)	1 kg (< 1 mm)	908	3.168	2.326	402.5
23	5	9.7 (< 1 mm)	30 (< 1 mm)	1 kg (< 1 mm)	941.1	7.172	3.281	361
23	5	9.7 (< 1 mm)	30 (< 1 mm)	1 kg (< 1 mm)	941.1	7.172	1.549	4235
23	6	9.7 (< 1 mm)	30 (< 1 mm)	1 kg (< 1 mm)	916.1	7.455	2.909	1987
23	6	9.7 (< 1 mm)	30 (< 1 mm)	1 kg (< 1 mm)	916.1	7.455	1.613	4100
23	6	9.7 (< 1 mm)	30 (< 1 mm)	1 kg (< 1 mm)	916.1	7.455	1.694	4235
23	6	9.7 (< 1 mm)	30 (< 1 mm)	1 kg (< 1 mm)	916.1	7.455	1.365	5806
12	2	9.7 [0.5 - 1 mm]	30 (< 1 mm)	1 kg (< 1 mm)	904	9.94	0.662	4235
12	3	9.7 [0.5 - 1 mm]	30 (< 1 mm)	1 kg (< 1 mm)	904	9.303	0.601	4235
12	5	9.7 [0.5 - 1 mm]	30 (< 1 mm)	1 kg (< 1 mm)	1021	12.288	0.813	4235
12	6	9.7 [0.5 - 1 mm]	30 (< 1 mm)	1 kg (< 1 mm)	951	11.206	1.074	4235
RDI	RDI	9.7 (< 1 mm)	30 (< 1 mm)	1 kg (< 1 mm)	870	2.000	3.450	197.5
RDI	RDI	9.7 (< 1 mm)	30 (< 1 mm)	1 kg (< 1 mm)	870	2.500	1.887	3700.0
RDI	RDI	9.7 (< 1 mm)	30 (< 1 mm)	1 kg (< 1 mm)	870	4.000	3.376	136.7

			mm)	mm)				
RDI	RDI	9.7 (< 1 mm)	30 (< 1 mm)	1 kg (< 1 mm)	870	4.000	3.437	136.7
RDI	RDI	9.7 (< 1 mm)	30 (< 1 mm)	1 kg (< 1 mm)	870	4.000	2.274	197.5
RDI	RDI	9.7 (< 1 mm)	30 (< 1 mm)	1 kg (< 1 mm)	870	5.000	3.893	136.7
RDI	RDI	9.7 (< 1 mm)	30 (< 1 mm)	1 kg (< 1 mm)	870	5.000	1.311	136.7

APPENDIX XII: Rice husk particle size distribution analysis of the rice husk samples used in the dry and wet seasons

I) Rice husks used by RDI Cambodia before January 2011

In the factory of RDI-Cambodia, the rice husk used has a grain size smaller than 1 mm.

The rice husk was sieved with a sieve of 1 mm in the sieving machine, but the shape of rice husk is stretched.

The shape of rice husk might influence the pore sizes of the filter pots, which are created in the kiln when the rice husk is burning.

A sample of RDIC rice husks was sieved again with a sieve 0.56 mm by using sieving machine for 35 minutes.

The results of the sieving into proportions between 1 mm and 0.56 mm are shown in the table below:

Table. Proportion between Coarse and Sieved Rice Husks

Rice Husk	Ø1 mm	Ø 0.56 mm	Total
Weight (g)	377.53	402.52	780.05
Percentages (%)	40	52	100

The differences between rice husk 1 mm and rice husk 0.56 mm can be seen in the figure below.



Figure. Rice Husk 1 mm (Left) and Rice Husk 0.56 mm (Right)

II) Rice Husks used by RDI Cambodia after January 2011)

In April 2011, a change in supplier of rice husk at RDIC occurred. Filter pots that were produced in the pilot production line with rice husks deliveries after April showed higher flow rates than the pots before April.

This was our reason for a more accurate sieve analysis on rice husks from different batches / deliveries.



Figure: Rice husk used for the pilot research at RDIC was sieved by hand with a sieve of 1 mm

A sample of RDIC rice husks of January 2011 was sieved by using a multiple sieving machine.

The results of sieving into 5 different proportions from 1 mm until 0.25 mm are shown in the table below.

Table. Rice husk from January 2011

Sieves	Weight sieve	I			II			Average and cum.	
		[g]	[d g]	%	[g]	[d g]	%	average	cum. %
1	413,9	413,9	0	0,0%	413,9	0	0,0%	0,0%	100,0%
0,8	368,8	371,9	3,1	1,9%	370,9	2,1	1,1%	1,5%	100,0%
0,63	387,1	427	39,9	24,0%	435,5	48,4	25,2%	24,6%	98,5%

0,4	348,9	429	80,1	48,2%	450,6	102	52,9%	50,6%	73,9%
0,25	360,5	384,4	23,9	14,4%	381,6	21,1	11,0%	12,7%	23,3%
0	377,5	396,6	19,1	11,5%	396,3	18,8	9,8%	10,6%	10,6%
0			166,1			192			0

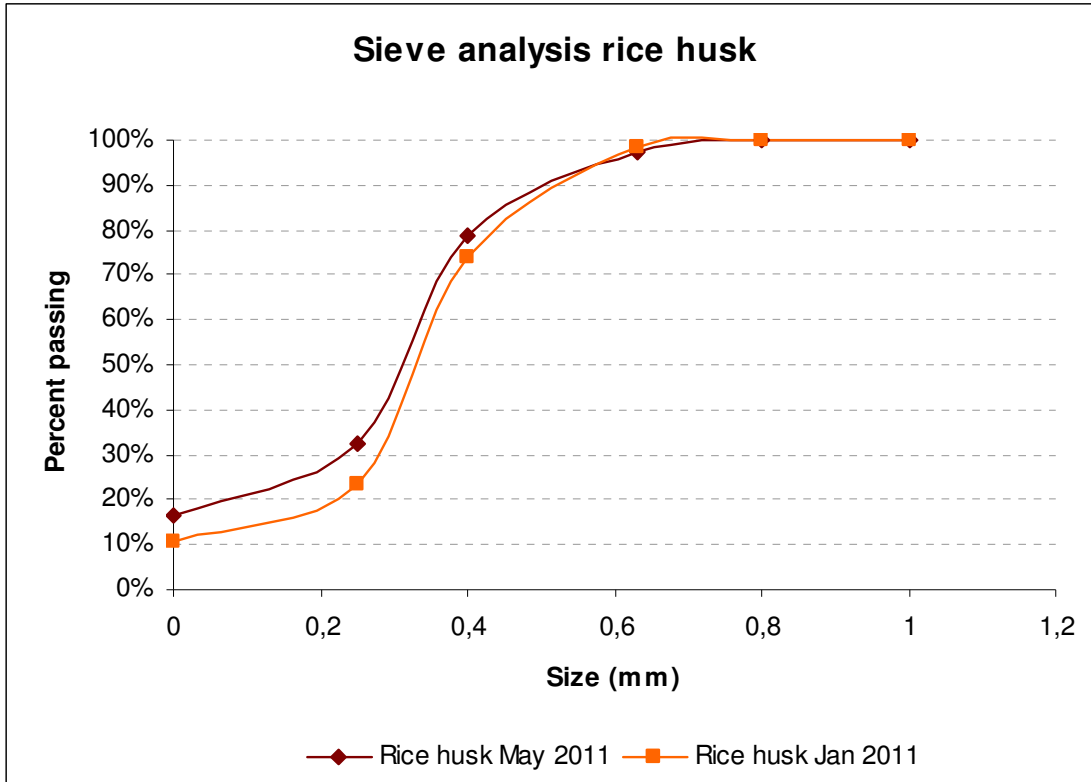
A sample of RDIC rice husks of May 2011 was sieved by using a multiple sieving machine.

The results of sieving into 5 different proportions from 1 mm until 0.25 mm are shown in the table below.

Table23. Rice husk from May 2011

Sieves [mm]	Weight sieve [g]	I			II			Average and cum.	
		[g]	[d g]	%	[g]	[d g]	%	average	cum. %
1	413,9	414,1	0,2	0,1%	414	0,1	0,1%	0,1%	100,0%
0,8	368,8	373,1	4,3	2,6%	373,3	4,5	3,0%	2,8%	99,9%
0,63	387,1	417,1	30	18,0%	415,2	28,1	18,9%	18,4%	97,1%
0,4	348,9	426,8	77,9	46,7%	417,1	68,2	45,8%	46,2%	78,7%
0,25	360,5	386,8	26,3	15,8%	384,7	24,2	16,2%	16,0%	32,5%
0	377,5	405,7	28,2	16,9%	401,4	23,9	16,0%	16,5%	16,5%
0			166,9			149			0

The results of the sieving of both samples of January and May 2011 are shown in the graph below.



The differences between the grain sizes of the two samples of rice husks look quite small.

We had expected that the larger fractions in rice husks would be better represented in May than in January, but we found the opposite.

According to the Ceramic Water Filter Handbook of Resource Development International- Cambodia:

- *RDIC seeks rice husks to be less than 1mm in size, and alters the quantity of rice husks added to the mix based on the size of the grounds.*
- *RDIC sources ground rice husks from three different suppliers. The size of the rice husk particles can vary between suppliers. Larger particles create larger pores in the clay decreasing the thickness of the walls between pores, which results in an overall increased flow rate through the filter when compared to the same mass of small rice husk particles. Therefore when particles are larger, less mass of rice husks is added to the clay mix.*

During our visit in May 2011 we learned that RDIC can also change the amount of rice husk in the clay mix for the full scale production, depending on the dry and wet season conditions. Normally (in the dry season) the weight ratio of clay, laterite and rice husk is 30 : 1 : 9,7 (in kg). In the wet season RDIC increases the rice husk proportion (in kg) in the clay mixture to maintain the flow rate of the pots at the desired level.

APPENDIX XIII: Long-term Flow Rate Raw Data (Pond Water – part 1)

Batch ID	Before Ag app.	28/6/11	29/6/11	30/6/11	1/7/2011	4/7/2011	5/7/2011 (after scrubbing)
B7 (9.7 kg)	1.817	1.13	0.695	0.364	0.501	0.386	4.079
B7 (9.7 kg)	1.881	0.928	1.12		0.673		2.445
B18 (11 kg)	3.814	1.77	1.683	0.664	0.471	0.549	6.996
B18 (11 kg)	4.568	2.535	1.983	0.961	0.88	1.172	3.942
B13 (12 kg)	6.114	2.43	2.215	0.856	0.757	1.016	5.171
B13 (12 kg)	5.915	2.24	1.458	0.533	0.602	0.782	6.969
B4 (13 kg)	13.240	3.341	5.852	2.558	2.624	2.028	8.434
B4 (13 kg)	8.972	3.993	5.579	2.291	1.982	2.048	9.086
B17 (14 kg)	9.329	2.547	1.904	1.032	1.242	0.709	7.189
B17 (14 kg)	11.164	3.174	2.68	1.129	0.787	1.153	7.816
Turbidity	78.3	85.4	39.1	25.8	103	55.7	82.4

	6/7/2011	7/7/2011	8/7/11	10/7/11	12/7/11	13/7/2011	14/07/11
B7 (9.7 kg)	1.382	1.641	1.081	0.863	1.742	1.654	0.929
B7 (9.7 kg)	0.983	2.291	0.783	1.666	0.741	1.462	0.695
B18 (11 kg)	3.297	1.535	1.497	0.75		1.739	1.048
B18 (11 kg)	1.633	1.59	2.064	1.938	0.814	1.183	0.979
B13 (12 kg)	1.901	1.328	1.837	2.971	0.976	0.681	1.659
B13 (12 kg)	2.523	1.285	1.326	1.246	0.586	2.178	1.142
B4 (13 kg)	3.577	2.151	2.273	2.803	1.621	1.47	1.266
B4 (13 kg)	6.353	2.133	2.354	2.9	1.666	3.105	1.292
B17 (14 kg)	2.536	1.802	1.698	1.862	1.111	0.758	1.486
B17 (14 kg)	2.548	1.551	1.094	1.433	1.714	1.448	1.452
Turbidity	60	41.2	15.2	80.8	33.2	29.9	85.9

	19/7/11	20/7/11	21/7/11	22/7/11	25/7/11	26/07/11
B7 (9.7 kg)	0.197	0	0.887	0.922	1.001	0.69
B7 (9.7 kg)	1.257	0.007	1.246	0.765	1.184	0.652
B18 (11 kg)	0.304	0.003	1.776	0.317	1.47	0.843
B18 (11 kg)	0	0.716	2.054	0.729	1.829	0.884
B13 (12 kg)	0.476	1.747	1.579	0.715	1.325	1.079
B13 (12 kg)	0	0.099	2.361	0.478	1.502	1.043
B4 (13 kg)	1.433	1.637	1.143	0.666	1.22	0.847
B4 (13 kg)	1.226	0.979	2.779	0.912	1.118	1.031
B17 (14 kg)	0.97	0.002	3.041	1.073	1.615	1.155
B17 (14 kg)	1.727	1.459	1.253	0.691	1.033	0.852
Turbidity	12.9	199	140	76.5	30	25

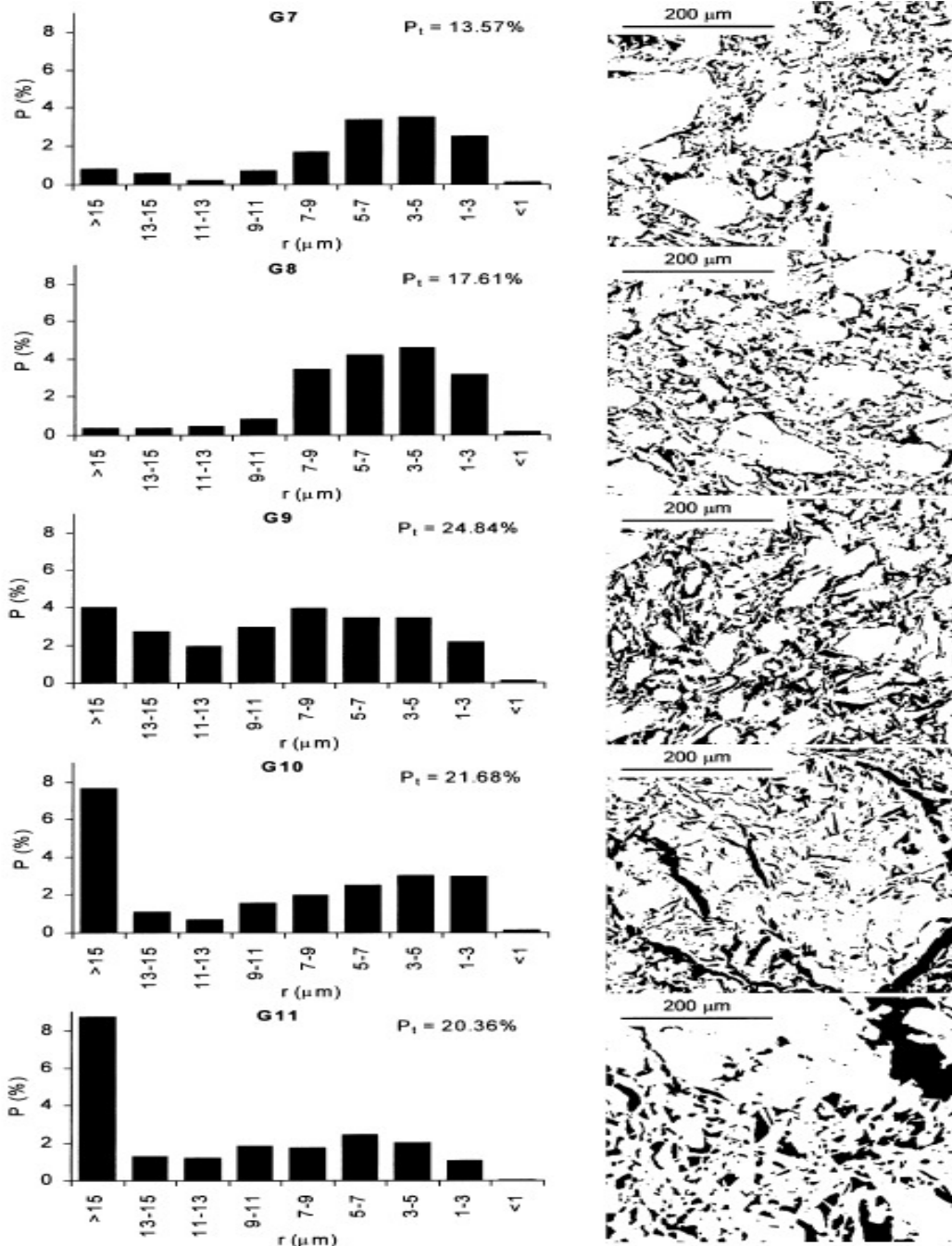
APPENDIX XIV: Long-term Flow Rate Raw Data (Well Water – part 2)

	1/8/11 (after scrub	3/8/11	5/8/11	8/8/11	9/8/11	11/8/11
B7 (9.7 kg)	1.8	0.67	1.931	1.074	1.26	1.199
B7 (9.7 kg)	2.168	0.84	2.207	1.185	1.3	1.029
B18 (11 kg)	4.208	1.56	1.893	1.704	1.755	2.083
B18 (11 kg)	3.512	1.07	1.345	1.491	1.557	1.448
B13 (12 kg)	4.564	1.51	1.684	2.038	2.007	2.02
B13 (12 kg)	4.073	1.46	2.243	2.58	2.447	2.089
B4 (13 kg)	6.993	2.64	3.042	2.934	3.733	2.537
B4 (13 kg)	6.399	1.78	2.036	1.489	1.777	1.649
B17 (14 kg)	10.29	4.27	4.715	3.337	3.83	3.233
B17 (14 kg)	8.171	3.09	4.345	2.504	2.758	2.419
Turbidity	9.68	9.23	18.2	12.5	16.7	7.46

	12/8/11	17/8/11	18/8/11	22/8/11	23/8/11	25/8/11
B7 (9.7 kg)	1.285	1.475	1.494	1.231	1.339	1.28
B7 (9.7 kg)	1.155	1.177	1.194	1.131	1.141	1.184
B18 (11 kg)	1.572	1.526	1.423	1.392	0.885	4.909
B18 (11 kg)	1.625	1.51	1.392	1.197	1.203	1.304
B13 (12 kg)	1.934	1.829	1.633	1.477	1.383	1.512
B13 (12 kg)	2.362	2.111	2.134	1.666	1.593	1.642
B4 (13 kg)	2.887	2.995	2.494	2.967	2.173	2.142
B4 (13 kg)	2.125	1.773	1.31	1.345	1.274	1.461
B17 (14 kg)	3.053	2.524	2.466	2.27	2.552	2.341
B17 (14 kg)	2.466	2.673	2.384	2.364	2.036	2.427
Turbidity	6.03	27.1	10.5	20.2	9.89	12.1

	26/08/11	29/8/11	30/8/11	1/9/11
B7 (9.7 kg)	1.181	1.253	1.187	1.397
B7 (9.7 kg)	0.981	2.623	1.751	1.348
B18 (11 kg)	2.811	2.567	2.398	1.852
B18 (11 kg)	0.929	4.531	2.539	1.811
B13 (12 kg)	1.36	1.435	1.373	1.5
B13 (12 kg)	1.516	1.795	1.672	1.627
B4 (13 kg)	2.132	2.711	2.496	1.973
B4 (13 kg)	1.513	1.25	1.228	1.326
B17 (14 kg)	2.552	2.214	2.147	2.25
B17 (14 kg)	1.955	2.365	1.964	1.982
Turbidity	7.64	5.08	2.84	12

APPENDIX XV: DIA of SEM photomicrographs from Cultrone et al. (2003)



The pore-size distribution histograms of non-calcareous bricks (G) fired at 700 – 1100 deg. C, as well as the corresponding DIA porosity (Pt) data and binary images (pores in black) are presented (Cultrone et al. 2003). G7, G8, G9, G10 and G11 correspond to 700, 800, 900, 1000 and 1100 deg. C., respectively.